

# **SIMULATION AND EXPERIMENTAL INVESTIGATION TO PRODUCE ETHYL TERT-BUTYL ETHER USING REACTIVE DISTILLATION**

**A Thesis  
Submitted to the College of Engineering  
of Nahrain University in Partial Fulfillment  
of the Requirements for the Degree of  
Master of Science  
in  
Chemical Engineering**

**by**

**NADEEN KHALID M. AL-JANABI  
(B. Sc., 2008)**

**Thu Al-Hija**

**1431**

**November**

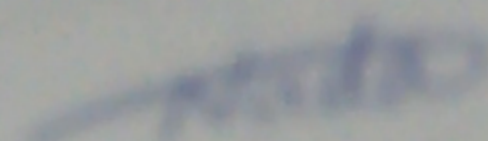
**2010**



## Certification

I certify that this thesis entitled "Simulation and Experimental Investigation to Produce Ethyl Tert-Butyl Ether Using Reactive Distillation" was prepared by Nadeen Khalid Mohammed Al-Janabi under my supervision at Nahrain University / College of Engineering in partial fulfillment of the requirements for the degree of Master of Science in Chemical Engineering.

Signature:



Name:

**Prof. Dr. Nada B. Nakkash**  
(Supervisor)

Date:

1 / 12 / 2010

Signature:



Name:

**Assist. Prof. Dr. Basim O. Hasan**  
(Head of Department)


Date:


8 / 12 / 2010

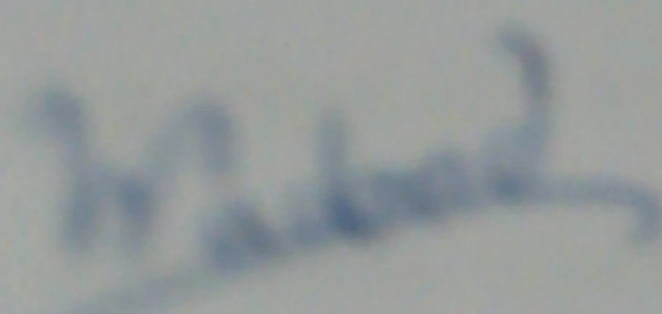


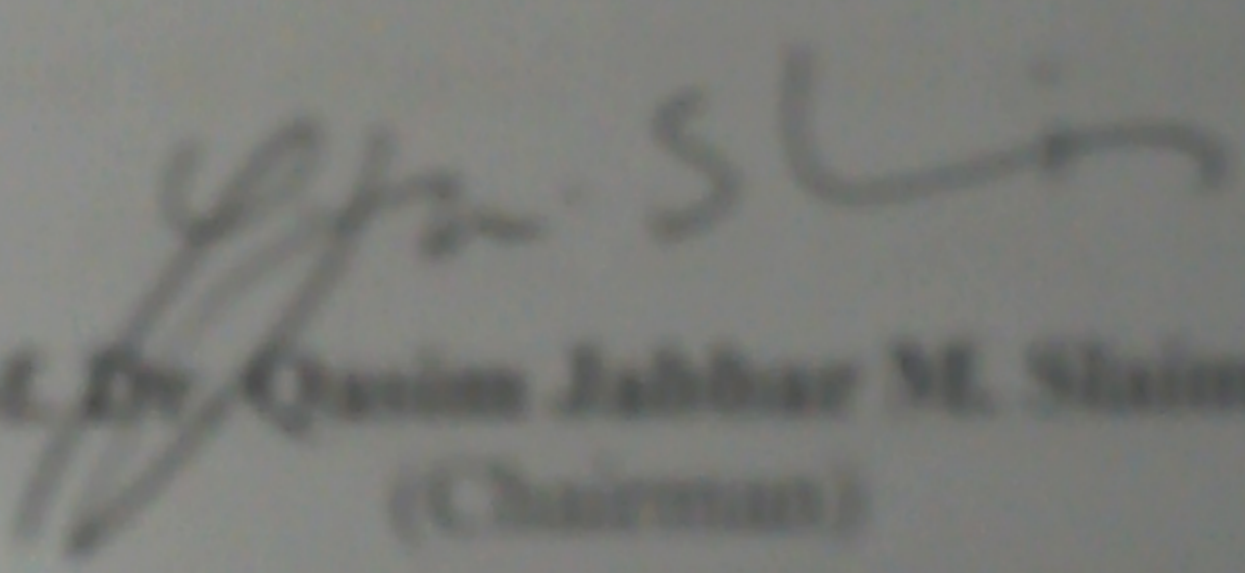
## Certificate

We certify, as an examining committee, that we have read this thesis entitled "**Synthesis and Experimental Investigation to Produce Ethyl Tert-Butyl Ether Using Reactive Distillation**", examined the student (**Nadeen Khalid Mahammed Al-Jasabi**) in its content and found it meets the standard of thesis for the degree of Master of Science in Chemical Engineering.

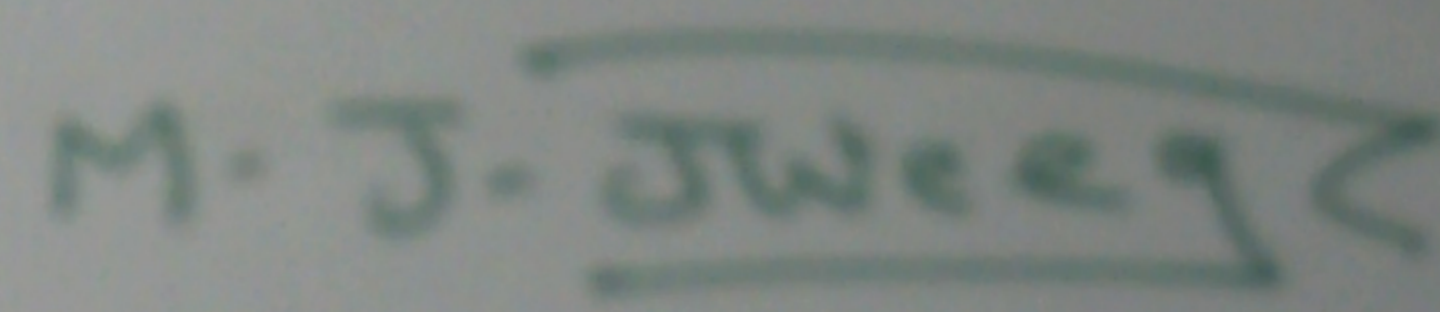
Signature:   
Name: **Prof. Dr. Nadeh B. Nakkash**  
(Supervisor)  
Date: **1 / 18 / 2010**

Signature:   
Name: **Dr. Sarmad Talib Najim**  
(Member)  
Date: **18 / 11 / 2010**

Signature:   
Name: **Asst. Prof. Dr. Wafiq Taber**  
(Member)  
Date: **18 / 11 / 2010**

Signature:   
Name: **Prof. Dr. Qasim Jabbar M. Shaiman**  
(Chairman)  
Date: **1 / 18 / 2010**

### Approval of the College of Engineering

Signature:   
Name: **Prof. Dr. Muhsin J. Jweeg**  
(Dean)  
Date: **19 / 12 / 2010**



## Abstract

Ethyl tert-butyl ether (ETBE) is primarily used for the production of high octane number gasoline. It is produced by reaction of ethanol (ETOH) and tert-butanol (TBA) over an acidic catalyst where water is also produced as a by-product, using reactive distillation unit which can be considered as reaction and distillation combined into one unit operation.

The present work concerned with studying the behavior of batch reactive packed distillation column to produce ETBE experimentally and theoretically. The main objectives of the experimental work is the design and construct a batch packed reactive distillation unit with a heat resistance glass distillation column of 70 cm total height and 3.5 cm inside diameter packed with glass rasching ring of 10 mm length, 6 mm outside diameter, and 3 mm inside diameter. The designed distillation unit has been used for producing ethyl tert-butyl ether by the reaction of ethanol (ETOH) and tert-butanol (TBA) over three types of catalysts Zeolite (13X),  $\text{H}_2\text{SO}_4$ , and  $\text{KHSO}_4$ . The reaction was carried out first using bench experiment to check the performance of catalysts used and their ability to produce ETBE. Zeolite (13X) failed to produce ETBE, while,  $\text{H}_2\text{SO}_4$  and  $\text{KHSO}_4$  catalysts produced ETBE in different purities. Then the reaction is carried out in the batch reactive distillation unit and the effect of many operating conditions on ETBE purity such as feed molar ratio of ethanol to tert-butanol (1:1, 2:1, 4:1), reflux ratios (3, 4, and 5), boiler heat duties of (65, 90, and 146 W), type of catalyst ( $\text{H}_2\text{SO}_4$  and  $\text{KHSO}_4$ ), and the amount of catalyst have been studied, when the catalyst and the reactants are mixed in the still.

The best operating conditions when the reaction takes place in the still are feed molar ratio (FMR) 1:1, reflux ratio 5, boiler heat duty 146W, and  $\text{H}_2\text{SO}_4$  catalyst shows a higher purity of ETBE 0.61317% and conversion 94.789% than  $\text{KHSO}_4$  even when three times the amount of  $\text{KHSO}_4$  has been used.

For the above best operating conditions an experiment was carried out using an intermediate reactive section with  $\text{KHSO}_4$  catalyst placed in pockets of cloth and is supported in the middle section of distillation column. The results give purity of ETBE 0.79407% and 99.465% conversion which are higher than that gained from reactive still but it is also need large amounts of catalyst. All experiments were carried out at atmospheric pressure.

In the theoretical part, Equilibrium (EQ) and Rate-Based or Non Equilibrium (NEQ) models were developed using MATLAB (R2009b) to solve **MESH**R equations, **M**: Material balance, **E**: Equilibrium relation, **S**: Summation equations, **H**: Heat balance, and **R**: Reaction equations. First the equilibrium model was developed and the results were compared with the results of an existed program ASPEN PLUS (10.2) for a certain operating conditions, and it shows a good agreement. The equilibrium model does not take into account the influence of heat and mass transfer on the overall process. Therefore, NEQ model was developed taking into account the effect of mass and heat transfer in material and energy balances. For the operating conditions studied, the results of experimental work compared with the results of the two developed programs of EQ and NEQ models and the deviation shows with about  $\pm 10\%$  error, this deviation may be due to the little difference in the size and shape of the packings and the manual set of the distillation column. The results of the two models EQ and NEQ were also compared.

Also, the results show the composition profiles obtained from NEQ model were near to the experimental profiles more than that of EQ model since the NEQ model taking into account the effect of heat and mass transfer. The comparison of EQ and NEQ models showed that there was a difference between the two models which is due to the consideration of a Murphee vapor efficiency of 1 in the equilibrium model.

## List of Contents

<b>Contents</b>	<b>Page</b>
Abstract	I
List of Contents	III
Notations	VIII
List of Tables	XIII
List of Figures	XVI
<b>Chapter One : Introduction</b>	
1.1 Introduction	1
1.2 Reactive Distillation Models	2
1.3 Aims of This Work	4
<b>Chapter Two : Literature Survey</b>	
2.1 Introduction	5
2.2 Selection of Octane Enhancer in the Present Work	6
2.2.1 Introduction	6
2.3 ETBE Synthesis	6
2.3.1 ETBE Reaction Chemistry	7
2.3.2 ETBE Reaction Mechanism	7
2.4 Reactive Distillation Processes	9
2.4.1 Continuous Reactive Distillation Process	9
2.4.2 Batch Reactive Distillation Process	12
2.5 Thermodynamics of Vapor-Liquid Equilibria	15
2.5.1 Fugacity Coefficient Model	16
2.5.2 Activity Coefficient Model	18
2.6 Models for Design of Reactive Distillation Columns	21
2.6.1 Unsteady state EQ Model	21
2.6.2 Unsteady state Rate-Based or Nonequilibrium Model (NEQ)	23

2.6.2.1 Rate-Based Model Equations	27
2.6.2.2 Rate Expressions	28
2.6.2.3 Transport Correlations	30
<b>Chapter Three : Theoretical Aspects</b>	
3.1 Introduction	33
3.2 Simulation of Equilibrium Model	33
3.2.1 Equilibrium Model Assumptions	33
3.2.2 Equilibrium Model Equations	34
3.2.3 Estimation of Equilibrium Model Parameters	35
3.2.3.1 Enthalpy Calculation	35
3.2.3.2 Calculation of Liquid Activity Coefficient	37
3.2.3.2a Wilson EOS	37
3.2.3.2b UNIQUAC EOS	37
3.2.3.2c UNIFAC EOS	38
3.2.3.3 Activity Coefficient Models Results	40
3.2.3.3 Calculation of Vapor Fugacity Coefficient	41
3.2.3.3a Virial EOS	41
3.2.3.3b Lee-Kesler Equation	42
3.2.3.4 Vapor Pressure Calculation	42
3.2.3.5 Bubble Point Calculation	42
3.2.3.6 Holdup	43
3.2.3.7 Physical Properties	43
3.2.4 Solution Procedure of the Equilibrium Model	44
3.3 Simulation of Rate-Based or Non Equilibrium Model	45
3.3.1 Rate-Based Model Assumptions	45
3.3.2 Non Equilibrium Model Equations	46

3.3.3 Estimation of Non Equilibrium Model Parameters	48
3.3.4 Solution Procedure of the Rate-Based Model	48
<b>Chapter Four : Experimental Work</b>	
4.1 Introduction	51
4.2 Bench Experiment	51
4.3 Reactive Distillation Unit Description	51
4.3.1 The Main Column	52
4.3.2 The Still Pot	52
4.3.3 The Condenser	55
4.3.4 Experimental Measurements	55
4.3.4a Temperature Measurement	55
4.3.4b Composition Measurement	56
4.5 Operating Procedure	56
4.5.1 Start-up Period	56
4.5.2 Production Period	57
4.5.3 Shutdown Period	57
4.6 Experimental Procedure	58
4.6.1 Reactive Still	58
4.6.1a Feed Molar Ratio (FMR)	58
4.6.1b Reflux Ratio	58
4.6.1c Boiler Heat Duty	59
4.6.1d Type of Catalyst	59
4.6.1e Catalyst Amount	59
4.6.2 Intermediate Reactive Section	60
4.7 Purification of Products	64



## **Chapter Five : Results and Discussions**

5.1 Introduction	66
5.2 Results of Bench Experiment	66
5.3 Experimental Studied Variables in Reactive Still	67
5.3.1 Feed Molar Ratio (FMR)	67
5.3.2 Effect of Changing Reflux Ratio (Rr)	68
5.3.3 Effect of Changing the Boiler Heat Duty	71
5.3.4 Effect of Changing the Catalyst Type	73
5.3.5 Effect of Changing the Catalyst Amount	77
5.4 Experimental Results of the Intermediate Reactive Section	79
5.5 Results of Purification Experiments	80
5.6 Theoretical Results	83
5.6.1 Checking the Validity of the Unsteady State Equilibrium Model	83
5.6.2 Comparison of Experimental and Equilibrium model Results	86
5.6.3 Comparison of Experimental and Non-Equilibrium model Results	95
5.6.4 Comparison of Equilibrium and Non-Equilibrium model Results	104

## **Chapter Six : Conclusions and Recommendations**

6.1 Conclusions	115
6.2 Recommendations for the Future Work	116

<b>References</b>	117
-------------------	-----

### **Appendices**

<b>A.</b> Equilibrium model properties	A-1
<b>B.</b> Non Equilibrium Model Properties	B-1

**C. Experimental Calibrations**

C-1

**D. Results Data**

D-1



## Notations

Symbols	Notations	Units
A1, A2, A3, A4, A5	Antoine Equation Constants	—
a	Interfacial Area	m <sup>2</sup>
a <sub>i</sub>	Activity	—
a, b, c, d	Constants for Heat Capacity Equation in Liquid Phase	—
ad	Wetted Specific Surface Area of Packing	m <sup>2</sup> /m <sup>3</sup>
ap	Specific Surface Area of Packing	m <sup>2</sup> /m <sup>3</sup>
a <sub>v</sub> , b <sub>v</sub> , c <sub>v</sub> , d <sub>v</sub>	Constants for Heat Capacity Equation in Vapor Phase	—
B <sup>o</sup> , B <sup>'</sup>	Second Virial Equation Constants	—
C	Concentration	mol/ m <sup>3</sup>
Ca	Capillary Number	—
Cp	Specific Heat	J/mole.K
D <sub>t</sub>	Distillate Flow Rate	mol/s
D <sup>V</sup>	Diffusivity of Vapor Mixture	m <sup>2</sup> /s
D <sup>L</sup>	Diffusivity of Concentrated Liquid Mixture	m <sup>2</sup> /s
D <sup>o</sup> <sub>ik,j</sub>	Diffusivity of Dilute Liquid Mixture	m <sup>2</sup> /s
d <sub>h</sub>	Hydraulic Diameter	m
dp	Nominal Size of Packing	m
E	Energy	J
e	Rate of Heat Transfer	J/s
f	Fugacity of Pure Component	atm
$\bar{f}$	Partial Fugacity of species in mixture	atm
F	Feed Flow Rate	mol/s
Fr	Froude Number	—

G	NRTL Parameter- Empirical Constant	—
g	Interaction Energies Between Groups- NRTL Parameter- Empirical Constant	—
$H_v$	Enthalpy of Vapor Phase	J/mol
h	Enthalpy of Liquid Phase	J/mol
$H_{mix}$	Heat of Mixing	J/mol
$Hr^\circ$	Reference Heat of Reaction	J/mol
$\Delta H_{vb}$	Heat of Vaporization at Normal Boiling Point	J/mol
Hr	Heat of Reaction	J/mol
$h^v$	Heat Transfer Coefficient in Vapor Phase	W/K
$h^L$	Heat Transfer Coefficient in Liquid Phase	W/K
J	Diffusion Flux	mol/ m <sup>2</sup> s
K	Equilibrium Constant	—
k	Mass Transfer Coefficient	m/s
$k_{OL}$	Overall Liquid Phase Mass Transfer Coefficient	kmol/ m <sup>3</sup> .s
$k_{OV}$	Overall Vapor Phase Mass Transfer Coefficient	kmol/ m <sup>3</sup> .s
$L_T$	Packed Height	m
L	Liquid Flow Rate	mol/s
$M_{cat}$	Mass of Catalyst	kg
M	Liquid Hold-Up	mol
m	Mass of Fluid	kg
N	Mass Transfer Rate	mol/s
$N_T$	Number of Stages	—
Le	Lewis Nmber	—
Pr	Prandtl Number	—
n	Total Number of Component	—
P	Pressure	atm



$P^{\text{sat}}$	Saturated Pressure	atm
$P_c$	Critical Pressure	atm
$P_r$	Reduced Pressure	—
$Q$	Heat Duty	J/mol
$R$	Gas Constant = 8.314	Pa. m <sup>3</sup> /mol.K
$R_i$	Reaction Rate	mol/s
$Re$	Reynold Number	—
$Sc$	Schmidt Number	—
$T_c$	Critical Temperature	K
$T^0$	Reference Temperature	K
$T_r$	Reduced Temperature	—
$V$	Vapor Flow Rate	mol/s
$V_c$	Critical Volume	m <sup>3</sup> /mol
$v$	Volume	m <sup>3</sup> /mol
$v$	Molar Volume	m <sup>3</sup> /kmol
$We$	Weber Number	—
$x$	Liquid Mole Fraction	—
$y$	Vapor Mole Fraction	—
$Z$	Compressibility Factor	—
$z$	Feed Composition	—

### Greek Letters

$\emptyset$	Fugacity Coefficient	—
$\gamma$	Activity Coefficient	—
$\wedge$	Wilson Model Parameter	—
$\lambda$	Binary Interaction Coefficient, Wilson Parameters	J/mol
$\alpha$	NRTL Parameter- Empirical Constant	—

$\tau$	Interaction Parameter Between Groups- NRTL Parameter- Empirical Constant	—
$\nu$	Stoichiometric Coefficient	—
$\varepsilon$	Reaction Fractional Volume	—
$\epsilon$	Energy Transfer Due to Mass Transfer	J/s
$\rho$	Density	kg/m <sup>3</sup>
$\mu$	Viscosity	kg/m.s
$\sigma$	Surface Tension	dyne/cm
$\sigma_c$	Critical Surface Tension	dyne/cm
$\eta$	Dimensionless Function	—

### Subscripts

i, k, j	Component indices
L	Liquid
V	Vapor
b	at Boiling Point
t	Total Number of Stages
t+1	Reboiler

### Superscripts

Sat	Saturated
L	Liquid
V	Vapor
w	Omega
R	Residual
C	Combinatorial
(i)	Pure Component



F	at Feed Stage
p	Vapor or Liquid
T	Total
I	Interface

### **Abbreviations**

DAA	Di-Acetone Alcohol
EG	Ethylene Glycol
EO	Ethylene Oxide
EOS	Equation of State
EQ	Equilibrium Model
ETBE	Ethyl Tert-Butyl Ether
ETOH	Ethanol
FMR	Feed Molar Ratio
FVR	Feed Volume Ratio
IB	Isobutene
RD	Reactive Distillation
MTBE	Methyl Tert-Butyl Ether
NEQ	Non Equilibrium Model
R <sub>r</sub>	Reflux Ratio
TAA	Tert-Amyl Alcohol
TAAE	Tert-Amyl Ethyl Ether
TAME	Tert-Amyl Methyl Ether
TBA	Tert-Butanol
TEL	Tert-Ethyl Lead
TML	Tert-Methyl Lead
VLE	Vapor Liquid Equilibria

## List of Tables

Table	Title	Page
2-1	Equations of fugacity coefficient methods	16
2-2	Equations of liquid phase activity coefficient methods	19
3-1	Comparison of Methods of Activity Coefficient	40
3-2	Variables and Equations of Equilibrium Model	44
3-3	Variables and Equations of the Non Equilibrium Model	50
4-1	Studied Operating Conditions for Changing FMR	59
4-2	Studied Operating Conditions for the Present Experimental Work	60
4-4	Purification Experiments	65
5-1	Results of Bench Experiment	66
5-2	Results of 0% Water in Feed and Catalyst $\text{KHSO}_4$	81
A-1	Heat of Formation	A-1
A-2	Liquid Heat Capacity Coefficients	A-1
A-3	Vapor Heat Capacity Coefficients	A-1
A-4	Group Number for Each Component	A-2
A.5	Group Paarameters for Each Component	A-2
A-6	Group Interaction Parameter $a_{mk}$	A-2
A-7	Virial Fugacity Coefficient of Ethanol	A-13
A-8	Fugacity Coefficient of Ethanol	A-14
A-9	Fugacity Coefficient of Tert-butanol	A-14
A-10	Fugacity Coefficient of ETBE	A-14
A-11	Fugacity Coefficient of $\text{H}_2\text{O}$	A-14
A-11	Antoine Parameters	A-15
A-12	Physical Properties	A-15
C-1	Constants of Liquid Viscosity	C-1

C-2	Sugden Parachor Constant	C-2
C-3	Molecular Volume	C-3
C-1	Actual Heating Rates for Heater Reading	C-3
D-1	Data of Figure (5.2)	D-1
D-2	Liquid Mole Fractions at Reflux Ratio=3	D-1
D-3	Liquid Mole Fractions at Reflux Ratio=4	D-2
D-4	Liquid Mole Fractions at Reflux Ratio=5	D-2
D-5	Liquid Mole Fractions at Reflux Ratio=5, Heat Duty=65W	D-3
D-6	Liquid Mole Fractions at Reflux Ratio=5, Heat Duty=90W	D-3
D-7	Liquid Mole Fractions with 90% water, catalyst H <sub>2</sub> SO <sub>4</sub>	D-4
D-8	Liquid Mole Fractions with 0% water, catalyst KHSO <sub>4</sub>	D-4
D-9	Liquid Mole Fractions with 0% water, catalyst H <sub>2</sub> SO <sub>4</sub>	D-5
D-10	Liquid Mole Fractions with 0% water, catalyst 3* KHSO <sub>4</sub>	D-5
D-11	Liquid Mole Fractions	D-6
D-12	Liquid Mole Fractions, 0% Water in Feed, H <sub>2</sub> SO <sub>4</sub>	D-6
D-13	Liquid Mole Fractions, Three Times Catalyst KHSO <sub>4</sub>	D-6
D-14	Liquid Mole Fractions, Intermediate Reactive Section	D-7
D-15	Operating Conditions for Comparison of Proposed EQ Program and Aspen Plus	D-7
D-16	Liquid Mole Fractions, Distillate of ASPEN PLUS	D-8
D-17	Liquid Mole Fractions, Distillate of Proposed Program	D-8
D-18	Liquid Mole Fractions, Rr=3	D-9
D-19	Liquid Mole Fractions, Rr=4	D-9
D-20	Liquid Mole Fractions, Rr=5	D-9
D-21	Liquid Mole Fractions, Heat Duty=65W	D-10
D-22	Liquid Mole Fractions, Heat Duty=90W	D-10
D-23	Liquid Mole Fractions, 0% Water in Feed, KHSO <sub>4</sub>	D-10



D-24	Liquid Mole Fractions, Three Times $\text{KHSO}_4$	D-11
D-25	Liquid Mole Fractions, Intermediate Reactive Section	D-11
D-26	Liquid Mole Fractions, $R_r=3$	D-11
D-27	Liquid Mole Fractions, $R_r=4$	D-12
D-28	Liquid Mole Fractions, $R_r=5$	D-12
D-29	Liquid Mole Fractions, Heat Duty=65W	D-12
D-30	Liquid Mole Fractions, Heat Duty=90W	D-13
D-31	Liquid Mole Fractions, 0% Water in Feed, $\text{KHSO}_4$	D-13
D-32	Liquid Mole Fractions, Three Times $\text{KHSO}_4$	D-13
D-33	Liquid Mole Fractions, Intermediate Reactive Section	D-14

## List of Figures

Figure	Title	Page
2-1	Liquid Mole Fraction in the Distillate	12
2-2	Schematic diagram of EQ segment	22
2-3	Schematic diagram of NEQ segment j	23
2-4	Two-film theory of NEQ segment	24
3-1	Packed Batch RD Column	34
3-2	Schematic Diagram of EQ Segment	34
3-3	The Non Equilibrium Segment	46
4-1	Photographic Picture of RD Unit	53
4-2	Schematic Sketch of RD Unit	54
4-3	Experimental Unit with Intermediate Reactive Section	62
4-4	Photographic Picture of the Upper Section during the Total Reflux of Intermediate Reactive Section	63
4-5	photographic picture of the purification mixture	64
5-1	Liquid Mole Fractions with Different FMR	68
5-2	Liquid mole fraction profile when $R_r=3$	69
5-3	Liquid mole fraction profile when $R_r=4$	70
5-4	Liquid mole fraction profile when $R_r=5$	70
5-5	Effect of Changing $R_r$ on ETBE Purity in the Distillate after 6hr	71
5-6	Liquid mole fraction profile when $R_r=5$ , heat duty=65W	72
5-7	Liquid mole fraction profile when $R_r=5$ , heat duty=90W	72
5-8	Effect of Changing Heat Duty on ETBE Purity in Distillate after 6hr	73
5-9	Liquid mole fraction profile with 90% water and catalyst $H_2SO_4$	74

5-10	Liquid mole fraction profile with 0% water and catalyst $\text{KHSO}_4$	75
5-11	Conversion profile for 0% water and catalyst $\text{KHSO}_4$	75
5-12	Liquid mole fraction profile with 0% water and catalyst $\text{H}_2\text{SO}_4$	76
5-13	Conversion profile for 0% water and catalyst $\text{H}_2\text{SO}_4$	76
5-14	Liquid mole fraction profile with 0% water and 3* $\text{KHSO}_4$	78
5-15	Conversion profile for 0% water and 3* $\text{KHSO}_4$	78
5-16	Liquid mole fraction profile using intermediate reactive section	79
5-17	Conversion profile using intermediate reactive section	80
5-18	Liquid Composition Profile in the Upper Layer, 0% Water in Feed $\text{H}_2\text{SO}_4$	81
5-19	Liquid Composition Profile in the Upper Layer, Three Times Catalyst $\text{KHSO}_4$	82
5-20	Liquid Composition Profile in the Upper Layer, Intermediate Reactive Section	82
5-21	Comparison of the Proposed EQ Program and Aspen Plus, Distillate	84
5-22	Comparison of the Proposed EQ Program and Aspen Plus, Bottom	84
5-23	Comparison of the Proposed EQ Program and Aspen Plus, Bottom	85
5-24	Error between the Two Programs in the Distillate	85
5-25	Experimental and EQ Model Composition profile in the Distillate for $R_r=3$ , Heat Duty=146W	86



5-26	Experimental and EQ Model Composition profile in the Distillate for $R_r=4$ , Heat Duty=146W	87
5-27	Experimental and EQ Model Composition profile in the Distillate for $R_r=5$ , Heat Duty=146W	87
5-28	Experimental and EQ Model Composition profile in the Distillate for Heat Duty=65W	88
5-29	Experimental and EQ Model Composition profile in the Distillate for Heat Duty=90W	88
5-30	Experimental and EQ Model Composition profile in the Distillate for 0% Water in Feed	89
5-31	Experimental and EQ Model Composition profile in the Distillate for 0% Water in Feed with Three Times Catalyst $KHSO_4$	89
5-32	Experimental and EQ Model Composition profile in the Distillate for Intermediate Reactive Section	90
5-33	Error between Experimental and EQ Model for $R_r=3$	91
5-34	Error between Experimental and EQ Model for $R_r=4$	91
5-35	Error between Experimental and EQ Model for $R_r=5$	92
5-36	Error between Experimental and EQ Model for Heat Duty=65W	92
5-37	Error between Experimental and EQ Model for Heat Duty=90W	93
5-38	Error between Experimental and EQ Model for 0% Water in Feed Catalyst $KHSO_4$	93
5-39	Error between Experimental and EQ Model for 0% Water in Feed with Three Times Catalyst $KHSO_4$	94

5-40	Error between Experimental and EQ Model for Intermediate Reactive Section	94
5-41	Experimental and EQ Model Composition profile in the Distillate for $R_r=3$	95
5-42	Experimental and EQ Model Composition profile in the Distillate for $R_r=4$	96
5-43	Experimental and EQ Model Composition profile in the Distillate for $R_r=5$	96
5-44	Experimental and EQ Model Composition profile in the Distillate for Heat Duty=65W	97
5-45	Experimental and EQ Model Composition profile in the Distillate for Heat Duty=90W	9
5-46	Experimental and EQ Model Composition profile in the Distillate for 0% Water in feed, Catalyst $\text{KHSO}_4$	98
5-47	Experimental and EQ Model Composition profile in the Distillate for 0% Water in feed, Catalyst $\text{KHSO}_4$	98
5-48	Experimental and EQ Model Composition profile in the Distillate for Intermediate Reactive Section	99
5-49	Error between Experimental and NEQ Model for $R_r=3$	100
5-50	Error between Experimental and NEQ Model for $R_r=4$	100
5-51	Error between Experimental and NEQ Model for $R_r=5$	101
5-52	Error between Experimental and NEQ Model for Heat Duty=65W	101
5-53	Error between Experimental and NEQ Model for Heat Duty=90W	102
5-54	Error between Experimental and NEQ Model for 0% Water in Feed, $\text{KHSO}_4$	102

5-55	Error between Experimental and NEQ Model for 0% Water in Feed Three Times Catalyst $\text{KHSO}_4$	103
5-56	Error between Experimental and NEQ Model for 0% Water in Feed Intermediate Reactive Section	103
5-57	NEQ and EQ Model Composition profile in the Distillate for for $R_r=3$	104
5-58	NEQ and EQ Model Composition profile in the Distillate for for for $R_r=4$	105
5-59	NEQ and EQ Model Composition profile in the Distillate for for $R_r=5$	105
5-60	NEQ and EQ Model Composition profile in the Distillate for for Heat Duty=65W	106
5-61	NEQ and EQ Model Composition profile in the Distillate for for Heat Duty=90W	106
5-62	NEQ and EQ Model Composition profile in the Distillate for for 0% Water in Feed Catalyst $\text{KHSO}_4$	107
5-63	NEQ and EQ Model Composition profile in the Distillate for for 0% Water in Feed Three Times Catalyst $\text{KHSO}_4$	107
5-64	NEQ and EQ Model Composition profile in the Distillate for for Intermediate Reactive Section	108
5-65	ETOH Liquid Composition Profile, $R_r=5$ , Heat Duty=146W	109
5-66	TBA Liquid Composition Profile, $R_r=5$ , Heat Duty=146W	110
5-67	ETBE Liquid Composition Profile, $R_r=5$ , Heat Duty=146W	110
5-68	Water Liquid Composition Profile, $R_r=5$ , Heat Duty=146W	111
5-69	ETBE Liquid Composition Profile, $R_r=3$ , Heat Duty=146W	111
5-70	ETBE Liquid Composition Profile, $R_r=4$ , Heat Duty=146W	112



5-71	ETBE Liquid Composition Profile, $R_r=5$ , Heat Duty=65W	112
5-72	ETBE Liquid Composition Profile, $R_r=5$ , Heat Duty=90W	113
5-73	ETBE Liquid Composition Profile, for 0% Water in Feed with 0.04 kg Catalyst / kg Reactant	113
5-74	ETBE Liquid Composition Profile, for 0% Water in Feed with 0.12 kg Catalyst / kg Reactant	114
5-75	ETBE Liquid Composition Profile, for Intermediate Reactive Section	114
A-1	$\gamma$ of ETOH, Wilson	A-3
A-2	$\gamma$ of TBA, Wilson	A-3
A-3	$\gamma$ of ETBE, Wilson	A-4
A-4	$\gamma$ of H <sub>2</sub> O, Wilson	A-4
A-5	$\gamma$ of ETOH, UNIFAC	A-5
A-6	$\gamma$ of TBA, UNIFAC	A-5
A-7	$\gamma$ of E TBE, UNIFAC	A-6
A-8	$\gamma$ of H <sub>2</sub> O, UNIFAC	A-6
C-1	Temperature vs. Time at Different Heating Power	C-2

# Chapter One

## Introduction

### 1.1 Introduction

Reactive distillation (RD) is an alternative to a separated reaction-distillation processes, whereby reaction and separation take place within a single counter current column. Reactants are converted to products in a reaction zone with simultaneous separation of the products and recycle of unreacted reactants to the reaction zone (Kenig et al., 2004). Among suitable reactive distillation processes is etherification process to produce octane enhancer such as production of ethyl tert-butyl ether (ETBE), methyl tert-butyl ether (MTBE), tert-amyl methyl ether (TAME), tert-amyl ethyl ether (TAEE) which are the best known oxygenates to be used to increase the octane level and to promote cleaner burning of gasoline, and thus decrease harmful emissions from vehicles (Ozbey and Oktar, 2009). There is an increasing interest in the use of ETBE as a replacement of methyl tert-butyl ether (MTBE) because :

1. ETBE has lower blend Reid vapor pressure (4 psi) than MTBE (9 psi) which allows ETBE to be used successfully in obtaining gasoline with less blend Reid vapor pressure than (7.8 psi) as required in some hot places during summer (Assabumrungrat et al., 2004).
2. From environmental view point, ETBE is derived from ethanol which can be obtained from renewable resources like biomass (Assambrungrat et al., 2004).
3. Also, ETBE may become a more attractive option for the reasons of higher octane number (111) than MTBE (109) (Yang et al., 2001).

Ethyl tert-butyl ether can be synthesized from tert-butanol. There are two ways to produce ETBE from tert-butanol; an indirect and a direct method. In the indirect method, tert-butanol is dehydrated to isobutene in a reactor and then isobutene is reacted with ethanol to form ETBE in the presence of acidic catalyst. While, in the

direct method, ETBE can be produced by reacting tert-butanol directly with ethanol in the presence of an acidic catalyst, during which the water is produced as a by-product (Ozbey and Oktar, 2009).

In general, reactive distillation can be performed by a continuous or batch processes. Batch reactive distillation often means lower cost than continuous distillation, but it is also complex since the composition profiles and operating conditions may change over a wide range of values during the entire operation and the state estimators must be designed to deal with the time-varying nature of the batch columns. Also, batch distillation is an attractive choice in reactive distillation, when the reaction is slow and a large resident time is required to attain high conversion and when the reaction is so fast that a significant reaction may occur before the column reaches steady state (Bahar and Ozgen, 2008).

## **1.2 Reactive Distillation Models**

Models for reactive distillation may be split into two categories; the equilibrium (EQ) stage model and the rate-based or the non equilibrium (NEQ) stage model, where the stage may be a tray or a segment of packing (Higler, 1999). The equilibrium model includes the assumption that the streams leaving the stages are at physical equilibrium. Component material balance, phase equilibrium equations, summation equations, energy balances for each stage, and reaction equations (MESHR equations) are solved to give composition, temperature, and flow profiles. On the other hand, the nonequilibrium models are commonly based on the two film theory. The equations are the component material balances and energy balance equations for each phase together with mass and energy transfer rate equations and equilibrium equations at the interface (Gomez et al., 2006).

In the non equilibrium model, it is the rate of mass and heat transfer, and not the physical equilibrium, that often limit the separation. The non equilibrium model can be

classified, depending on the way that heat and mass transfer rates are calculated, into differential and integral nonequilibrium models. According to the differential model, Maxwell Stefan equations are integrated on the thickness of the film. On the other hand, the integral model uses mass and heat transfer coefficients to determine the flux at the interface, and it is not necessary to determine the thickness of the film in this case (Gomez et al., 2006).

The non equilibrium model is preferred to the equilibrium model because it takes into account the technical characteristics of the column (type of plate, or type of packing), which is more near reality. Also, an important reason for using the non equilibrium model is that the reactive distillation operations deal with multicomponent mixtures exhibiting large thermodynamic non-idealities. Furthermore, chemical reactions taking place in the homogeneous liquid phase could significantly influence interphase mass transfers. Also, equilibrium model does not take into account the coupling between chemical reaction and mass transfer and it assumes that the reaction occurs in the bulk of liquid only and not in the mass transfer film (Higler et al., 1998).

Building the NEQ model of a reactive separation process is not as straightforward as it is for the EQ stage model in which a term added to account for reaction to the liquid-phase material balances. For a reactive separation process, it is first needed to know whether the reaction is heterogeneous or homogeneous, for homogeneous systems reactions takes place in the liquid bulk, if it is sufficiently rapid, the reaction will also take place in the liquid film adjacent to the phase interface, and very fast reactions may occur only in the film. For a heterogeneous reaction, there are two approaches for the description of the reaction term. The simplest approach is to treat the reaction homogeneously, whereby catalyst diffusion and reaction is lumped into an overall reaction term. In this case, one only needs to specify catalyst mass and activity. A more rigorous approach would involve if the catalyst is porous, or reaction at the surface or not. In this case information about the catalyst geometry (surface area, mean pore diameter, etc) is required (Taylor and Krishna, 2000).

### **1.3 Aims of This Work**

The present work consists of two parts; experimental and theoretical.

1. The aim of experimental work is to construct a packed reactive distillation column which is used for production of ethyl tert-butyl ether (ETBE) from ethanol and tert-butanol using homogeneous catalyst. Then examine the effect of changing the operating conditions such as FMR, reflux ratio, amount of catalyst, and heat duty of the reactive distillation unit on the purity of ETBE in the distillate in order to reach the best purity with high selectivity and conversion.
2. The aims of theoretical part are:
  - Simulation of equilibrium program for unsteady state (or dynamic) packed reactive distillation.
  - Simulation rate-based or non equilibrium program.
3. The results of experimental part are compared with the theoretical results of the two developed models.
4. Comparison of the results of equilibrium and rate-based model.



## **Chapter Two**

### **Literature Survey**

#### **2.1 Introduction**

Reactive distillation (RD) can be considered as reaction and distillation combined into one unit operation. The reactions in reactive distillation considered include heterogeneous catalysis reactions, homogeneous catalysis reactions, and thermal (non catalysis) reactions (Harmsen, 2007). Reactive distillation is a favorable alternative to conventional series of reaction-separation processes due to:

1. It can reduce the capital investment because two process steps can be carried out in the same device, such as integration leads to lower costs in pumps, piping, and instrumentation (Lei et al., 2005).
2. The operating costs are also reduced via overcoming distillation boundaries such as azeotrop due to the presence of reactions (Budi et al., 2004).
3. Product selectivities can be improved due to a fast removal of reactants or products from the reaction zone. Thus, the probability of consecutive reactions, which may occur in the sequential operation mode, is lowered (Lei et al., 2005).
4. If RD is applied to exothermic reaction; the heat of reaction is utilized for the evaporation of liquid phase component which can reduce the heat duty (Jhon and Lee, 2003).
5. The maximum temperature in reaction zone is limited to the boiling point of the reaction mixture, so that the danger of hot spot formation on the catalyst is reduced significantly (Lei et al., 2005).

Reactive distillation is a favorable technique for production octane enhancer, such as methyl tert-butyl ether, ethyl tert-butyl ether, and tert-amyl ethyl ether (Budi et al., 2004).

## **2.2 Selection of Octane Enhancer in the Present Work**

### **2.2.1 Introduction**

The use of lead compounds such as tetra-ethyl lead (TEL) and tetra-methyl lead (TML) as octane boosters and anti-knocking agent is no more used in practice in most parts of world due to stringent environmental protection regulations. Therefore, oxygenated compounds have gained importance on octane enhancing fuel blending compounds (Umar et al., 2009a).

Alcohols and ethers are among these oxygenated compounds, proposed as octane enhancers. Addition of oxygenates into gasoline also reduces exhaust emissions of CO and unburned hydrocarbons and helps to reduce the formation of atmospheric ozone. Tert-ethers are generally preferred to alcohols as gasoline components, due to their lower blending vapor pressure (Ozbay and Oktar, 2009).

The tert-ethers like methyl tert-butyl ether (MTBE), ethyl tert-butyl ether (ETBE), and tert-amyl methyl ether (TAME) were considered to be the most suitable and preferred sources over alcoholic oxygenates (Umar et al., 2009b).

Methyl tert-butyl ether (MTBE) has been the most widely used oxygenates. Currently, there are pending legislations on the use of MTBE because it has the tendency to pollute the underground water. Therefore, ETBE is the most suitable alternative (Jhon and Lee, 2003).

### **2.3 ETBE Synthesis**

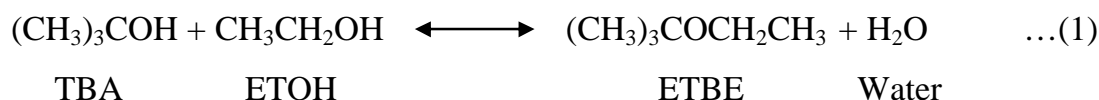
Mostly ETBE has been synthesized by exothermic reversible reaction between isobutene (IB) and ethanol (ETOH), but the availability of isobutene is limited, it is only produced in refinery using catalytic and steam cracking operations, and it is produces ETBE under high pressure.

Therefore, alternative routes to synthesize ETBE are under substantial consideration. The most important substitute of isobutene is tert-butanol (TBA) (Umar et al., 2009b).

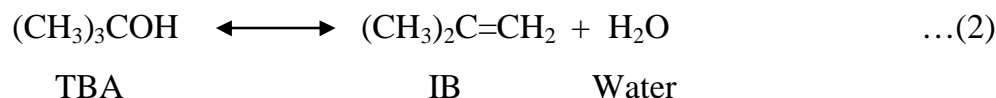
TBA is relatively less expensive and produces ETBE under atmospheric pressure (Umar et al., 2009a).

### 2.3.1 ETBE Reaction Chemistry

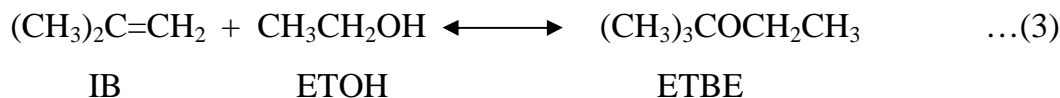
In the synthesis of ETBE from TBA and ETOH, following sequence of reactions take place (Umar et al., 2009a).



The above main reaction is accompanied by side reaction, i.e. dehydration of TBA into isobutene and water.



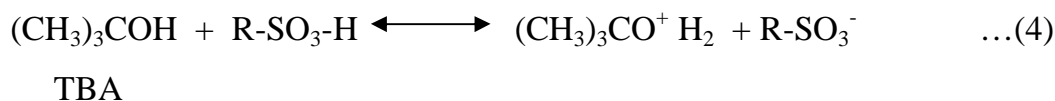
The third reaction which may take place is the indirect formation of ETBE by ethanol and isobutene.

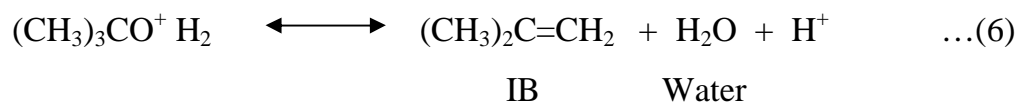
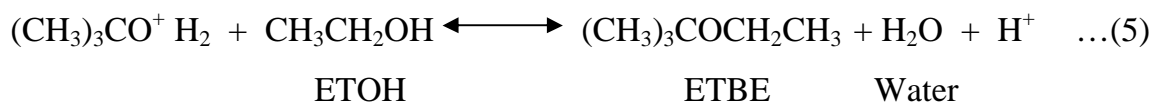


As isobutene exists only in the gaseous state at atmospheric pressure, backward reaction in reaction (2) and the reaction (3) can safely be neglected (Assambrungrat et al., 2004; Umar et al., 2008).

### 2.3.2 ETBE Reaction Mechanism

The following mechanism was assumed for the ETBE synthesis (Słomkiewicz, 2004; Umar et al., 2009b):





In the first step (reaction 4), TBA converted to a solvated carbocation, a reactive unstable intermediate in the presence of strong acidic media. The solvated carbocation combines with ethanol in reaction 5 to form ETBE, water and hydrogen ion. The solvated carbocation could also be decomposed to isobutene, water, and hydrogen ion as in reaction 6. The hydrogen ion  $\text{H}^+$  formed in reactions 5 and 6 helps the catalyst to regain its original matrix as in reaction 7.

**Matouq et al., 1996** used different catalysts for production of ethyl tert-butyl ether from ethanol and tert-butanol using total reflux conditions, such as potassium hydrogen sulfate  $\text{KHSO}_4$ , sodium hydrogen sulfate  $\text{NaHSO}_4$ , sulfuric acid  $\text{H}_2\text{SO}_4$ , and Amberlyst 15. From the experimental results,  $\text{NaHSO}_4$  failed to produce ETBE,  $\text{H}_2\text{SO}_4$ , and Amberlyst 15 produces ETBE with 70% and 71% in the distillate, and  $\text{KHSO}_4$  produces 10% ETBE and 62% when the catalyst amount is doubled.

**Quitain et al., 1999b** prepared and used ion exchange resin catalyst Amberlyst 15 in  $\text{H}^+$  form as a catalyst. Cylindrical pellet of catalyst were made by mixing Amberlyst 15 particles with poly ethylene powder (15 wt %) in a mold of 8 mm diameter and heated to 393 K to bind the particles. The mentioned catalyst causes a production of ETBE with 53% concentration with zero reflux ratio, and 60% with reflux ratio of seven in the distillate.

**Assabumrungrat et al., 2004** used  $\beta$ -Zeolite with (Si/Al) ratio of 55 to produce ETBE. About 20% ETBE produced in the distillate with 1.5 reflux ratio and feed molar ratio of TBA: ETOH:  $\text{H}_2\text{O}$  = 1:1:38

**Umar et al., 2009a** examined ion exchange resin catalyst CT-145-H for production of ETBE from tert-butanol, the catalyst produces about 7% ETBE in the distillate and 42% selectivity.

**Valsenko et al., 2009** studied the possibility of increasing the productivity of acidcation-exchange resin catalysts for ETBE synthesis. Commercial acidic micro porous gel type ion exchange resin and Amberlyst 15 have been studied.

## **2.4 Reactive Distillation Processes**

### **2.4.1 Continuous Reactive Distillation Process**

There are two main advantages of continuous RD process relative to the conventional alternatives are the possibility of carrying equilibrium limited chemical reactions to completion, and the simultaneous separation of the reaction products in only one unit. This reduces or eliminates reactor and recycle costs (Hamodi, 2004).

**Sneesby et al., 1997a** presented continuous mathematical models for reactive distillation of ETBE synthesis from isobutene and ethanol using both Pro II and Speed Up simulation software. Comparison between the two programs shows excellent agreement with each other.

**Quitain et al., 1999a** proposed an industrial scale process for synthesis of ETBE from tert-butanol and simulated using ASPEN PLUS. Their results show that when the reboiler heat duty changed from 700 kW to 1200 kW the conversion increased from 88.5% to 99.9 mole%. There is also a corresponding decrease in flow rate of the residue from 13.4 to 9.9 mol/s.

**Al-Arfaj and Luyben, 2000** explored the effect of number of trays in the rectifying and stripping sections of reactive distillation columns for ETBE and a hypothetical system. They have demonstrated that adding additional trays in a reactive distillation column does not degrade performance, provided the specified degrees of freedom are appropriately chosen.



**Tade and Tian, 2000** showed that the conversion could be inferred from multiple process temperatures. For 10-stages ETBE reactive distillation pilot plant process with six temperature measurements, a third-order nonlinear inferential model was developed using MATLAB software to infer the reactant conversion with sufficiently high accuracy. The two temperatures employed in the model were the bottom reactive section temperature and the reboiler temperature, respectively.

**Al-Arfaj and Luyben, 2002** explored two process configurations for ETBE synthesis: a design with two fresh reactant feed streams and a design with a single mixed reactant feed. Several control structures are investigated. Their results showed that the double feed system requires internal composition control to balance the stoichiometry along with temperature control to maintain product purity, while, the single feed case is effectively controlled with only a temperature controller.

**Li et al., 2003** studied the variation of reflux ratio, reboiler rate, and feed molar ratio of ETOH/IB and their influence on the conversion of IB on ETBE purity. Experimental results showed that higher conversion of IB was obtained with feed molar ratio of 1 to 1.1, reflux ratio 6, and 0.115 m<sup>3</sup>/hr reboiler rates. For these conditions conversion was exceeded 90%.

**Murat et al., 2003** developed an equilibrium simulation model for staged reactive distillation of synthesizing MTBE. The simulation model developed using FORTRAN90 programming language.

**Singh et al., 2004** prepared a biodiesel from vegetable oils and alcohol through transesterification process in the presence of a catalyst. In their study a novel reactor system using reactive distillation techniques was developed and studied for biodiesel preparation from yellow mustard seeds oil.

**Bisowarno et al., 2004** presented a mathematical design model of single and double feed reactive distillation column for ETBE production and investigated the effects of separation and reaction stages on the overall performance. Their results showed that for the single feed column, longer column requires both reflux ratio and reboiler duty to be

adjusted to optimize the ETBE purity, while the increasing of reflux ratio does not reduce the ETBE purity for the shorter column. For the double feed column, increasing reflux ratio does not degrade the column performance.

**Nakkash and Al-Khazraji, 2005** developed a simulation computer programs to analyze multicomponent multistage continuous reactive distillation processes for ideal and non ideal systems. A rigorous method was used to build the simulation programs using FORTRAN program for ethyl acetate production. The influence of various parameters such as feed plate location, reflux ratio, and number of stages were studied upon the performance of continuous reactive distillation.

**Bolun et al., 2006** modeled a process for synthesis of ETBE with ASPEN PLUS simulation package. They observed the input multiplicity for a range of reboiler duty of several values of reflux ratio. These results can be used to avoid the excessive energy consumption and achieve optimum design of reactive distillation column. They found that the best reflux ratio is 5 over a narrow range of reboiler duty (78-83 kW).

**Al-Harhi, 2008** developed a mathematical model for MTBE production via reactive distillation using simulation software Pro II, and then the developed model was used to assess the effect of some critical design and operating parameters on column performance. Also, the effect of feed molar ratio of methanol/isobutene ratio and the number of trays on conversion and selectivity were studied.

**Mohammed M. Z., 2009** developed a steady state model for ETBE and MTBE synthesis using MATLAB program. Liquid composition, vapor composition, and temperature profiles were determined. Also, the residue curve maps were plotted for reacted system and system without reaction.

## 2.4.2 Batch Reactive Distillation Process

Reactive distillation has proved to be an important process alternative to the conventional reactor-separator configuration. Advantages of reactive distillation and flexibility of a batch process can be combined in a batch reactive distillation (Hamodi, 2004). Batch reactive distillation is suitable when the reaction products have lower boiling point temperature than the reactants (Mujtaba, 2004). Therefore, in the present work batch reactive distillation process is considered.

Matouq et al., 1996 synthesized ethyl tert-butyl ether from tert-butanol and ethanol in the presence of different acid catalysts ( $\text{KHSO}_4$ ,  $\text{NaHSO}_4$ ,  $\text{H}_2\text{SO}_4$ , and Amberlyst 15) at low alcohol grade (mixture of 80% mole percent water). The observed mole fraction in the distillate shown in Fig. 2-1.

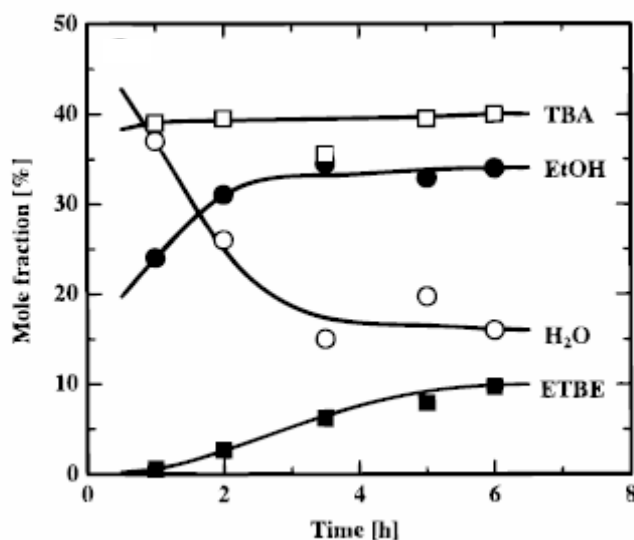


Figure 2-1 Liquid Mole Fraction in the Distillate

Sneesby et al., 1997b presented a dynamic simulation model for ETBE synthesis from isobutene and ethanol. The simulation was developed using Speed Up simulation software, then the system was utilized for the study of transient open-loop responses and control system design.

**Quitain et al., 1999b** synthesized ETBE from tert-butanol. Then, the effect of feed molar ratio of ETOH/TBA and type of catalyst on conversion and was studied. At zero reflux ratio, results show that 53.3 mol% ETBE can be obtained in the distillate and pure water in the residue. Increasing the reflux ratio from 7 to 14 has no significant effect on ETBE (about 60 mol%) in the distillate. The experimental results were compared with results from ASPEN PLUS simulator and showed good agreement.

**Bisowarno and Tade, 2000** used dynamic simulation model to understand the effect of start up policy on the ETBE reactive distillation. This start up policy would results in the targeted ETBE purity within the shortest possible time without using excessive energy.

**Yang et al., 2001** developed a dynamic mathematical model for synthesis of ETBE from tert-butanol using ASPEN PLUS. The model incorporated reaction kinetics. The rapid solution for this model was obtained using Newton-Raphson method. Their simulation results showed good agreement with the literature results.

**Jhon and Lee, 2003** presented dynamic simulation model using MATLAB software for reactive distillation column of 20 stages with ETBE synthesis. A structured and simple iterative algorithm was devised to estimate the vapor flows with the fast convergence under the rigorous energy balance. Both total and partial condensers are considered, and the reactive distillation performance for these condensers was observed. By comparison of their influence on purity of ETBE, total condenser is the better one.

**Assabumrungrat et al., 2004** used the experimental results of packed reactive distillation column for synthesis of ETBE from TBA to validate a simulation model using ASPEN PLUS software. They investigated the effect of various operating parameters such as condenser temperature, feed molar flow rate, reflux ratio, heat duty, and molar ratio of H<sub>2</sub>O: ETOH on the reactive distillation performance.

**Varisli and Dogu, 2005** produced tert-amyl ethyl ether (TAEE) and tert-amyl alcohol (TAA) by simultaneous etherification and hydration of 2-methyl-2-butene in a batch

reactive distillation column. The effect of changing reboiler temperature in the range of (90-124) C° on total conversion was studied.

**Hamza, 2005** studied a batch reactive distillation in packed column for esertification of methanol with acetic acid to produce methyl acetate using sulfuric acid as a homogeneous catalyst. The influence of various parameters such as batch time, reflux ratio, and feed molar ratio of methanol to acetic acid on performance of batch reactive distillation was studied, and the best conditions found are reflux ratio 2, feed molar ratio 2, and batch time 90 min.

**Umar et al., 2008** used a packed reactive distillation column to generate experimental data of ETBE synthesis from TBA. The effect of different key variables on reactant conversion and product purity in distillate was investigated.

In their second paper, **Umar et al., 2009b** studied the experimental synthesis of the same system with different macro porous and gelular ion exchange resin catalyst. Effect of various parameters such as temperature, reactants feed molar ratio, and catalyst loading were studied for optimization of reaction condition.

**Nakkash et al., 2010** presented a batch reactive multistage multi component distillation; rigorous model was used to build the simulation program using MATLAB to solve MESH equations. The validity and accuracy of the developed program model were checked with previous work for methyl acetate production. The influence of various parameters, such as number of stages, batch time and liquid hold up on the performance of batch reactive distillation was studied.

## 2.5 Thermodynamics of Vapor-Liquid Equilibria

The starting point for vapor-liquid equilibria calculations is:

$$\bar{f}_{iL}(x_i, T, P) = \bar{f}_{iv}(y_i, T, P) \quad (2.1)$$

An equation of state can be used to obtain the fugacity in the vapor phase in terms of temperature, pressure, and composition (Orbey and Sandler, 1998).



To relate  $\bar{f}_{iv}$  to temperature, pressure, and mole fraction it is by introducing fugacity coefficient  $\phi_i$ .

$$\phi_i^v \quad (2.2)$$

The fugacity of a component in the liquid phase is related to the composition of liquid phase through the activity coefficient  $\gamma_i$ .

$$\gamma_i = \frac{\bar{f}_{iL}}{x_i f_{iL}(T, P)} \quad (2.3)$$

Where  $f_{iL}(T, P)$  is the fugacity of pure component i as a liquid at the temperature and pressure of mixture (Orbey and Sandler, 1998).

$$f_{iL}(T, P) = f_i^{sat} \exp\left[\frac{1}{RT} \int_{P_i^{sat}}^P v_i dp\right] \quad (2.4)$$

Since  $v_i$ , the liquid-phase molar volume, is a weak function of P at a temperature below  $T_c$ , an approximation is often obtained when  $v_i$  is assumed constant at the value for saturated liquid,  $v_i^L$ .

$$f_{iL}(T, P) = f_i^{sat} \exp\left[\frac{v_i^L (P - P_i^{sat})}{RT}\right] \quad (2.5)$$

Substituting  $f_i^{sat} = \phi_i^{sat} P_i^{sat}$  gives:

$$f_{iL}(T, P) = \phi_i^{sat} P_i^{sat} * \exp\left[\frac{v_i^L (P - P_i^{sat})}{RT}\right] \quad (2.6)$$

Substituting equations (2.6), (2.2) and (2.3) in (2.1)

$$\phi_i^v y_i P = \gamma_i x_i \phi_i^{sat} P_i^{sat} * \exp\left[\frac{v_i^L (P - P_i^{sat})}{RT}\right] \quad (2.7)$$

$$y_i = \frac{\gamma_i x_i P_i^{sat}}{\phi_i P} \quad (2.8)$$

Where  $\phi_i$  is given by equation (2.9)

$$\phi_i = \frac{\phi_i^v}{\phi_i^{sat}} * \exp\left[-\frac{v_i^L (P - P_i^{sat})}{RT}\right] \quad (2.9)$$

At low pressures (up to at least 1 bar), vapor phase usually approximate ideal gas for which  $\phi_i^v = \phi_i^{sat} = 1$  and the exponential term is nearly 1, therefore, equation (2.8) becomes:

$$y_i = \frac{\gamma_i x_i P_i^{sat}}{P} \quad (2.10)$$

### 2.5.1 Fugacity Coefficient Model

Deviations from the ideal gas law can be accounted for by the use of fugacity coefficient  $\phi_i$ . There are several methods could be used in order to determine the vapor fugacity coefficient in pure and vapor mixture as listed in Table 2-1.

**Table 2-1** Equations of fugacity coefficient methods

Methods	Equations
1. Soave-Redlich-Kowng equation (Soave, 1972)	$\phi = \exp\left[\frac{b_k}{b}(Z-1) - \ln(Z-B) - \frac{A}{B}\left(\frac{2\sum_i y_i a_{ik}}{a} - \frac{b_k}{b}\right) \ln\left(\frac{Z+B}{Z}\right)\right]$ <p>Where</p> $a_{ik} = \frac{0.42747R^2Tc^2}{Pc}$ $b_k = \frac{0.08664RTc_k}{Pc_k}$ $Z = \frac{Pv}{RT}, A = \frac{aP}{R^2T^2}, B = \frac{bP}{RT}$ $b = \sum_i y_i b_i$ $a = \sum_i \sum_j y_i y_j a_{ij}$

<p>2. Peng-Robinson equation (Peng and Robinson, 1976)</p>	$\phi = \exp\left[\frac{b_k}{b}(Z-1) - \ln(Z-B) - \frac{A}{2\sqrt{2}B}\left(\frac{2\sum_i y_i a_{ik}}{a} - \frac{b_k}{b}\right) \ln\left(\frac{Z+(1+\sqrt{2})B}{Z+(1-\sqrt{2})B}\right)\right]$ <p>Where</p> $a_{ik} = \frac{0.45724R^2Tc^2}{Pc}$ $b_k = \frac{0.07780RTc_k}{Pc_k}$ $Z = \frac{Pv}{RT}, A = \frac{aP}{R^2T^2}, B = \frac{bP}{RT}$ $b = \sum_i y_i b_i$ $a = \sum_i \sum_j y_i y_j a_{ij}$
<p>3. Van der Waals (Walas, 1985)</p>	$\phi = \exp\left[Z - 1 - \frac{a}{RTv} - \ln\left[Z\left(1 - \frac{b}{v}\right)\right]\right]$ $Z = \frac{Pv}{RT}, a = 3P_c V_c^2, b = V_c / 3$
<p>4. Virial equation (Smith et al., 2001)</p>	$\phi = \exp\left[\frac{Pr}{Tr}(B^\circ + \omega B')\right]$ $B^\circ = 0.083 - \frac{0.422}{Tr^{1.6}}$ $B' = 0.139 - \frac{0.172}{Tr^{4.2}}$

<p>5. Redlich/Kowng Equation (Smith et al., 2001)</p>	$\phi = \exp\left[\frac{b_i}{b}(Z-1) - \ln Z(1-h) + \frac{a}{bRT^{1.5}}\left(\frac{b_i}{b} - \frac{2\sum_k y_k a_{ki}}{a}\right)\right] \ln(1+h)$ $a_{ki} = \frac{0.42748R^2 Tc_{ki}^{2.5}}{Pc_{ki}}$ $b_i = \frac{0.08664RTc_i}{Pc_i}$ $Z = \frac{1}{1-h} - \frac{a}{bRT^{1.5}}\left(\frac{h}{1+h}\right)$ $h = \frac{bP}{ZRT}$ $b = \sum_i y_i b_i$ $a = \sum_i \sum_j y_i y_j a_{ij}$
<p>6. Lee/Kesler Equation (Smith et al., 2001)</p>	$\phi_i = \phi_i^s (\bar{\phi}_i)^w$

### 2.5.2 Activity Coefficient Model

When liquids contain dissimilar species, particularly those who can form or break hydrogen bonds, the ideal liquid solution assumption is invalid and the regular solution theory is not applicable. At moderate pressures, a vapor solution may still be ideal even though the gas mixture does not follow the ideal gas law. Non idealities in the liquid phase can be severing even at low pressures (Seader and Henley, 1998).

Several models can be used to calculate activity coefficients, such as Wilson equation of state, NRTL (Non Random Two Liquid), UNIQUAC (UNIversal QUAsi

Chemical), UNIFAC (UNIQuac Functional Activity Coefficient), and ASOG (Analytical Solution Of Groups) as listed in Table 2-2.

**Table 2-2** Equations of liquid phase activity coefficient methods

Methods	Equations
1. Wilson (Yang and Wang, 2001)	$\ln \gamma_i = -\ln\left(\sum_{j=1}^n x_j \wedge_{ij}\right) + 1 - \sum_{k=1}^n \left(\frac{x_k \wedge_{ki}}{\sum_{j=1}^n x_j \wedge_{kj}}\right)$ $\wedge_{ij} = \frac{v_j}{v_i} \exp\left[-\frac{\lambda_{ij}}{RT}\right], \wedge_{ii} = \wedge_{jj} = \wedge_{kk} = 1$
2. NRTL (Renon and Prausnitz, 1968)	$\ln \gamma_i = \frac{\sum_{j=1}^c \tau_{ij} G_{ij} x_j}{\sum_{k=1}^c G_{ki} x_k} + \sum_{j=1}^c \left[ \frac{x_j G_{ij}}{\sum_{k=1}^c G_{kj} x_k} \left( \tau_{ij} - \frac{\sum_{k=1}^c x_k \tau_{kj} G_{kj}}{\sum_{k=1}^c G_{kj} x_k} \right) \right]$ $G_{ji} = \exp(-\alpha_{ij} \tau_{ij})$ $\tau_{ij} = \frac{g_{ij} - g_{jj}}{RT}, \tau_{ji} = \frac{g_{ij} - g_{ii}}{RT}$
3. UNIQUAC (Abrams and Prausnitz, 1975)	$\ln \gamma_i = \ln \gamma_i^c + \ln \gamma_i^R$ $\ln \gamma_i^c = \ln \frac{\phi_i}{x_i} + \frac{z}{2} q_i \ln \frac{\theta_i}{\phi_i} + l_i - \frac{\phi_i}{x_i} \sum_j X_j l_j$ $\ln \gamma_i^R = q_i \left[ 1 - \ln \left( \sum_j \theta_j \tau_{ji} \right) - \sum_j \frac{\theta_j \tau_{ij}}{\sum_k \theta_k \tau_{kj}} \right]$ $l_i = \frac{z}{2} (r_i - q_i) - (r_i - 1), \quad z=10$

<p>4. UNIFAC (Fredenslund et al., 1975)</p>	$\ln \gamma_i = \ln \gamma_i^c + \ln \gamma_i^R$ $\ln \gamma_i^c = \ln \frac{\phi_i}{x_i} + \frac{z}{2} q_i \ln \frac{\theta_i}{\phi_i} + l_i - \frac{\phi_i}{x_i} \sum_j x_j l_j$ $\ln \gamma_i^R = \sum_k \mu_k^{(i)} (\ln \Gamma_k - \ln \Gamma_k^{(i)})$
<p>5. ASOG (Tochigi and Kojima, 1976)</p>	$\ln \gamma_i = \ln \gamma_i^S + \ln \gamma_i^G$ $\ln \gamma_i^S = 1 + \ln r_i - r_i$ $\ln \gamma_i^G = \sum_k v_{ki} (\ln \Gamma_k - \ln \Gamma_k^{(i)})$

**Quitain and Goto, 1998** measured the liquid phase activity coefficient at 15, 25, and 35 C°. UNIQUAC and NRTL equations are fitted to the experimental data using ASPEN PLUS. Both the experimental and correlated values of the equilibrium compositions are compared with values predicted by UNIFAC method for ETBE-ETOH-H<sub>2</sub>O-TBA system at low TBA concentration. From comparison of experimental and predicted values, it is found that existence of 2.5% TBA in the mixture of ETBE-ETOH-H<sub>2</sub>O decreases ETBE concentration in the organic phase by about 10%. However, concentration of H<sub>2</sub>O in the aqueous phase increases by about 1%.

**Quitain et al., 1999b** used the UNIFAC method for prediction of activity coefficients in the simulation of ethyl tert-butyl ether synthesis from tert-butanol using ASPEN PLUS.

**Yang et al., 2001** determined the liquid phase activity coefficient using Wilson method, and they found that it is suitable to be used for the analysis of ETBE synthesis from tert-butanol.

**Yang and Wang, 2002** reported the vapor-liquid equilibrium data for ETBE-TBA-ETOH-H<sub>2</sub>O system at different temperatures under atmospheric pressure. They were used UNIFAC and Wilson models for prediction of activity coefficients and compare the developed data from the two models with their experimental data. The predicted

vapor-liquid equilibrium of the developed model agreed well with the experimental data, which shows that both models can be used for prediction of VLE for multicomponent system contains water, alcohol, and branched ether.

**Ozbey and Oktar, 2009** performed a detailed thermodynamic analysis of ETBE synthesis reaction between TBA and ethanol. UNIFAC method was used to determine the activity coefficients. Predicted values showed good agreement with experimental results.

## **2.6 Models for Design of Reactive Distillation Columns**

Models of reactive distillation systems are classified into: The equilibrium reactive model (EQ) which adopts an equilibrium stage approach with a reaction rate expression, and the more complex non-equilibrium (NEQ) stage model that takes into account both reaction rates and interface mass and energy transfer fluxes.

Stages in the above models are either a tray or segment of packing. The major objective of the present system is to develop an unsteady state EQ and NEQ (Rate-based) models for packed reactive distillation.

### **2.6.1 Unsteady state EQ Model**

All previous work for unsteady state equilibrium model was discussed in section 2-4-2. The equilibrium model for reactive distillation consists of the conventional **MESH** equations (Lei et al., 2005). The configuration of each EQ segment in the packed tower is shown in Fig. 2-2.



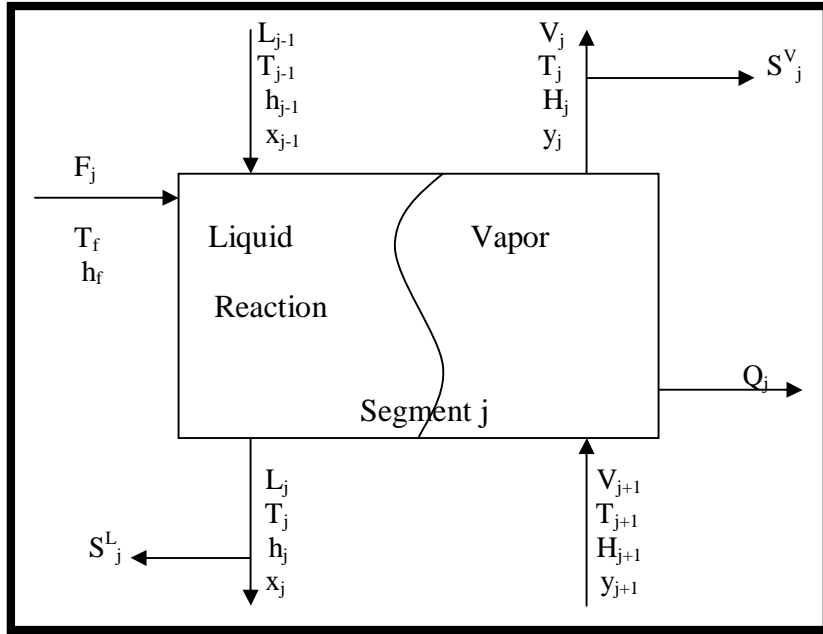


**Figure 2-2** Schematic diagram of EQ segment (Lei et al., 2005).

The **M** equations are the material balance equations. The total material balance takes the form:

$$\frac{dM_j}{dt} = V_{j+1} + L_{j-1} + F_j - (1 - r_j^V)V_j - (1 - r_j^L)L_j + \sum_{k=1}^n \sum_{i=1}^c \nu_{i,k} R_{k,j} \varepsilon_j \quad (2.11)$$

The component material balance (neglecting the vapor hold up) is

$$\frac{dM_j x_{ij}}{dt} = V_{j+1} y_{i,j+1} + L_{j-1} x_{i,j-1} + F_j z_{i,j} - (1 - r_j^V)V_j y_{i,j} - (1 - r_j^L)L_j x_{i,j} + \sum_{k=1}^n \nu_{i,k} R_{k,j} \varepsilon_j \quad (2.12)$$

In the material balance equations given above,  $r_j$  is the ratio of side stream flow to interstage flow:

$$r_j^V = \frac{S_j^V}{V_j}, \quad r_j^L = \frac{S_j^L}{L_j} \quad (2.13)$$

The **E** equations are the phase equilibrium relations

$$y_{i,j} = K_{i,j} x_{i,j} \quad (2.14)$$

Where,  $K_{i,j}$  is the chemical equilibrium constant.

The **S** equations are the summation equations.

$$\sum_{i=1}^c x_{i,j} = 1, \quad \sum_{i=1}^c y_{i,j} = 1 \quad (2.15)$$

The enthalpy balance, **H** equation is given by:

$$\frac{dM_j H_j}{dt} = V_{j+1} H_{j+1} + L_{j-1} h_{j-1} + F_j h_j^F - (1-r_j^V) V_j H_j - (1-r_j^L) L_j h_j - Q_j + R_j H_r \quad (2.16)$$

**R** equations are the reaction rate equations.

### 2.6.2 Unsteady state Rate-Based or Nonequilibrium Model (NEQ)

Distillation operations are better simulated using non equilibrium models that take account of mass and energy transfer (and some times of fluid flow patterns) in a manner that is more rigorous than EQ models (Sundmacher and Kienle, 2002). Schematic diagram of NEQ segment *j* is shown in Fig. 2-3.

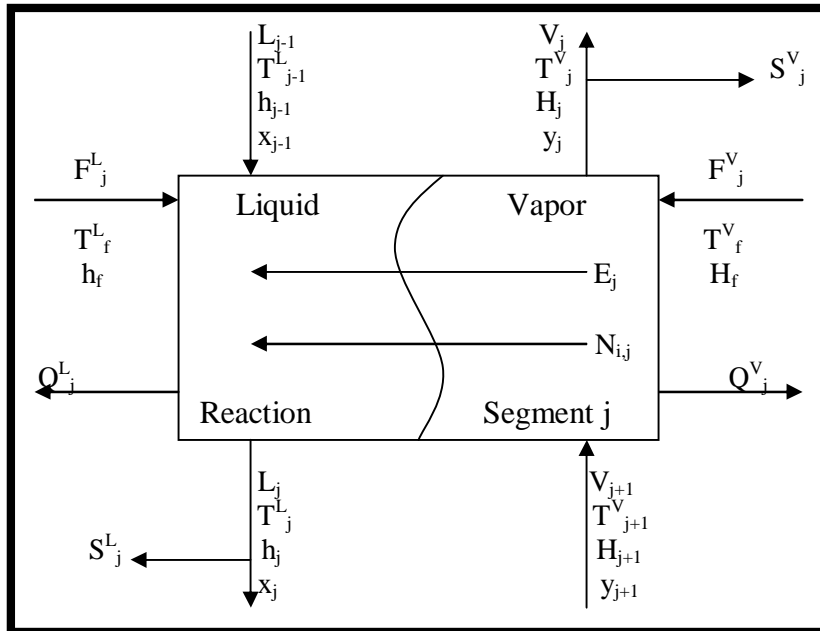


**Figure 2-3** Schematic diagram of NEQ segment *j* (Lei et al., 2005).

In addition, in the NEQ model it is assumed that the resistance to mass and energy transfer is located in a thin film adjacent to the vapor-liquid interface according to the two film theory, as in Fig. 2-4, (Lei et al., 2005).

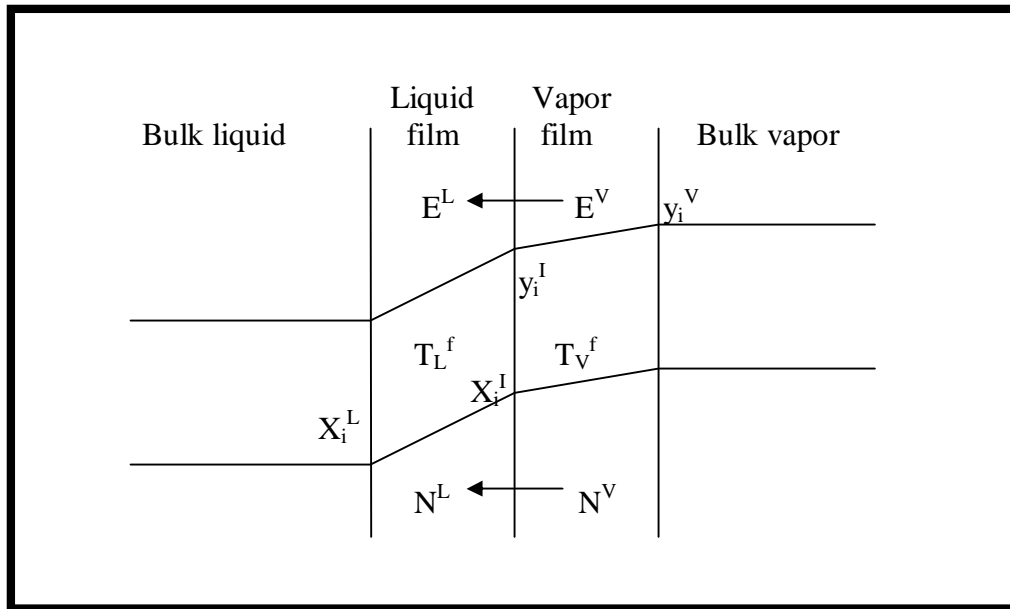


**Figure 2-4** Two-film theory of NEQ segment (Lei et al., 2005).

In the rate-based model, the mass and energy balances around each equilibrium segment are replaced by separate balances for each phase around the segment (Seader and Henley, 1998).

**Sundmacher, and Hoffmann, 1996** presented a detailed three phase non equilibrium model for a packed catalytic distillation column. Then, this model was used for prediction of suitable operating conditions and optimal arrangement of feed streams and packings. Finally, the simulated results were validated by comparison with experimental data obtained from two runs of a laboratory scale MTBE column.

**Podrebarac et al., 1998** developed a steady state rate-based model for the reaction zone of catalytic distillation column of the aldol condensation of acetone to diacetone alcohol (DAA). Their model considered external mass transfer between the liquid phase and the catalyst surface. The model fits the experimental data quite well.

**Higler et al., 1998** proposed a steady state non equilibrium model for simulation of homogeneous reactive distillation. Their calculations were done for process of production ethyl acetate. They found that the reactions could have a significant impact

on component efficiencies, thus emphasizing the need for the rate-based models for RD.

**Higler et al., 1999** developed a generic NEQ model for packed reactive distillation columns. The nonequilibrium model was demonstrated with a case study for production of MTBE. Multiple steady state behaviors were observed when the bottom product flow rate of MTBE was varied. The results of the NEQ model show significant quantitative differences from an EQ model.

**Baur et al., 2000a** compared the EQ and the NEQ stage models for reactive distillation column using two case studies; synthesis of MTBE, and hydration of ethylene oxide (EO) to ethylene glycol (EG). An important conclusion were drawn that the hardware design can have a significant influence on the conversion and selectivity, also, they concluded that for design of RD columns the NEQ model must be adopted.

**Baur et al., 2000b** developed a NEQ cell model to describe the dynamic of RD tray columns, where each stage is divided into a number of contacting cells; these cells describe just a small section of a single tray using three case studies; metathesis of 2-propene in RD column, distillation of methanol-isopropanol-water, and synthesis of MTBE.

**Baur et al., 2001a** proposed a generic, rate-based cell model for reactive distillation tray column. The utility of the developed model is demonstrated by carrying out simulations of a RD column for production of ethylene glycol by hydration of ethylene oxide. They found the introduction of staging in the vapor and liquid phases improves the conversion of EO and also reduces the formation of unwanted di-ethylene glycol.

**Baur et al., 2001b** developed a dynamic rate-based model for reactive distillation column by examining the response of a column for synthesis of MTBE. Also, they emphasized the differences between the dynamic behavior of trayed and random packed columns.

**Peng et al., 2002** compared a steady state EQ and rate-based model for packed reactive distillation column for production of tert-amyl ethyl ether (TAME) and methyl

acetate. Both models yield good agreement with experimental data. The influence of changing reflux ratio, operating pressure, catalyst amount, and heat duty was studied.

**Peng et al., 2003** developed a dynamic rate-based and an equilibrium model for a packed reactive distillation produces TAME. A new approach was proposed to simplify the dynamic rate-based model by assuming that the mass transfer coefficients are time invariant. This approach was demonstrated to be superior to the conventional simplification methods. It can reduce the number of equations by up to two third and still accurately predicts the dynamic behavior.

**Kenig et al., 2004** presented a rigorous rate-based modeling approach to RD equipment in detailed, where the attention was devoted to the mass transfer model, including the reaction in the film region, to the catalyst efficiency determination based on the mass transfer inside the catalyst and to the hydrodynamic models for reactive trays.

**Gomez et al., 2006** proposed a mixed integer nonlinear programming (MINLP) formulation for optimal design of a reactive distillation column based on a generic nonequilibrium model. Catalytic distillation of ethyl tert-butyl ether production from isobutene and ethanol is considered as an illustrative example.

**Kotora et al., 2009** presented a steady state simulation model for catalytic distillation. Computer program was developed to solve the mathematical model using FORTRAN programming language. The described model was verified using experimental data obtained from continuous distillation column equipped with catalytic packing. Comparison of experimental and simulation data was presented for the synthesis of propyl propionate from 1-propanol and propionic acid.

### **2.6.2.1 Rate-Based Model Equations**

Rate-based model equations are the same as EQ model equations but, it is written for each phase separately around each segment (Lei et al., 2005).

Vapor phase component material balance:

$$\frac{dM_{i,j}^V}{dt} = (1 + r_j^V)V_j y_{i,j} - V_{j+1} y_{i,j+1} - F_j^V z_{i,j}^V + N_{i,j}^V \quad (2.17)$$

Liquid phase component material balance:

$$\frac{dM_{i,j}^L}{dt} = (1 + r_j^L)L_j x_{i,j} - L_{j-1} x_{i,j-1} - F_j^L z_{i,j}^L - N_{i,j}^L - \sum_{k=1}^n v_{i,k} R_{k,j} \epsilon_j \quad (2.18)$$

The overall molar balances are obtained by summing equations (2.18) and (2.19) over the total number of components.

$$\frac{dM_j^V}{dt} = (1 + r_j^V)V_j - V_{j+1} - F_j^V + N_j^T \quad (2.19)$$

$$\frac{dM_j^L}{dt} = (1 + r_j^L)L_j - L_{j-1} - F_j^L + N_{j,j}^T - \sum_{i=1}^c \sum_{k=1}^n v_{i,k} R_{k,j} \epsilon_j \quad (2.20)$$

Vapor phase energy balance:

$$\frac{dE_j^V}{dt} = (1 + r_j^V)V_j H_j - V_{j+1} H_{j+1} - F_j^V z_{i,j}^V H_j^{VF} + Q_j^V + e_j^V \quad (2.21)$$

Liquid phase energy balance:

$$\frac{dE_j^L}{dt} = (1 + r_j^L)L_j h_j - L_{j-1} h_{j-1} - F_j^L z_{i,j}^L h_j^{LF} + Q_j^L - e_j^L + R_j Hr \quad (2.22)$$

Summation mole fractions on vapor and liquid phases:

$$\sum_{i=1}^c x_{i,j} = 1 \quad , \quad \sum_{i=1}^c y_{i,j} = 1 \quad (2.15)$$

The interface energy transfer rates  $E^I$  have convective and conductive contributions.

$$E^{I,L} = -h^{I,L} A \frac{dT^{I,L}}{d\eta} + \sum_{i=1}^c N_i^{I,L} H_i^{I,L} \quad (2.23)$$

Where  $h^I$  is the heat transfer coefficient in the liquid phase. A relation analogous to equation (2.23) holds for vapor phase.

At the vapor liquid interface phase equilibrium is assumed:

$$y_{i,j}^I = K_{i,j} x_{i,j}^I \quad (2.24)$$

Continuity of mass and energy have been given as:

$$N^{IV}_i = N^{IL}_i, \quad E^{IV}_i = E^{IL}_i \quad (2.25)$$

For both equilibrium and rate-based models, thermodynamics and physical properties are required. Moreover, in the rate-based model the mass and energy transfer models are also necessary.

## 2.6.2.2 Rate Expressions

### a. Mass Transfer Rate Expression

Mass transfer is a rate process driven by gradients in concentration. Thus, the rate of mass transfer in the vapor phase depends on the difference between the bulk vapor compositions,  $y^V_{i,j}$ , and the vapor compositions at the interface,  $y^I_{i,j}$ , Figure (2.3). Similarly, the rate of mass transfer in the liquid phase depends on the difference between the bulk liquid compositions,  $x^L_{i,j}$ , and the liquid compositions at the interface,  $x^I_{i,j}$  (Krishnamurthy and Taylor, 1985).

The general form of components mass transfer rates across vapor and liquid films respectively, in a packed segment, are as follows, where both diffusive and convective (bulk flow) contributions are included:

$$N_{ij}^V = a_j^I J_{ij}^V + y_{ij} N_j^T \quad (2.26)$$

$$N_{ij}^L = a_j^I J_{ij}^L + x_{ij} N_j^T \quad (2.27)$$

Where,  $a_j^I$  is the total interfacial area of packing. The diffusion fluxes  $J^V_i$  and  $J^L_i$  are given in equations (2.28) and (2.29):

$$J^V_{ij} = C_t^V [k^V] (y_{ij} - y_{ij}^I) \quad (2.28)$$

$$J^L_{ij} = C_t^L [k^L] (x_{ij}^I - x_{ij}) \quad (2.29)$$

In the nonequilibrium stage model of Krishnamurthy and Taylor (1985a), the total mass transfer rates are obtained by combining equations (2.26) and (2.28) and multiplying by the interfacial area available for mass transfer.



$$N_j^V = C_{ij}^V [k_j^V] a_j (y_{ij} - y_{ij}^I) + N_j^{TV} y_{ij} \quad (2.30)$$

Analogous relation can be written for the liquid phase total mass transfer rate.

$$N_j^L = C_{ij}^L [k_j^L] a_j (x_{ij}^I - x_{ij}) + N_j^{TL} x_{ij} \quad (2.31)$$

Seader and Henley (1998), mentioned that it is convenient to determine the matrix  $[k^P]$  from a reciprocal mass transfer coefficient function,  $R$ . For an ideal gas solution:

$$[k^V] = [R^V]^{-1} \quad (2.32)$$

For nonideal liquid solution:

$$[k^L] = [R^L]^{-1} [\Gamma^L] \quad (2.33)$$

Where the elements of  $R^V$  in terms of vapor mole fractions:

$$R_{ii,j} = \frac{y_{ij}}{k_{i,nc} a_j} + \sum_{\substack{k \neq 0 \\ k=1}}^{nc} \frac{y_{k,j}}{k_{ik,j} a_j} \quad (2.34)$$

$$R_{il,j} = -y_{l,j} + \left( \frac{1}{k_{il,j} a_j} - \frac{1}{k_{inc,j} a_j} \right), \quad i \neq 1 \quad (2.35)$$

The previous equations are written for vapor phase (composition  $y$ ) but it can also be written for liquid phase (composition  $x$ ).

Binary elements of matrix of thermodynamic factors in Equation (2.33) were defined by:

$$\Gamma_{ik,j} = \delta_{ik,j} + x_{ij} \left( \frac{\partial \ln \gamma_{i,j}}{\partial x_{k,j}} \right) \quad (2.36)$$

Where  $\delta = 1$  if  $i=k$  and zero if not.

## b. Energy Transfer Rate Expression

The general forms of rates of heat transfer across the vapor and liquid films respectively are (Seader and Henley, 1998):

$$e_j^V = a_j^I h^V (T^V - T^I) + \epsilon_j^V \quad (2.37)$$

$$e_j^L = a_j^I h^L (T^I - T^L) + \epsilon_j^L \quad (2.38)$$

Where  $\epsilon_j^V$  and  $\epsilon_j^L$  are the energy transfer rates due to mass transfer, and can be calculated from the following equations:

$$\epsilon_j^V = \sum_{i=1}^{nc} N_{ij}^L \bar{H}_{ij}^V \quad (2.39)$$

$$\epsilon_j^L = \sum_{i=1}^{nc} N_{ij}^L \bar{H}_{ij}^L \quad (2.40)$$

## 2.6.2.3 Transport Correlations

### a. Mass Transfer Coefficient

Mass transfer models are the basis of nonequilibrium model, and it is possible to change the behavior of a column by selecting different mass transfer correlations (Kooijman, 1995).

**Onda et al., 1968** developed correlations of mass transfer coefficients for gas absorption, desorption, and vaporization in different size of random packings. They stated that these correlations can be applicable for distillation since the distillation process is equimolar counter current diffusion, while the gas absorption or vaporization is unidirectional, but this difference may have little effect on the individual mass transfer coefficients. Also, in gas absorption, it is reasonable to obtain the average film coefficient in a packed column, but in the distillation column it is meaningless, because the temperature and concentration of mixture differ greatly at each point through the column. The vapor phase mass transfer coefficient is obtained from:

$$k^V = A \text{Re}_v^{0.7} \text{Sc}_v^{0.333} (apD^V)(ap * dp)^{-2} \quad (2.41)$$

Where  $A = 2$  if  $dp < 0.012$ , and  $A = 5.32$  otherwise.

The liquid phase mass transfer coefficient is:

$$k^L = 0.0051(\text{Re}_L^I)^{2/3} \text{Sc}_L^{-0.5} (ap * dp)^{0.4} (\mu^L g / \rho^L)^{1/3} \quad (2.42)$$

Where  $\text{Re}_L^I$  is the liquid Reynolds number based on the interfacial area density.

$$\text{Re}_L^I = \frac{\rho^L u^L}{\mu^L a d} \quad (2.43)$$

The interfacial area density,  $ad$ , is computed from:

$$ad = ap[1 - \exp(-1.45(\sigma_c/\sigma)^{0.75} \text{Re}_L^{0.1} \text{Fr}_L^{-0.05} \text{We}_L^{0.2})] \quad (2.44)$$

**Bravo and Fair, 1982** used the correlations of Onda et al., (1968) for the estimation of mass transfer coefficients for distillation in random packings by using an alternative relation for the interfacial area density:

$$ad = 0.498(\text{Ca}_L \text{Re}_v)^{0.392} \sigma^{0.5} H^{-0.4} ap \quad (2.45)$$

Where  $H$  is the height of packed section and  $\text{Ca}_L$  is the capillary number.

$$\text{Ca}_L = a_L \mu_L / \rho^L \sigma \quad (2.46)$$

**Billet and Schultes, 1992** described an advanced theoretical model which is dependent on pressure drop/hold up calculations. The correlations can be used for both random and structured packings. Mass transfer coefficients of liquid and vapor phases are computed from equations (2.47) and (2.48) respectively.

$$k^L = C_l \left( \frac{g \rho_L}{\mu_L} \right)^{1/6} \sqrt{\frac{D^L}{d_h}} \left( \frac{u_L}{ap} \right)^{1/3} \quad (2.47)$$

$$k^V = C_{vl} \left( \frac{1}{\sqrt{\epsilon - h_t}} \right) \sqrt{\frac{a}{d_h}} D^V (\text{Re}_v)^{3/4} (S_{C_v})^{1/3} \quad (2.48)$$

The hydraulic diameter  $d_h$  is given by:

$$d_h = 4 \epsilon / ap \quad (2.49)$$

The interfacial area density  $ad$  is:

$$ad = ap(1.5/\sqrt{ap d_h}) (u_L d_h \rho^L / \mu^L)^{-0.2} (u_L^2 \rho^L d_h / \sigma)^{0.75} (u_L^2 / g d_h)^{-0.45} \quad (2.50)$$

**Al-Zaidi M. D., 2009** estimated the mass transfer coefficient in batch packed bed distillation column for rasching ring packing with 15 mm size, as function of physical properties: vapor to liquid molar rates ratio, relative volatility, ratio of vapor to liquid diffusivities, ratio of vapor to liquid densities, and ratio of vapor to liquid viscosities.

The vapor phase mass transfer coefficient is given by:

$$k_{ov} = 3.29 * 10^{-10} \alpha^{-0.70311} \left(\frac{D^V}{D^L}\right)^{0.64634} \left(\frac{L}{V}\right)^{3.54823} \left(\frac{\rho_V}{\rho_L - \rho_V}\right)^{1.248} \left(\frac{\mu_V}{\mu_L}\right)^{-4.96566} \quad (2.51)$$

$$k_{oL} = 2.8 * 10^{-6} \alpha^{-0.94613} \left(\frac{D^V}{D^L}\right)^{0.031} \left(\frac{L}{V}\right)^{1.1539} \left(\frac{\rho_V}{\rho_L - \rho_V}\right)^{0.07687} \left(\frac{\mu_V}{\mu_L}\right)^{-0.89661} \quad (2.52)$$

## b. Heat Transfer Coefficient

Heat transfer coefficients for the vapor film are estimated from the Chilton-Colburn analogy between heat and mass transfer (Seader and Henley, 1998).

$$h^V = k^V \rho^V C_p^V (Le^V)^{2/3} \quad (2.53)$$

Where  $N_{Le}^V$  is the Lewis number, and it is given by:

$$Le^V = \frac{Sc^V}{Pr^V} \quad (2.54)$$

For the liquid phase:

$$h^L = k^L \rho^L C_p^L (Le^L)^{1/2} \quad (2.55)$$

## **Chapter Three**

### **Theoretical Aspects**

#### **3.1 Introduction**

Unsteady state equilibrium and non equilibrium models for packed reactive distillation column are developed. In this chapter, the equations that are required to solve the equilibrium and the nonequilibrium models are given together with the models parameters.

Then, the detailed solution procedure of the proposed programs in the present work was discussed.

#### **3.2 Simulation of Equilibrium Model**

##### **3.2.1 Equilibrium Model Assumptions**

Consider the batch packed reactive distillation column and the schematic model of  $j$ th segment shown in Fig. 3-1 and 3-2, respectively, the mathematical equilibrium model was formulated using the following assumptions (Peng et al., 2003).

1. Vapor-liquid equilibria is achieved on each segment.
2. Constant pressure drop across the column.
3. Hold-up per segment equal to liquid hold-up on segment (i.e. vapor phase molar hold-up neglected).
4. Walls of column are perfectly insulated, therefore, the heat losses neglected.
5. Reactions take place in liquid phase.
6. Each segment is at physical, mechanical, and thermal equilibrium.

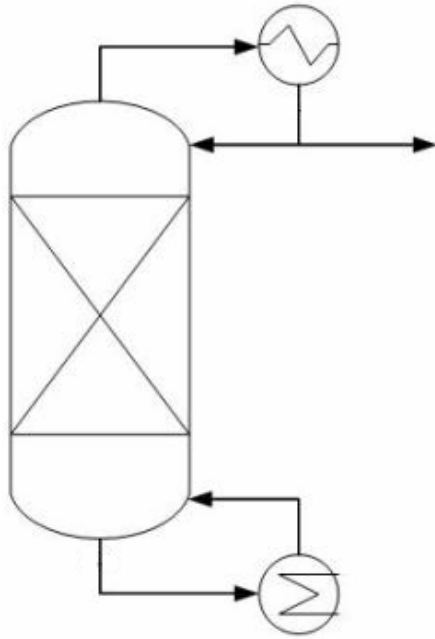


**Figure 3-1** Packed Batch  
RD Column

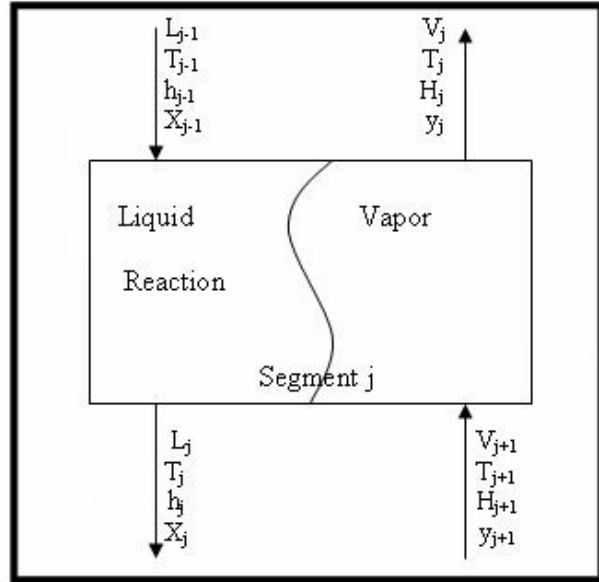


**Figure 3-2** Schematic Diagram of  
EQ Segment

### 3.2.2 Equilibrium Model Equations

Equations that model the equilibrium segment are shown as **MESH**R equations. MESH is an acronym referring to the different types of equations.

**M.** Total and component material balances.

The total material balance in Equation (2.11) and component material balance in Equation (2.12) with no vapor and liquid side streams and no feed stream can be reduced to Equations (3.1) and (3.2) respectively.

$$\frac{dM_j}{dt} = V_{j+1} + L_{j-1} - V_j - L_j + R_j \quad (3.1)$$

$$\frac{dM_j x_{ij}}{dt} = V_{j+1} y_{i,j+1} + L_{j-1} x_{i,j-1} - V_j y_{i,j} - L_j x_{i,j} + R_{i,j} \quad (3.2)$$

**E.** Equilibrium relation

$$y_{i,j} = K_{i,j} x_{i,j} \quad (3.3)$$

### S. Summation equations

$$\sum_{i=1}^c x_{i,j} = 1 \quad , \quad \sum_{i=1}^c y_{i,j} = 1 \quad (2.15)$$

**H.** Enthalpy equation, the energy balance of Equation (2.16) reduced to Equation (3.4) with no side streams and no feed stream.

$$\frac{dM_j H_j}{dt} = V_{j+1} H_{j+1} + L_{j-1} h_{j-1} - V_j H_j - L_j h_j + R_j H_r \quad (3.4)$$

**R.** Reaction rate equations (Umar et al., 2009b)

$$R = M_{cat} \frac{K_1 (a_A a_B - \frac{a_C a_D}{K_{eq}})}{1 + K_w a_D} \quad (3.5)$$

$$K_1 = \exp(3.55 - \frac{2286}{T}) \quad (3.6)$$

$$K_w = \exp(-16.16 - \frac{6636}{T}) \quad (3.7)$$

$$K_{eq} = \exp(-2101.93 - \frac{38672.73}{T} + 411.41 \log T - 1.592T + 1.345 * 10^{-3} T^2 - 5.7517 * 10^{-7} T^3) \quad (3.8)$$

The activity of i-th component was calculated using the following equation:

$$a_i = x_i \gamma_i \quad (3.9)$$

## 3.2.3 Estimation of Equilibrium Model Parameters

### 3.2.3.1 Enthalpy Calculation

Enthalpy of component in liquid phase can be estimated through basing the heat of formation at reference temperature and adding the sensible heat at a desired temperature (Perry and Green, 1997).

$$h_i = \Delta H_{fi}^{298} + \int_{298}^T C_p^L dT \quad (3.10)$$



Values of heat of formation of all components can be found in Appendix A.1. Evaluation of integral in Equation (3.10) requires knowledge of the temperature dependence of heat capacity. This is usually given by:

$$Cp_i^L = a + bT + cT^2 + dT^{-2} \quad (3.11)$$

The constants a, b, c, and d for all components are listed in Appendix A.2. The total enthalpy of liquid phase is given by(Perry and Green, 1997):

$$h_{i,j} = \sum_{i=1}^c x_{i,j} h_i + H_{mix} \quad (3.12)$$

Where  $H_{mix}$  is the heat of mixing, for UNIFAC model heat of mixing is:

$$H_{mix} = RT \sum_{i=1}^c (x_i \ln \gamma_i) \quad (3.13)$$

The enthalpy of component in vapor phase was estimated through the integral of heat capacity in vapor phase at any temperature T with respect to a reference temperature  $T^0$ :

$$\Delta H_V = \int_{T^0}^T Cp_V dT \quad (3.14)$$

Heat capacity of components in the vapor phase is:

$$Cp_i^V = a_v + b_v T + c_v T^2 + d_v T^{-2} \quad (3.15)$$

Constants of heat capacity  $a_v$ ,  $b_v$ ,  $c_v$ ,  $d_v$  are given in Appendix A.3. Total enthalpy of vapor phase is:

$$H_{V,i,j} = y_{i,j} H_i \quad (3.16)$$

Heat of reaction at any temperature can be calculated from heat capacity data if the value for one temperature is known, the tabulation of data can be reduced to the completion of standard heats of formation at a single temperature (Seader and Henley, 1998). The calculation of standard heats of reaction has been given by:

$$Hr^{\circ} = \sum_{i=1}^c v_i H_{fi} \quad (3.17)$$

Where the sign of stoichiometric ratio  $\nu$  is positive for products and negative for reactants.

$$Hr = Hr^\circ + \int_{T^\circ}^T \Delta C p_i^\nu dT \quad (3.18)$$

### 3.2.3.2 Calculation of Liquid Activity Coefficient

Liquid activity coefficients in the present work have been estimated using Wilson, UNIQUAC, and UNIFAC equation of state (EOS). NRTL and ASOG have not been used due to the lack of sets of group parameters for the present system.

#### 3.2.3.2a Wilson EOS

In the Wilson method, the activity coefficient  $\gamma_i$  is expressed as (Yang and Wang, 2001):

$$\ln \gamma_i = -\ln\left(\sum_{j=1}^N x_j \wedge_{ij}\right) + 1 - \sum_{k=1}^N \left(\frac{x_k \wedge_{ki}}{\sum_{j=1}^N x_j \wedge_{kj}}\right) \quad (3.19)$$

Where

$$\wedge_{ij} = \frac{v_j}{v_i} \exp\left[\frac{-\lambda_{ij}}{RT}\right] \quad (3.20)$$

$$\wedge_{ii} = \wedge_{jj} = \wedge_{kk} = 1 \quad (3.21)$$

$\wedge_{ij}$ ,  $\wedge_{ii}$ ,  $\wedge_{jj}$ , and  $\wedge_{kk}$  are Wilson parameters.  $\lambda_{ij}$  is the binary interaction coefficient.

#### 3.2.3.2b UNIQUAC EOS

UNIQUAC (UNIversal QUAsi-Chemical) liquid phase activity coefficient for a species in a multicomponent mixture is obtained (Renon and Prausnitz, 1968):

$$\ln \gamma_i = \ln \gamma_i^c + \ln \gamma_i^R \quad (3.22)$$

$$\ln \gamma_i^c = \ln \frac{\phi_i}{X_i} + \frac{z}{2} q_i \ln \frac{\theta_i}{\phi_i} + l_i - \frac{\phi_i}{X_i} \sum_j X_j l_j \quad (3.23)$$

$$\ln \gamma_i^R = q_i \left[ 1 - \ln \left( \sum_j \theta_j \tau_{ji} \right) - \sum_j \frac{\theta_j \tau_{ij}}{\sum_k \theta_k \tau_{kj}} \right] \quad (3.24)$$

$$r_i = \sum_k \nu_k^{(i)} R_k, \quad q_i = \sum_k \nu_k^{(i)} Q_k \quad (3.25)$$

$$l_i = \frac{z}{2} (r_i - q_i) - (r_i - 1), \quad z=10 \quad (3.26)$$

$$\phi_i = \frac{r_i}{\sum_j r_j x_j}, \quad \theta_i = \frac{q_i}{\sum_j q_j x_j}, \quad \tau_{ij} = -\frac{u_{ij} - u_{jj}}{RT} \quad (3.27)$$

$$u_{11} = \frac{-\Delta U_1}{q_1}, \quad u_{22} = \frac{-\Delta U_2}{q_2} \quad (3.28)$$

$$u_{12} = u_{21} = (u_{11} u_{22})^{1/2} (1 - c_{12}) \quad (3.29)$$

$$\Delta U \cong \Delta H_{vi} - RT, \quad c_{ii} = \frac{\Delta U_i}{V_i^L}, \quad c_{12} = (c_{11} c_{22})^{1/2} (1 - l_{12}) \quad (3.30)$$

Where  $l_{12}$  can be assumed zero because it is very small compared to unity (Reid et al., 1987).  $\Delta H_v$  can be calculated from  $\Delta H_{v2} = \Delta H_{v1} \left( \frac{1 - T_{r2}}{1 - T_{r1}} \right)^n$  where  $\Delta H_{v1}$  is the enthalpy of vaporization at normal boiling point and it is given by Vetere method (Reid et al., 1987).

$$\Delta H_{vb} = RT_C T_{br} \frac{0.4343 \ln P_C - 0.69431 + 0.89584 T_{br}}{0.37691 - 0.37306 T_{br} + 0.15075 P_C^{-1} T_{br}^{-2}} \quad (3.31)$$

### 3.2.3.2c UNIFAC EOS

UNIFAC (UNIQuac Functional-group Activity Coefficient) method depends on the concept that a liquid mixture may be considered as a solution of structural units from which the molecules are formed. These structural units are called subgroups. UNIFAC method can be given by the following equations (Smith et al., 2001):

$$\ln \gamma_i = \ln \gamma_i^c + \ln \gamma_i^R \quad (3.32)$$

Where  $\gamma_i^c$  is the combinatorial term, and  $\gamma_i^R$  is the residual term.

$$\ln \gamma_i^c = 1 - J_i + \ln J_i - 5q_i \left(1 - \frac{J_i}{L_i} + \ln \frac{J_i}{L_i}\right) \quad (3.33)$$

$$\ln \gamma_i^R = q_i \left[1 - \sum_k \left(\theta_k \frac{\beta_{ik}}{S_k} - e_{ki} \ln \frac{\beta_{ik}}{S_k}\right)\right] \quad (3.34)$$

Where:

$$J_i = \frac{r_i}{\sum_j r_j x_j} \quad (3.35)$$

$$L_i = \frac{q_i}{\sum_j q_j x_j} \quad (3.36)$$

$$S_i = \sum_j \theta_m \tau_{mi} \quad (3.37)$$

In addition the following definitions were applied:

$$r_i = \sum_k \nu_k^{(i)} R_k \quad (3.38)$$

$$q_i = \sum_k \nu_k^{(i)} Q_k \quad (3.39)$$

$$e_{ki} = \frac{\nu_k^{(i)} Q_k}{q_i} \quad (3.40)$$

$$\beta_{ik} = \sum_m e_{mi} \tau_{mk} \quad (3.41)$$

$$\theta_k = \frac{\sum_i x_i q_i e_{ki}}{\sum_j x_j q_j} \quad (3.42)$$

$$\tau_{mk} = \exp \frac{a_{mk}}{T} \quad (3.43)$$

Subscript i identify species, and j is a dummy index running overall species. Subscript k identifies subgroups, and m is a dummy index running overall subgroups. The quantity of  $\nu_k^{(i)}$  is the number of subgroups of type k in a molecule of species i

(Smith et al., 2001). Values of subgroup parameters  $R_k$  and  $Q_k$  and of the group interaction parameters  $a_{mk}$  are listed in Appendix A.4

### 3.2.3.3 Activity Coefficient Models Results

Three equations of state were used to calculate the activity coefficient. Wilson, UNIQUAC, and UNIFAC models and programs have been developed using MATLAB (R2009b) software for the present system to calculate the activity coefficients of components for any feed composition and temperature. Wilson and UNIFAC programs results were checked with results of previous work of (Yang and Wang, 2002) and the comparison shows a good agreement, Appendix A.5. UNIQUAC results were checked with the results of Wilson and UNIFAC, and the comparison shows that the activity coefficients calculated by UNIQUAC method deviated from that calculated by Wilson and UNIFAC Table 3-1. Wilson, UNIQUAC, and UNIFAC programs written in MATLAB language given in Appendix A.6.

**Table 3-1** Comparison of Methods of Activity Coefficient

1. For temperature=346.33 K, $x_{\text{ETOH}}=0.3305$ , $x_{\text{TBA}}=0.1569$ , $x_{\text{ETBE}}=0.1015$ , $x_{\text{H}_2\text{O}}=0.4111$ .				
Activity coefficient	$\gamma_{\text{ETOH}}$	$\gamma_{\text{TBA}}$	$\gamma_{\text{ETBE}}$	$\gamma_{\text{H}_2\text{O}}$
Wilson method	1.0714	1.2846	2.2390	1.7513
UNIQUAC method	1.0505	0.9146	0.8453	1.1440
UNIFAC method	1.1034	1.2083	2.9552	2.0284
2. For temperature=348.83 K, $x_{\text{ETOH}}=0.4034$ , $x_{\text{TBA}}=0.2547$ , $x_{\text{ETBE}}=0.0612$ , $x_{\text{H}_2\text{O}}=0.2807$ .				
Activity coefficient	$\gamma_{\text{ETOH}}$	$\gamma_{\text{TBA}}$	$\gamma_{\text{ETBE}}$	$\gamma_{\text{H}_2\text{O}}$
Wilson method	0.9952	1.1480	1.7195	2.0996
UNIQUAC method	1.0270	0.9362	0.8646	1.1493
UNIFAC method	1.0505	1.1092	2.6284	2.3109

3. For temperature=351.7 K, $x_{\text{ETOH}}=0.1540$ , $x_{\text{TBA}}=0.1608$ , $x_{\text{ETBE}}=0.0126$ , $x_{\text{H}_2\text{O}}=0.6726$ .				
Activity coefficient	$\gamma_{\text{ETOH}}$	$\gamma_{\text{TBA}}$	$\gamma_{\text{ETBE}}$	$\gamma_{\text{H}_2\text{O}}$
Wilson method	1.4402	2.0929	3.1645	1.2539
UNIQUAC method	1.1909	0.9064	0.8759	1.0899
UNIFAC method	1.4830	2.0101	7.3765	1.4235

UNIFAC method was used in the present work for equilibrium and rate-based model programs because UNIFAC parameters are independent of temperature, and the binary interaction parameters are available for a wide range of functional groups and also the UNIFAC results agreed with the previous work of Yang and Wang (2002) more than the agreement with Wilson method.

### 3.2.3.4 Calculation of Vapor Fugacity Coefficient

Virial truncated to second term and Lee-Kesler equations of state have been used for evaluating the fugacity coefficients of components.

#### 3.2.3.4a Virial EOS

Vapor phase activity coefficient using virial equation for a species is obtained by:

$$\phi = \exp\left[\frac{Pr}{Tr}(B^\circ + \omega B')\right] \quad (3.44)$$

$$B^\circ = 0.083 - \frac{0.422}{Tr^{1.6}} \quad (3.45)$$

$$B' = 0.139 - \frac{0.172}{Tr^{4.2}} \quad (3.46)$$

Virial program has been developed using MATLAB (R2009b) software for the present system. Results show that the vapor fugacity coefficient is nearly equal to 1 (i.e. ideal gas) (Appendix A.7).

### 3.2.3.4b Lee-Kesler EOS

Generalized correlations by Lee/Kesler have been used for evaluating the component fugacity coefficient in vapor phase, which is generally used for all components with respect to their reduced temperature and pressure.

$$\phi_i = \phi_i^\circ (\bar{\phi}_i)^w \quad (3.47)$$

The quantities of  $\phi_i^\circ$  and  $(\bar{\phi}_i)$  are taken from tables established by Lee-Kesler correlation as a function of reduced temperature and reduced pressure. Results show that the vapor fugacity coefficients are nearly 1 which means that the gas phase is approximately ideal gas (Appendix A.8).

### 3.2.3.5 Vapor Pressure Calculation

The vapor pressure of each component for the present system was calculated using Antoine equation (Walas, 1985, Yang et al., 2001).

$$\ln P^{sat} = A1 + \frac{A2}{T + A3} + A4 * T + A5 \ln T + A6 * T^{A7} \quad (3.48)$$

Where vapor pressure  $P^{sat}$  in Pa and T in Kelvin. Parameters of Antoine equation for all components are given in Appendix A.9.

### 3.2.3.6 Bubble Point Calculation

Temperatures of segments have been calculated using iterative procedure of bubble point until the summation in Equation (3.49) equals to one.

$$\sum_{i=1}^m (K_{ij} x_{ij}) = 1 \quad (3.49)$$

Where K is the distribution coefficient and it can be calculated using:

$$K = \gamma_i \frac{P^{sat}}{P} \quad (3.50)$$

### 3.2.3.7 Holdup

The liquid holdup in a packed column is defined as the volume of liquid held under operating conditions per volume of packed bed. This holdup can be divided into two portions, the static and the dynamic (or operating) holdup. The static holdup consists of the liquid kept in the voids or dead spaces of the packing, while the dynamic portion flows down the column. The static holdup is influenced by the physical properties of the liquid and the packing surface but is independent of the liquid load. The static holdup is normally of no great significance in packed columns. The dynamic holdup is primarily a function of the liquid velocity (Wagner et al, 1997). Kister (1992) mentioned that Mackowiak (1991) evaluated liquid holdup predictions from several recent correlations. His evaluation selected a simplified version of the Mersmann and Deixler (1986) correlation over alternative methods and demonstrated that it fitted experimental holdup data to within  $\pm 20$  to 25 percent, and it has been extensively tested for random packing, the hold up correlations is given by:

$$M = \frac{1}{12\varepsilon} \left( \frac{\mu_L}{\rho_L} \right)^{1/6} (u_L a_P)^{0.5} \quad (3.51)$$

The holdup in reboiler based on the initial charge to the reboiler ( $M^\circ$ ) and it is given by (Seader and Henley, 1998):

$$M_{N_{t+1}} = M^\circ_{N_{t+1}} - \sum_{j=0}^{N_t} M_j - \int_0^t D_t dt \quad (3.52)$$

### 3.2.3.8 Physical Properties

All physical properties required for solving the equilibrium model such as density, latent heat, molecular weight, critical temperature, critical pressure, and boiling point of all components in the present system are listed in Appendix A.10.



### 3.2.4 Solution Procedure of the Equilibrium Model

A computer program to solve the MESH equations has been developed using MATLAB (R2009b) to determine the composition of components, segment temperatures, condenser and reboiler duties, liquid and vapor flow rates along stages, and reaction rate profile.

The program begins with specifying all parameters that consist of number of stages, reflux ratio, total pressure, feed compositions, distillate rate, batch time, step time, and mass of catalyst, as well as all physical properties of components. Time and temperature loops were started, respectively over all stages. The temperature of each stage has been calculated by trial and error until the equilibrium relation is applicable.

The new segment temperatures have been used in calculation of reaction rate, enthalpies of vapor, liquid and mixing. Then liquid and vapor flow rates were calculated by total material and energy balances. A tridiagonal matrix was used to find the component compositions by solving the MESH equations, solving the matrices by eigen value, and normalizing the new compositions for each component. New sets of composition are obtained with the previous procedure for each step time of the batch time. When the compositions at different times are evaluated the program ended and the results plotted.

Equilibrium model variables and equations as well as their numbers are listed in Table 3-2. Block diagram of the equilibrium model is given in Appendix A.11.

**Table 3-2** Variables and Equations of Equilibrium Model

Variable	Equation	Number
$V_{j+1}$	(3.4)	1
$L_j$	(3.1)	1
$y_{i,j+1}$	(3.3)	C

$x_{i,j}$	(3.2)	C
$H_{j+1}$	(3.14)	1
$h_{i,j}$	(3.10)	1
$T_j$	(3.49)	1
$M_j$	(3.51)	1
$M_{Nt}$	(3.52)	1
Total		2C+7

### 3.3 Simulation of Rate-Based or Non Equilibrium Model

#### 3.3.1 Rate-Based Model Assumptions

The rate-based model is more complicated than the equilibrium model. In the rate-based model, the design information of the column configuration must be specified so that the mass transfer coefficients, interfacial areas, liquid hold-ups can be calculated. The packed reactive distillation column is vertically divided into a number of segments. Schematic model of j-th non equilibrium segment is shown in Fig. 3-3. The following assumptions were made to simplify the model (Peng et al., 2003).

1. Each phase is perfectly mixed in each segment.
2. Vapor-liquid equilibrium is only assumed at the interface.
3. The segments are in mechanical equilibrium  $P_j^V = P_j^L = P_j$ .
4. Mass and energy transport are from vapor phase to liquid phase.
5. The walls of column are perfectly insulated; therefore, the heat losses can be neglected.
6. Hold-up per segment equal to liquid hold-up on segment (i.e. vapor phase molar hold-up neglected).

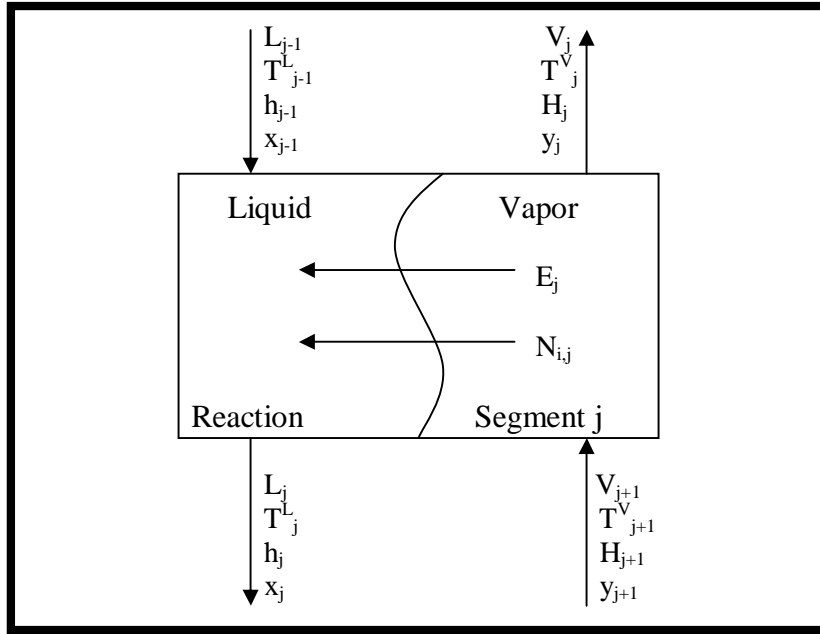


**Figure 3-3** The Non Equilibrium Segment

### 3.3.2 Non Equilibrium Model Equations

Non equilibrium model equations consist of material balance, energy balance, summation equations, equilibrium relation at the interface, and interface energy transfer for each phase. Component material balances for vapor and liquid phase in Equation (2.17) and (2.18) with no feed streams, no vapor and liquid side streams are reduced to Equation (3.53) and (3.54), respectively for the present work.

$$\frac{dM_{i,j}^V}{dt} = V_j y_{i,j} - V_{j+1} y_{i,j+1} + N_{i,j}^V \quad (3.53)$$

$$\frac{dM_{i,j}^L}{dt} = L_j x_{i,j} - L_{j-1} x_{i,j-1} - N_{i,j}^L - R_{i,j} \quad (3.54)$$

Total material balances in Equations (2.19) and (2.20) are reduced for the following:

$$\frac{dM_j^V}{dt} = V_j - V_{j+1} + N_j^T \quad (3.55)$$

$$\frac{dM_j^L}{dt} = L_j - L_{j-1} + N_{j,j}^T - R_j \quad (3.56)$$

Also, Equations (2.21) and (2.22) with no heat losses, no side and feed streams are:

$$\frac{dE_j^V}{dt} = V_j H_j - V_{j+1} H_{j+1} + e_j^V \quad (3.57)$$

$$\frac{dE_j^L}{dt} = L_j h_j - L_{j-1} h_{j-1} - e_j^L + R_j H_r \quad (3.58)$$

Where  $e_j^V$  and  $e_j^L$  are given by:

$$e_j^V = a_j^V h^V (T^V - T^I) + \epsilon_j^V \quad (3.59)$$

$$e_j^L = a_j^L h^L (T^I - T^L) + \epsilon_j^L \quad (3.60)$$

And:

$$\epsilon_j^V = \sum_{i=1}^{nc} N_{ij}^L \bar{H}_{ij}^V \quad (3.61)$$

$$\epsilon_j^L = \sum_{i=1}^{nc} N_{ij}^L \bar{H}_{ij}^L \quad (3.62)$$

Summation equations:

$$\sum_{i=1}^c x_{i,j} = 1 \quad , \quad \sum_{i=1}^c y_{i,j} = 1 \quad (2.15)$$

The interface energy transfer on vapor and liquid phases are:

$$E^{I,V} = -h^{I,V} A \frac{dT^{I,V}}{d\eta} + \sum_{i=1}^c N_i^{I,V} H_i^{I,V} \quad (3.63)$$

$$E^{I,L} = -h^{I,L} A \frac{dT^{I,L}}{d\eta} + \sum_{i=1}^c N_i^{I,L} H_i^{I,L} \quad (3.64)$$

Vapor-liquid equilibrium equation at the interface:

$$y_{i,j}^I = K_{i,j} x_{i,j}^I \quad (3.65)$$

### 3.3.3 Estimation of Non Equilibrium Model Parameters

Non equilibrium model parameters such as enthalpy, activity coefficient, fugacity coefficient, vapor pressure, liquid holdup, and bubble point calculation are the same of the equilibrium model given in section (3-2-3). Non equilibrium model requires other parameters over the equilibrium model such as rate of mass and energy transfer which were shown in details in chapter two. The mass transfer coefficient used in calculation of mass transfer rate is that given by Bravo and Fair, (1982) which is based on the correlations of Onda et al. (1968), both are for different size of packing. The calculation of mass transfer coefficients required the calculation of diffusivities. The binary diffusivity in concentrated liquid mixture is (Gomez et al., 2006):

$$D_{ik,j}^L = (D_{ik,j}^0)^{x_{ij}} (D_{ki,j}^0)^{x_{kj}} \quad (3.66)$$

The estimation of diffusion coefficients in dilute liquid mixtures is given by:

$$D_{ik,j}^0 = 117.4 * 10^{-8} \frac{(\varphi_k M_k)^{1/2} T_j^L}{\mu_{kj}^L \nu_i^{0.6}} \quad (3.67)$$

Diffusivity of vapor mixture is:

$$D_{ik,j}^V = 1.013 * 10^{-2} (T_j^V)^{1.75} \frac{\sqrt{[M_i + M_k] / M_i M_k}}{P[\sqrt[3]{\nu_i} + \sqrt[3]{\nu_k}]^2} \quad (3.68)$$

Other physical properties used in the non equilibrium model of vapor phase, and liquid phase for pure components and mixture are given in Appendix B.

### 3.3.4 Solution Procedure of the Rate-Based Model

In order to solve the NEQ model equations, a computer program using MATLAB (R2009b) has been developed to show the liquid and vapor mole fractions, interface, vapor and liquid temperatures, reaction rate profile, liquid and vapor enthalpies, liquid and vapor flow rates along stages, mass and energy transport rates for both phases, and total mass transfer flux.

The rate-based model program begins like the equilibrium program by specifying the model specifications, but in the rate-based model packing size and dimensions is also introduced in order to be used later in calculation of interfacial area and the mass and heat transfer coefficients. To simplify the model initial guesses for temperatures, vapor and liquid mole fractions are given, which is the results of the equilibrium model, also as initial guess the interface mole fractions are set equal to the liquid bulk mole fractions and the reaction rate initialized by zero which is the same assumptions used by Kooijman and Taylor in designing the non equilibrium part of ChemSep software (Kooijman and Taylor, 1995).

When all the specifications are given and the initial guesses are introduced to the program, a time loop starts over all stages, and the vapor and liquid flow rates are calculated using the total material balances on vapor and liquid phases respectively. Then the component material balances have been solved with the tridiagonal matrix, solving the matrices with eigen value and normalizing the new mole fractions for each phase separately. Equilibrium relation at the interface has been then used in determination of the temperature at the interface, when the summation of vapor interface mole fractions equal to 1, the temperatures of all stages are taken as the interface temperatures. The condenser and reboiler were treated as equilibrium segments therefore, their temperatures of liquid and vapor are taken equal to their interface temperatures. Calculation of mass transfer coefficients, heat transfer coefficients, and mass transfer fluxes for both phases comes next. Then, stages temperatures are estimated for each phase using the phase energy balance. Finally, reaction rate and interface mole fraction are calculated. When the iteration of time loop ended the model results are plotted. Non equilibrium model variables, equations and their numbers are listed in Table 3-3. Block diagram of the rate-based model program are given in Appendix B.7.

**Table 3-3** Variables and Equations of the Non Equilibrium Model

Variable	Equation	Number
$V_{j+1}$	(3.55)	1
$L_j$	(3.56)	1
$y_{i,j+1}$	(3.53)	C
$x_{i,j}$	(3.54)	C
$y_{i,j+1}^I$	(3.65)	C
$x_{i,j}^I$	(2.31)	C
$H_{j+1}$	(3.17)	1
$h_{i,j}$	(3.13)	1
$T_j^I$	(2.15)	1
$T_j^L$	(3.58)	1
$T_j^V$	(3.57)	1
$N_{ij}^L$	(2.27)	C
$N_{ij}^V$	(2.26)	C
$M_j$	(3.51)	1
$M_{Nt}$	(3.52)	1
Total		7C+9

## **Chapter Four**

### **Experimental Work**

#### **4.1 Introduction**

In this chapter, the description of experimental work is considered. First bench experiments were carried out in order to select the best catalyst to work with. In bench experiments three catalysts were used; Zeolit (13X), potassium hydrogen sulfate  $\text{KHSO}_4$ , and sulfuric acid  $\text{H}_2\text{SO}_4$ , these catalysts are the available in the local Iraqi markets. Full description of reactive distillation column unit, experimental measurements, operating and experimental procedure and the effect of different variables were studied.

#### **4.2 Bench Experiment**

Bench experiment to produce ETBE was carried out in a batch reactor, consists of 250ml two-necked round flask one neck handle thermometer and the other handling stirrer. Heat was supplied by a jacketed heating mantle with a constant heat duty of 220 W. 60 ml of ethanol and tert-butanol has been mixed with a measured amount of catalyst, and the mixture was introduced to the flask, stirred, and heated to a temperature of  $75\text{ C}^\circ$ , three types of catalyst have been used (Zeolite (13X),  $\text{KHSO}_4$ , and  $\text{H}_2\text{SO}_4$ ). After a certain time a sample was taken and analyzed using Gas Chromatography.

#### **4.3 Reactive Distillation Unit Description**

Laboratory scale packed batch reactive distillation unit has been constructed to perform the present work. A photographic picture and schematic sketch are illustrated in Figures 4-1 and 4-2, respectively.

The unit consists of a still pot (C), which is heated using heating mantle (B) having different heat duties. The distillation column is located above the still pot, and packed



with rasching ring. At the top of column, a double pipe condenser is connected, which is used to condense the vapor leaving the top of column. Part of condensate returns back to the distillation column and the other was drained with a constant reflux ratio.

### **4.3.1 The Main Column**

The distillation column is made of a heat resistance glass column. To avoid the heat loss, the column was insulated with rubber insulation. Insulation efficiency was checked by operating the column on pure water distillation by checking the top and bottom temperatures Appendix C.1. The main column is 70 cm total height which is equivalent to 7 theoretical stages according to height equivalent theoretical plates (HETP), the calculation is given in Appendix C.2. The main column is divided into three sections, upper, intermediate, and lower section. The heights of the three sections are 21, 28, and 21 cm respectively.

The inside diameter of column is 3.5 cm, packed with glass rasching ring of 10 mm length, 6 mm outside diameter, and 3 mm inside diameter. The column dimensions were checked with Assabumrungrat et al., 2004.

### **4.3.2 The Still Pot**

The still pot consists of a three neck-round flask connected to the distillation column through its central opening. The other two openings were connected to a thermometer to measure the bottom temperature (vapor temperature), and a line for recycling a portion of solution in the distillate. Heat for still pot was supplied by a jacketed heating mantle (made in England); its heat duty can be controlled using an electrical controller. Heat duties are 65, 90, and 146 W. The actual readings of heating mantle power (actual heating rate) were calibrated using pure water to find the actual amount of heat gained by the still content Appendix C.3.



**Figure 4-1** Photographic Picture of RD Unit

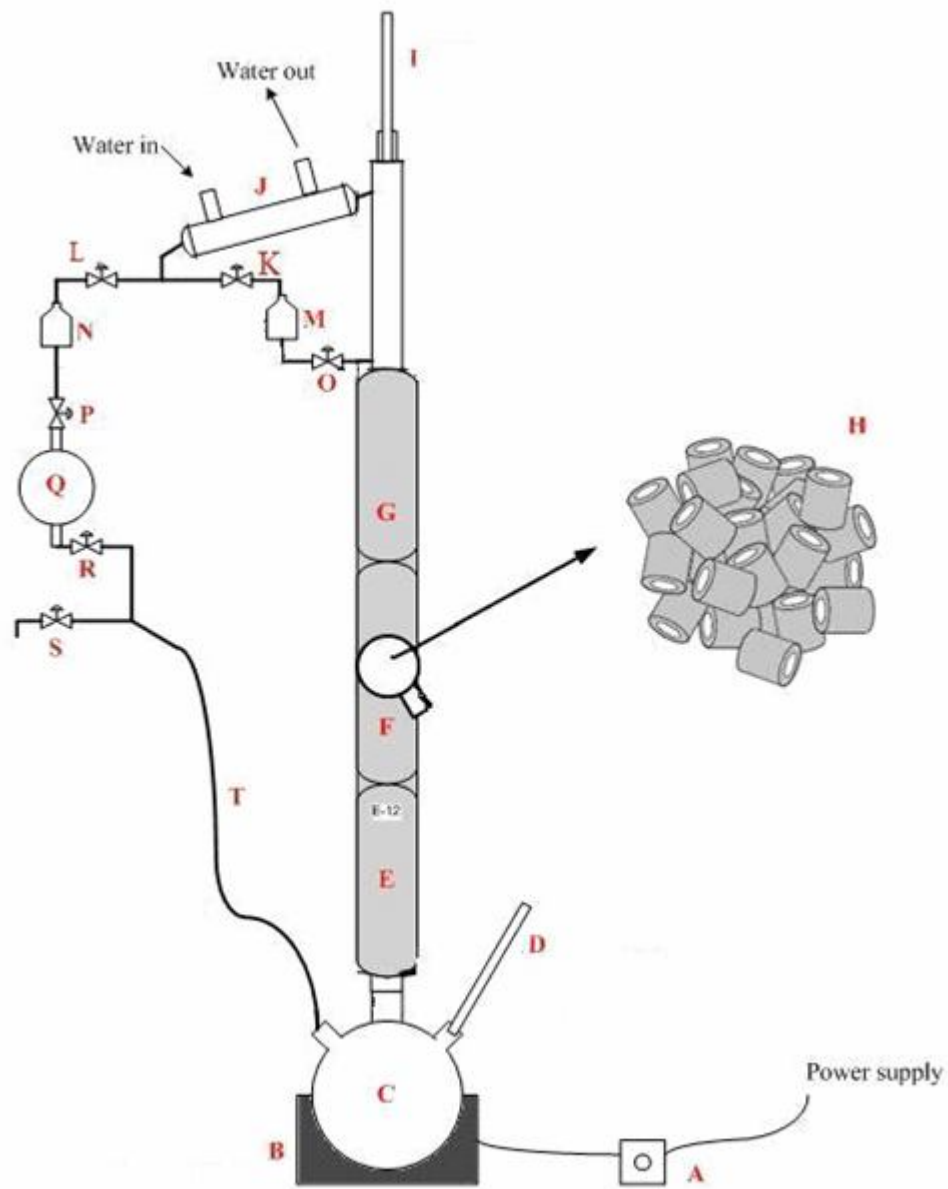


**Figure 4-2** Schematic Sketch of RD Unit

- A:** Heat duty controller; **B:** Heating mantle; **C:** Still pot; **D:** Bottom thermometer,  
**E:** Lower distillation column section; **F:** Intermediate distillation column section  
**G:** Upper distillation column section; **H:** Rasching ring; **I:** Top thermometer  
**J:** Condenser; **K, L, O, P:** Reflux valves; **M:** Container; **N:** Container,  
**Q:** Collecting vessel; **R:** Valve; **S:** Valve; **T:** Recycle line

### **4.3.3 The Condenser**

The upper part of distillation column was connected to a double pipe condenser. Water at room temperature was circulated counter currently through the external pipe of condenser to condense the vapor out from the upper part of distillation column totally.

A portion of condensate returns back to the distillation column and the other was drained with a constant reflux ratio. Both portions of condensate were passed through graduated containers before reaching the column and the collecting vessel.

The desired reflux ratio is calculated by the ratio of the amount of liquid distillate in M container to the amount of liquid distillate in N container. The level of distillate can be adjusted using four valves K, L, O, and P. The liquid distillate is collected in the collecting vessel Q.

### **4.3.4 Experimental Measurements**

Two measurements were obtained during the experiments; temperature and composition measurements.

#### **4.3.4a Temperature Measurement**

Bottom and top temperatures were measured using two mercury thermometers. Bottom temperature was measured by a thermometer connected to the still pot to measure the vapor temperature, and the top temperature was measured with a thermometer connected to the upper end of distillation column to measure the temperature of vapor before passing to the condenser.

The actual readings of the two thermometers were calibrated using boiling water and ice, both gave low errors compared with the boiling and freezing points of water Appendix C.4.

### **4.3.4b Composition Measurement**

In each run of the present experimental work, samples were taken from the distillate, every 1 hour and one sample from the residue at the end of experiment.

These samples were analyzed using Gas Chromatography (GC). The major advantage of GC over other separation techniques is the high selective ability to separate volatile components from the mixture. Analysis and samples were carried out in Iben Sina Company / Ministry of Industry and Minerals. The type of GC was Shemadzu-14A, porpak Q column. The temperatures of detector, injector, and oven were 250 C°, 225 C°, and 180 C° respectively. Helium gas (He) of high purity was used as the carrier gas with flow of 20 ml / min.

## **4.5 Operating Procedure**

Operating of batch reactive distillation column can be conveniently described in three parts:

1. Start-up period.
2. Production period.
3. Shutdown period.

Following sections describe briefly each of these operations for a conventional batch distillation column.

### **4.5.1 Start-up Period**

In practice, an empty conventional batch column is started-up in the following sequence:

1. The still (C) was charged with 10 moles of reactant mixture and a desired amount of catalyst.
2. The cooling water of condenser was turned on.

3. Heat supplied to still (C) at constant rate to bring the still contents to its boiling point temperature. A part of material in the still is vaporized and the vapor travels upward through the packings until reaches the condenser (J).
4. The reflux valves K and O were opened while L was closed when the condensed liquid collected.
5. The liquid begins to flow into the column and falls down through the packed column until the still was reached.
6. The column was run at total reflux operation until a steady state condition was reached; this takes approximately 1 hr in the present work. The steady state condition is reached when the top temperature remains unchanged with time.

#### **4.5.2 Production Period**

Generally, the production period was start when the removal of distillate from the process is started. This period can be operated under the following conditions:

1. The total reflux start-up period was ended when the unit reaches its steady state conditions. Product was collected at specified constant reflux ratio.
2. Samples from distillate product were withdrawn at intervals of 1 hr for six hours.

#### **4.5.3 Shutdown Period**

At the end of production period, a batch reactive distillation column can be shutdown in the following sequence:

1. Heat supply to the column was cut-off.
2. The cooling water of the condenser was turned off after 15 min on the heating off.

## **4.6 Experimental Procedure**

### **4.6.1 Reactive Still**

Measured amounts of reactants were introduced to the still pot together with a desired amount of catalyst ( $\text{KHSO}_4$ , or  $\text{H}_2\text{SO}_4$ ). Cooling water of condenser is started and heat to the still pot is supplied. In this case reaction takes place in the still between ethanol and tert-butanol then ethyl tert-butyl ether and water produced. Water has the highest boiling point among the still contents; therefore, during the distillation water accumulates in the still and little amount reaches the condenser. Samples were taken from the distillate each hour starting at the second hour because the amount of ETBE produced in the first hour is very small according to the literatures of Assambrungrat et al., (2004), Umar et al. (2008), and Umar et al., (2009a). In this case the studied variables considered are:

#### **4.6.1 a Feed Molar Ratio (FMR)**

Feed molar ratio (FMR) of ethanol to tert-butanol, (1:1, 2:1, 4:1). In practical purposes, one reactant is fed in excess to the limiting reactant to get maximum conversion of limiting reactant, therefore stoichiometric amounts of ETOH: TBA was used then doubles the amount of ethanol to 2:1 and 4:1.

#### **4.6.1 b Reflux Ratio**

In the first experiment, total reflux is considered with FMR of 1:1 to compare the experimental result with previous work of Matouq et al., (1996) which produces ETBE from tert-butanol and ethanol using batch reactive distillation with six plates, FMR of 1:1 and total reflux condition. Comparison with previous work was considered in details in chapter five. Then to find the best FMR the same conditions of the first experiment were used with feed molar ratio of ethanol: tert-butanol of 2:1 and other experiment with FMR 4:1. Table 4-1.

**Table 4-1** Studied Operating Conditions for Changing FMR

No.	Reflux ratio	FMR	Heat duty	Initial water content	Catalyst used
1	Total	1:1	146 W	95%	KHSO <sub>4</sub>
2	Total	2:1	146 W	95%	KHSO <sub>4</sub>
3	Total	4:1	146 W	95%	KHSO <sub>4</sub>

To find the effect of changing the reflux ratio on purity of ETBE reflux ratios of (3, 4, and 5) were considered, these ratios were taken according to the available operating conditions of the present experimental unit. Table 4-2.

#### **4.6.1 c Boiler Heat Duty**

Boiler heat duties, (65, 90, and 146W), the first value was the minimum operating heat duty of the present heating mantle and the last is the maximum value. Table 4-2.

#### **4.6.1 d Type of Catalyst**

Potassium hydrogen sulfate KHSO<sub>4</sub>, and sulfuric acid H<sub>2</sub>SO<sub>4</sub> are used as homogenous catalysts in the present work according to their availability in the local Iraqi market, and their success to produce ETBE in the bench experiment. For the same operating conditions experiments were carried out with different catalysts, Table (4.2). Comparisons are given in chapter five.

#### **4.6.1 e Catalyst Amount**

The amount of catalyst used was about 0.04 kg catalyst per 1kg bulk reactant (Assambrungrat et al., 2004). For higher catalyst concentration lower hold up times were required for a given conversion (Hamza, 2005). Therefore, the last experiment was carried out using KHSO<sub>4</sub> with three times the amount of KHSO<sub>4</sub> in the other experiments. Table 4-2.



**Table 4-2** Studied Operating Conditions for the Present Experimental Work

No.	Reflux ratio	FMR	Heat duty	Initial water content	Catalyst used
1	5	1:1	146 W	90%	KHSO <sub>4</sub>
2	4	1:1	146 W	90%	KHSO <sub>4</sub>
3	3	1:1	146 W	90%	KHSO <sub>4</sub>
4	5	1:1	90 W	90%	KHSO <sub>4</sub>
5	5	1:1	65 W	90%	KHSO <sub>4</sub>
6	5	1:1	146 W	90%	H <sub>2</sub> SO <sub>4</sub>
7	5	1:1	146 W	0%	KHSO <sub>4</sub>
8	5	1:1	146 W	0%	H <sub>2</sub> SO <sub>4</sub>
9	5	1:1	146 W	0%	3*KHSO <sub>4</sub>

The best FMR (which gives the highest purity of ETBE) are obtained by using a mixture of ethanol and tert-butanol with 95% water as considered by Assabmrungrat et al., 2004, the purities of ETBE obtained were very small therefore, the amount of water is reduced to 90% in the experiments to determine the best reflux ratio, and heat duty. The best operating conditions of FMR, reflux ratio, and heat duty obtained from the above experiments are used in experiments for the two catalysts with 0% water to find the maximum purity of ETBE when no water presented with reactants.

#### 4.6.2 Intermediate Reactive Section

An intermediate reactive section of 28 cm length has been packed with 160 g of KHSO<sub>4</sub> and the other two sections are packed with rasching ring packing. To prevent the KHSO<sub>4</sub> catalyst crystals from falling down through the column it has been located in a cloth bags, porous, and inert to the reactants and products U in Fig. 4-3. Ethanol and tert-butanol reactants were added to the still. Heat is supplied to the still by heating mantle; the vapor formed is rising up through the three sections passing the packing of

the lower section, the  $\text{KHSO}_4$  crystals section, and the packing of the upper section condensed and returns back to the column. In this case reaction takes place only in the middle section. One experiment was carried out using the best operating conditions of FMR 1:1, reflux ratio 5, and heat duty 146W obtained from previous experiments when the reaction was in the still. This experiment was carried out using only ethanol and tert-butanol with no water initially, because the large amount of water makes the  $\text{KHSO}_4$  crystals soluble (the solubility of  $\text{KHSO}_4$  in water is 50 g/100 ml).

During the operation at total reflux (the first hour) the liquid accumulated in the upper section above the catalyst section because  $\text{KHSO}_4$  is crystals with about 1.5 mm average diameter, so it is difficult for the liquid distillate to pass through this section as it passes through the rasching ring section. Therefore, when the vapor rising up through the upper section the liquid flow downward looks like bubbling. Figure 4-4 shows photographic picture for the upper section during the total reflux condition.

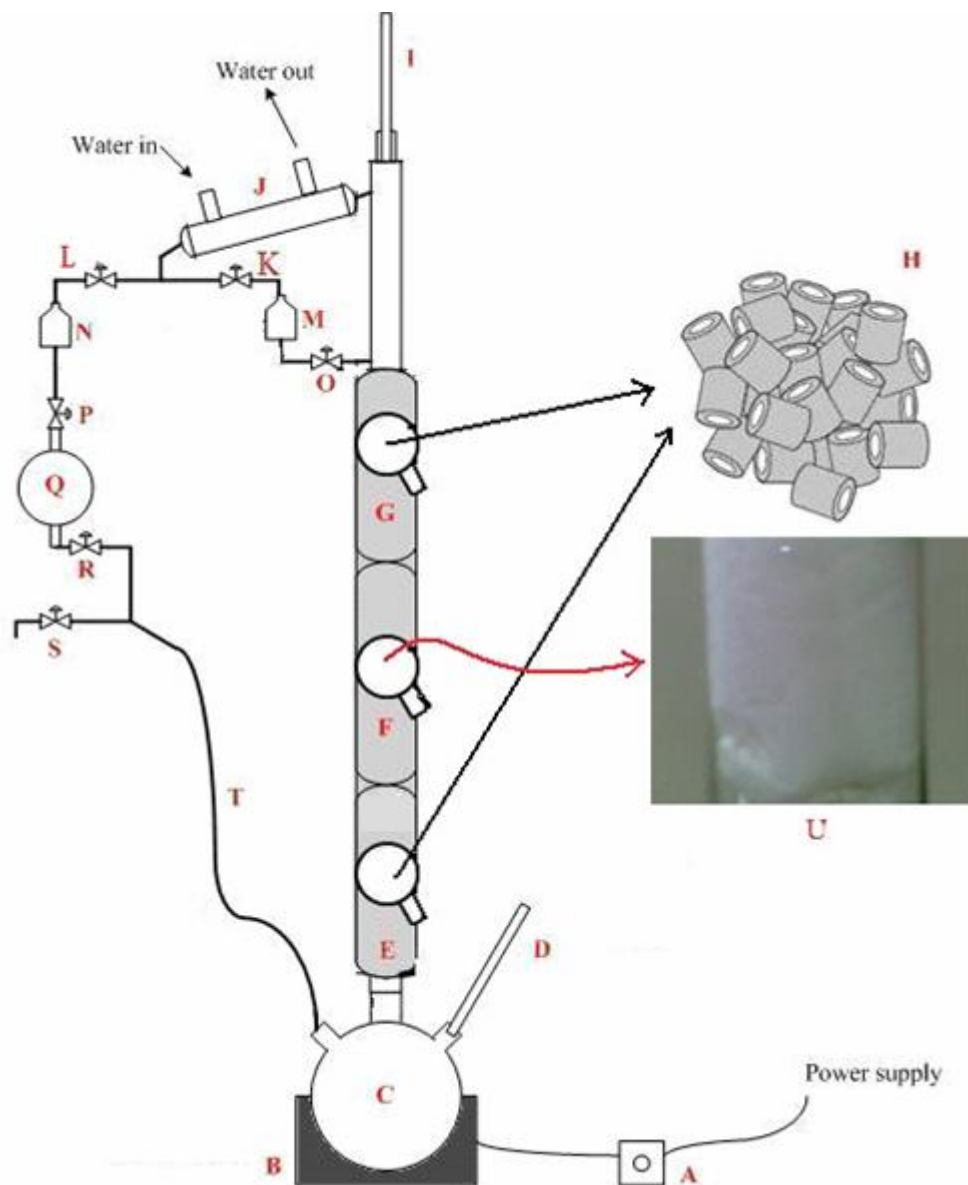


**Figure 4-3** Experimental Unit with Intermediate Reactive Section

- A:** Heat duty controller; **B:** Heating mantle; **C:** Still pot; **D:** Bottom thermometer,  
**E:** Lower distillation column section; **F:** Intermediate distillation column section  
**G:** Upper distillation column section; **H:** Rasching ring; **I:** Top thermometer  
**J:** Condenser; **K, L, O, P:** Reflux valves; **M:** Container; **N:** Container,  
**Q:** Collecting vessel; **R:** Valve; **S:** Valve; **T:** Recycle line,  
**U:** Catalyst bags in the glass section



**Figure 4-4** Photographic Picture of the Upper Section during the Total Reflux of Intermediate Reactive Section

## 4.7 Purification of Products

To increase the purity of ETBE, the distillate products of the experiments with 0% water in Table (4.2), and the intermediate reactive section experiment have been purified by mixing the distillate with pure water thoroughly and the distillate-water mixture leaving to allow it stabilize. After stabilization of the produced mixture two layers appeared; the upper layer consists mostly of ETBE and the lower layer is mostly water with ethanol and tert-butanol as observed in the previous work of Quitain et al., (1999b). Photographic picture shows the two layers are presented in Fig. 4-5. The set of experiments carried out to purify the distillate product given in Table 4-3 which was purified with different ratios of water to distillate to find the best amount of water must be added to reach high purity of ETBE.

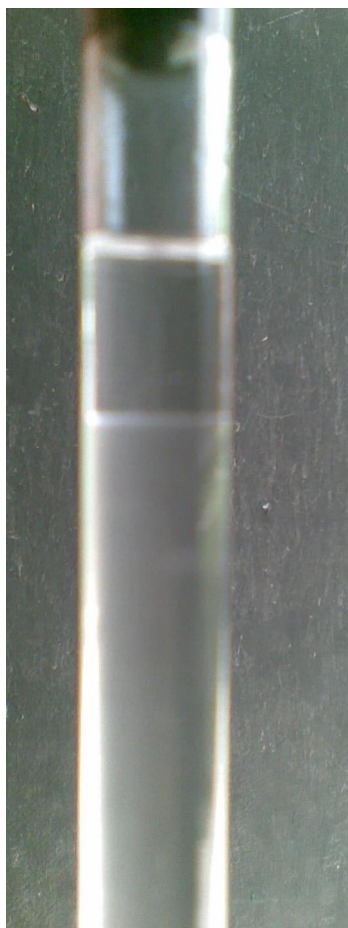


**Figure 4-5** Photographic picture of the purification mixture

**Table 4-3** Purification Experiments

No.	Reflux ratio	FMR	Heat duty	Water percent initially	Catalyst used	Ratios by volume of water to distillate used in purification
1	5	1:1	146 W	0%	KHSO <sub>4</sub>	1. 1:1 2. 2:1
2	5	1:1	146 W	0%	H <sub>2</sub> SO <sub>4</sub>	1. 1:1 2. 2:1 3. 4:1
3	5	1:1	146 W	0%	3*KHSO <sub>4</sub>	1. 1:1 2. 2:1 3. 4:1
4	5	1:1	146W	0%	Intermediate reactive section with KHSO <sub>4</sub>	1. 1:1 2. 2:1 3. 4:1

## Chapter Five

### Results and Discussions

#### 5.1 Introduction

In this chapter the results of the present work were included. The results of studied variables in experimental work presented first, and then validation of the predicted unsteady state equilibrium model has been discussed. The data obtained from the experimental work were compared with the results predicted from both equilibrium model and the rate-based model with error estimation. Furthermore, the results of purification experiments were presented.

#### 5.2 Results of Bench Experiment

Three experiments were carried out to show the performance of the three catalysts. The first catalyst Zeolit (13X) was failed to produce ETBE (i.e. no ETBE was produced when analyzing the product after about 3.5 h), while; the other two catalysts produce ETBE in different amounts. Results of bench experiment were shown in Table 5-1 together with the operating conditions.

**Table 5-1** Results of Bench Experiment

1. $\text{KHSO}_4 = 6\text{g}$							
Time (h)	FVR ETOH/TBA	$x_{\text{ETOH}}$	$x_{\text{TBA}}$	$x_{\text{ETBE}}$	$x_{\text{H}_2\text{O}}$	% Conversion	% Selectivity
3.5	2:1	0.738	0.152	0.092	0.018	53.669	52.119
2. $\text{H}_2\text{SO}_4 = 0.6\text{ml}$							
Time (h)	FVR ETOH/TBA	$x_{\text{ETOH}}$	$x_{\text{TBA}}$	$x_{\text{ETBE}}$	$x_{\text{H}_2\text{O}}$	% Conversion	% Selectivity
4.5	1:1	0.4232	0.0724	0.2497	0.2360	81.09	80.39

From Table (5.1), when  $\text{KHSO}_4$  catalyst has been used, after 3.5 h the % conversion (ratio of reacted tert-butanol to the initial tert-butanol) was 53.669%, and there was amount of tert-butanol still unreacted, also ethanol amount unreacted is very high since the feed volume ratio (FVR) of ethanol to tert-butanol used was 2:1, therefore, when  $\text{H}_2\text{SO}_4$  catalyst has been used the time increased to 4.5h and the FVR has been decreased to 1:1 and therefore, the % conversion increases to 81.09%.

## **5.3 Experimental Studied Variables in Reactive Still**

### **5.3.1 Feed Molar Ratio (FMR)**

Experiments 1, 2, and 3 in Table 4-1 were performed to study the effect of changing FMR on purity of ETBE in the distillate. Experiment 1 was carried out under total reflux, feed molar ratio of 1:1, using  $\text{KHSO}_4$  catalyst. The observed purity of ETBE in the distillate after 3h is 5.619 %mol which is nearly the same purity of ETBE that obtained by Matouq et al., 1996, Fig. 2-1, for the same system when operating at total reflux, FMR=1:1, using  $\text{KHSO}_4$  catalyst with reactive distillation column of 6 plates. For the same operating conditions of experiment 1, experiments 2 and 3 were carried out with feed molar ratio (FMR) of 2:1, and 4:1 respectively. Figure 5-1 shows the effect of changing FMR on the purity of ETBE and the best FMR obtained is 1:1. All experimental results are given in Appendix (D.1).



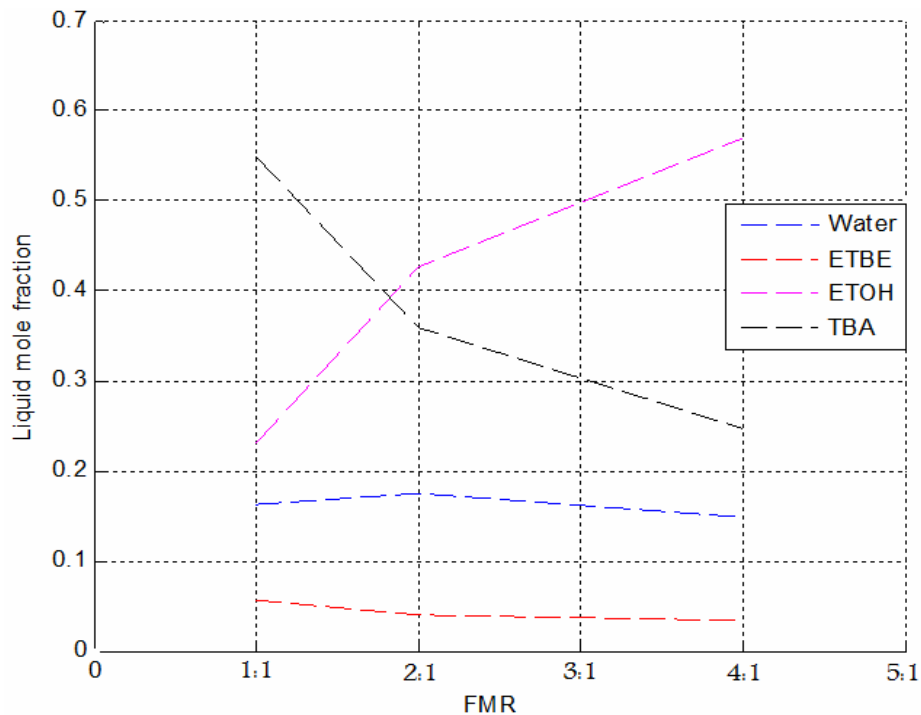


**Figure 5-1** Liquid Mole Fractions with Different FMR

From Figure (5.1) the purity of ETBE decreases as the ratio of ethanol to tert-butanol increases because the distillate contains the unreacted ethanol which reduces the amount of ETBE in the distillate.

### 5.3.2 Effect of Changing Reflux Ratio (Rr)

In the present experimental work the column was operated with reflux ratios of 3, 4, and 5 for the best value of FMR of 1:1. The purity of ETBE in the distillate when determining the best FMR was low, therefore, the percentage amount of water in the feed is reduced from 95% to 90% and the time increased to 6 h. Samples are taken from the distillate each 1 h starting from the second hour while from bottom one sample was taken at the end of experiment (at time 6h). Figures 5-2, 5-3, and 5-4 show the change of liquid mole fraction of each component in the distillate with time for reflux ratios 3, 4, and 5, respectively, and the effect of changing the reflux ratio on

ETBE purity after 6h is shown in Fig. 5-5. Experimental results of changing of reflux ratio are given in Appendix (D.2).

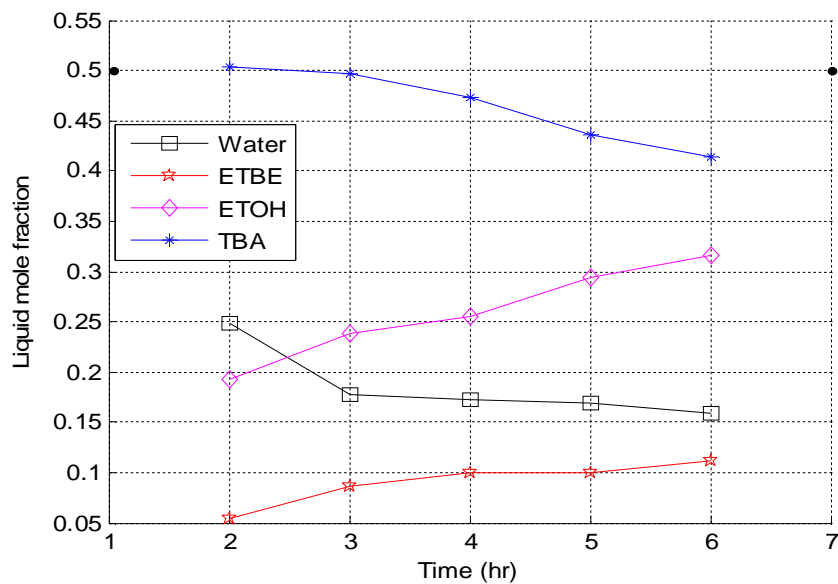


**Figure 5-2** Liquid mole fraction profile when Rr=3

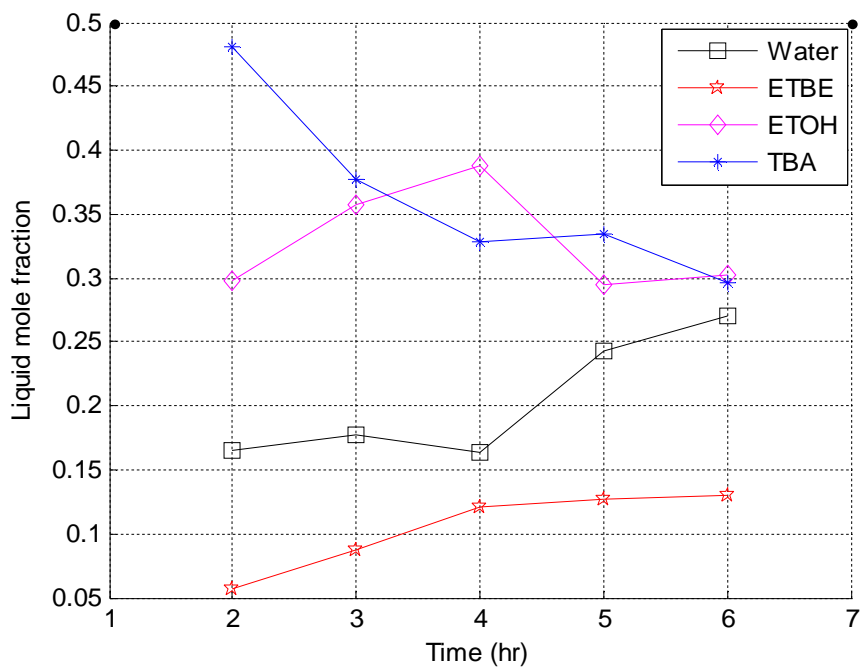


**Figure 5-3** Liquid mole fraction profile when Rr=4

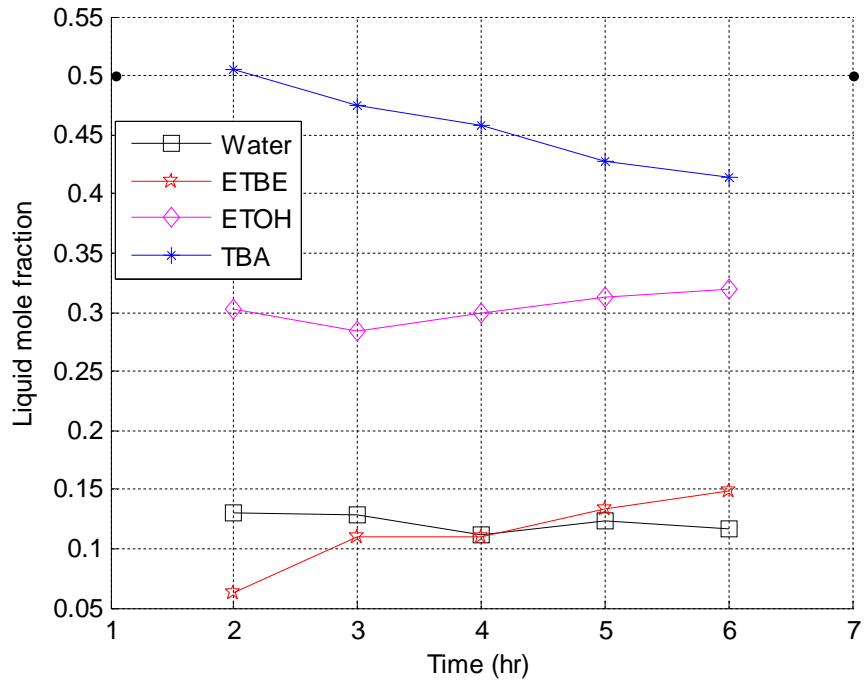


**Figure 5-4** Liquid mole fraction profile when Rr=5

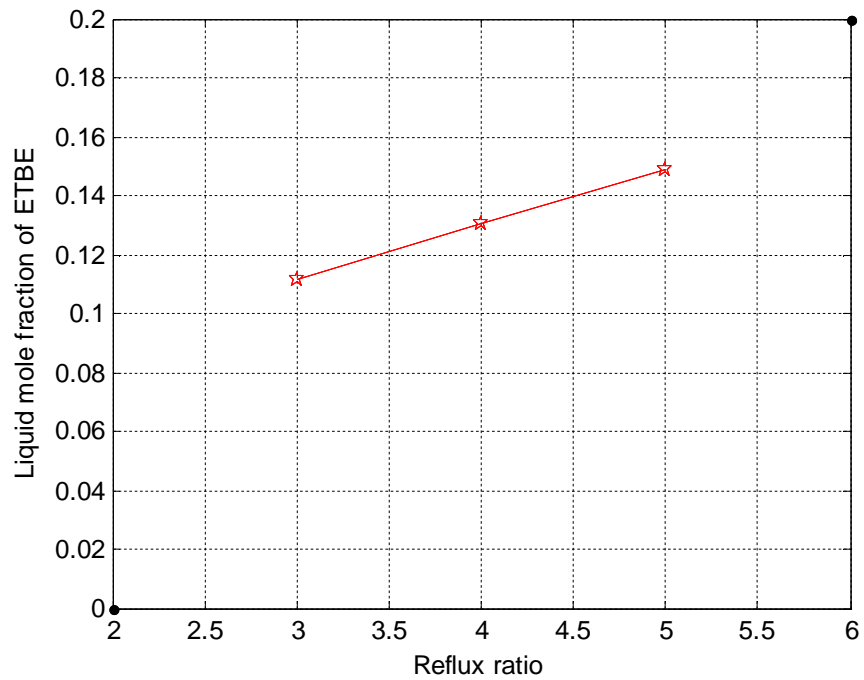


**Figure 5-5** Effect of Changing Rr on ETBE Purity in the Distillate after 6hr

From Fig. 5-5 the best reflux ratio which gives higher purity of ETBE is 5; also it was found that the purity of ETBE increases linearly with increasing the reflux ratio. This is because when reflux ratio increases the residence time of reactants increased and the concentration of reactants in the distillate reduced, therefore, the purity of ETBE increased.

### 5.3.3 Effect of Changing the Boiler Heat Duty

All the previous experiments have been carried out under boiler heat duty of 146 W, which is the maximum operating value of the heating mantle. In order to find the effect of changing the heat duty on the purity of ETBE in the distillate; experiments with the best FMR (1:1), best reflux ratio (5), and boiler heat duty of 65 and 90 W were performed. Figures 5-6 and 5-7 show the liquid mole fraction profiles of each component in the distillate with time for 65 and 90 W, respectively.

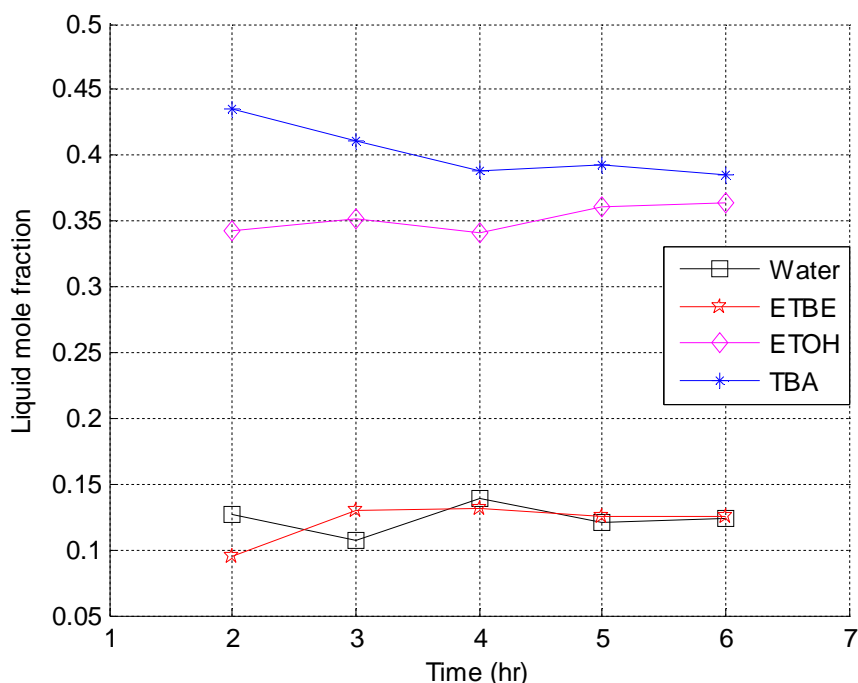


**Figure 5-6** Liquid mole fraction profile when  $R_r=5$ , heat duty=65W

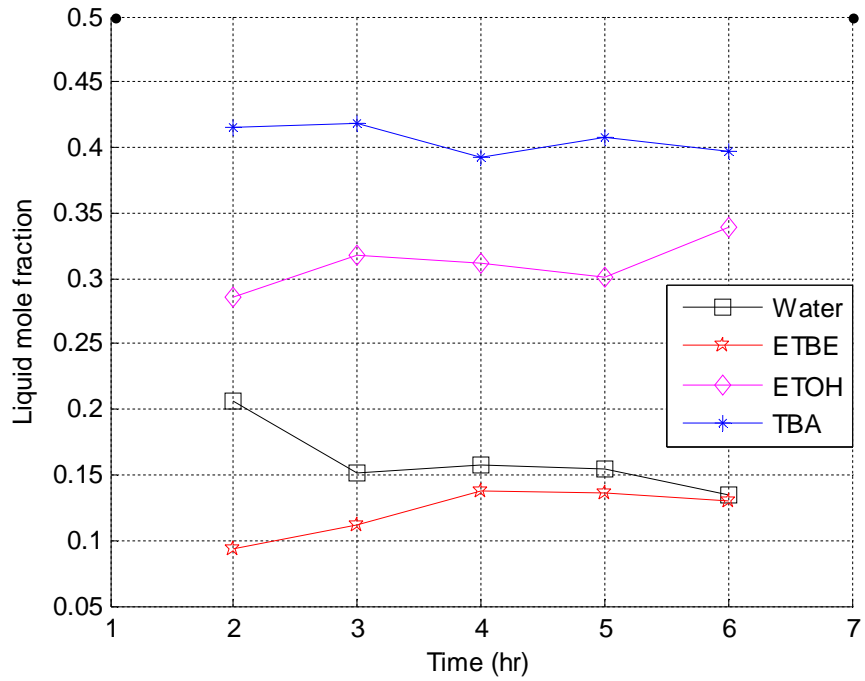


**Figure 5-7** Liquid mole fraction profile when  $R_r=5$ , heat duty=90W

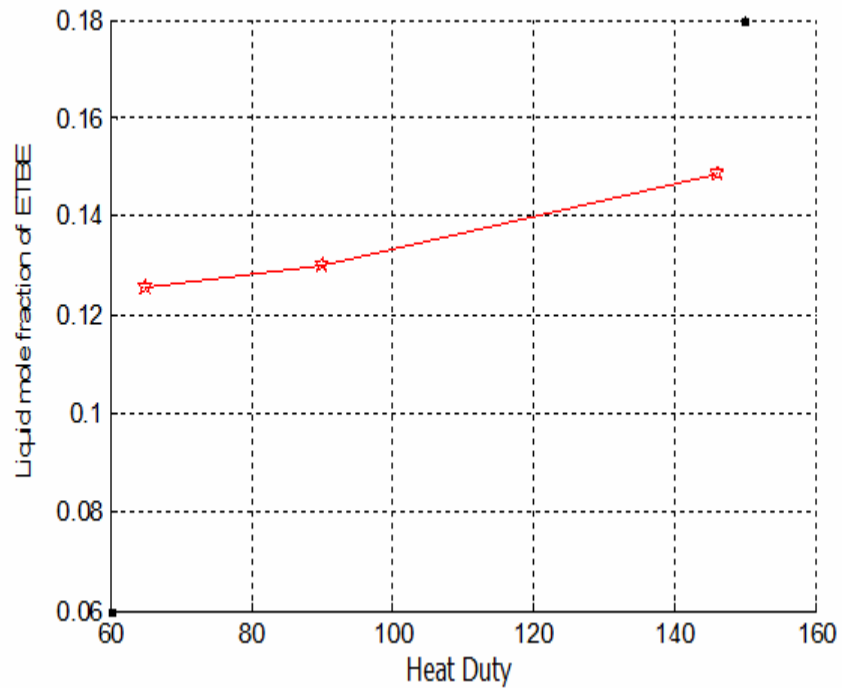


**Figure 5-8** Effect of Changing Boiler Heat Duty on ETBE Purity in Distillate after 6hr

Figure 5-8 shows the effect of changing the boiler heat duty after 6 h on liquid mole fraction of ETBE in the distillate, as the boiler heat duty increases the purity of ETBE increased and the best boiler heat duty was 146 W. When the heat duty increases the vapor rate is increased which transfers more volatile and lower boiling point component from the still to the distillate, therefore, the purity of ETBE which is the lower boiling point component in the system increases. Experimental results of changing the heat duty are given in Appendix (D.3).

### 5.3.4 Effect of Changing the Catalyst Type

In the previous experiments, potassium hydrogen sulfate  $\text{KHSO}_4$  was used as a catalyst. In order to increase the purity of ETBE in the distillate other catalyst has been chosen such as  $\text{H}_2\text{SO}_4$  with the same amount (0.04 kg catalyst/1kg bulk reactant), for both 90% and 0% water in the feed, with the best FMR (1:1), best reflux ratio (5), and best boiler heat duty (146W). Figure 5-9 shows the results of performed experiment with 90% water in feed and sulfuric acid ( $\text{H}_2\text{SO}_4$ ) as a catalyst.

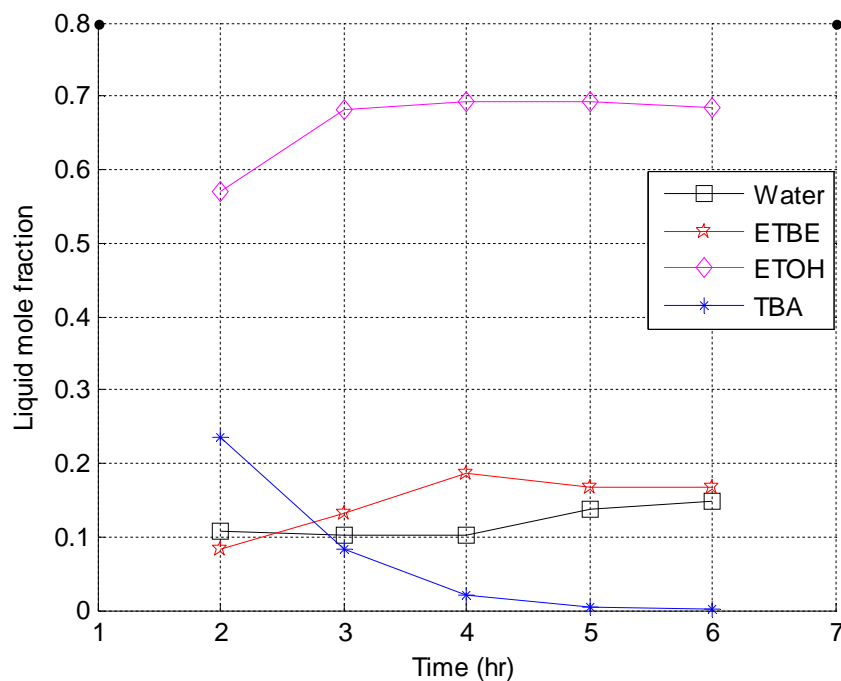


**Figure 5-9** Liquid mole fraction profile with 90% water and catalyst  $\text{H}_2\text{SO}_4$

Two experiments with 0% water in the feed for both catalysts  $\text{KHSO}_4$  and  $\text{H}_2\text{SO}_4$  were carried out. Figures 5-10 to 5-13 show the liquid mole fraction and %conversion profile using catalyst  $\text{KHSO}_4$  and  $\text{H}_2\text{SO}_4$ , respectively. Experimental results of changing the catalyst type are listed in Appendix (D.4).

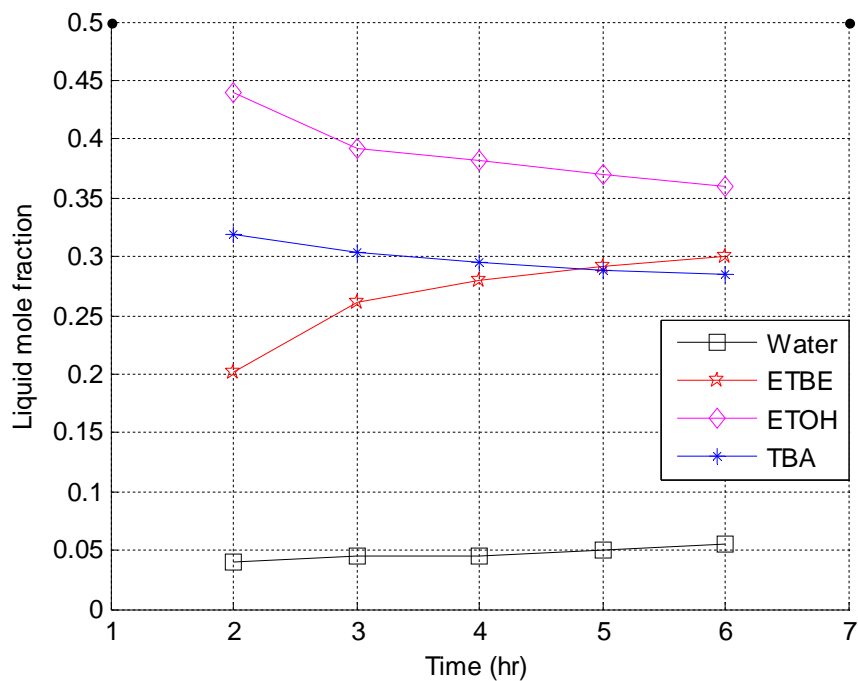


**Figure 5-10** Liquid mole fraction profile with 0% water and catalyst  $\text{KHSO}_4$

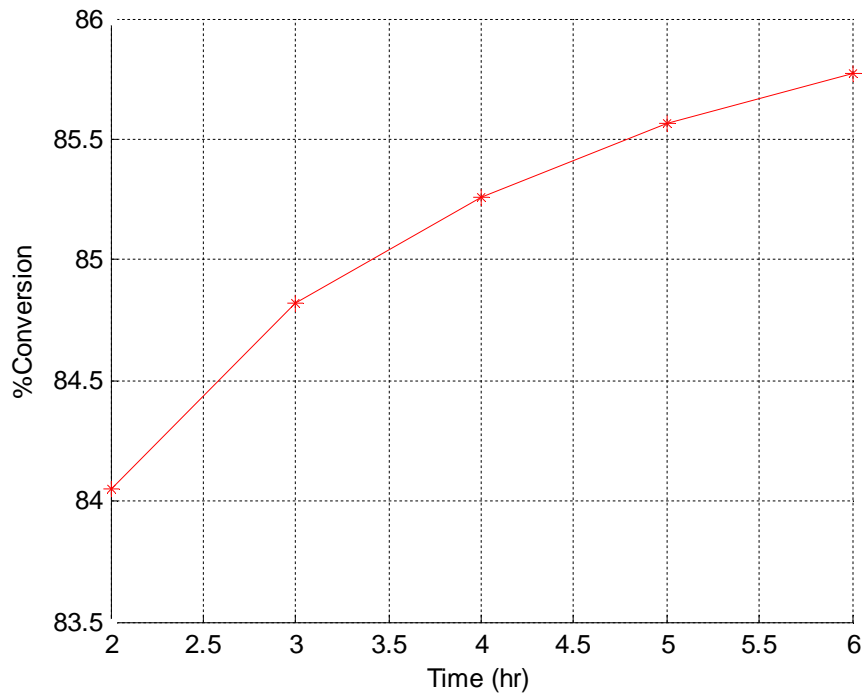


**Figure 5-11** Conversion profile for 0% water and catalyst  $\text{KHSO}_4$

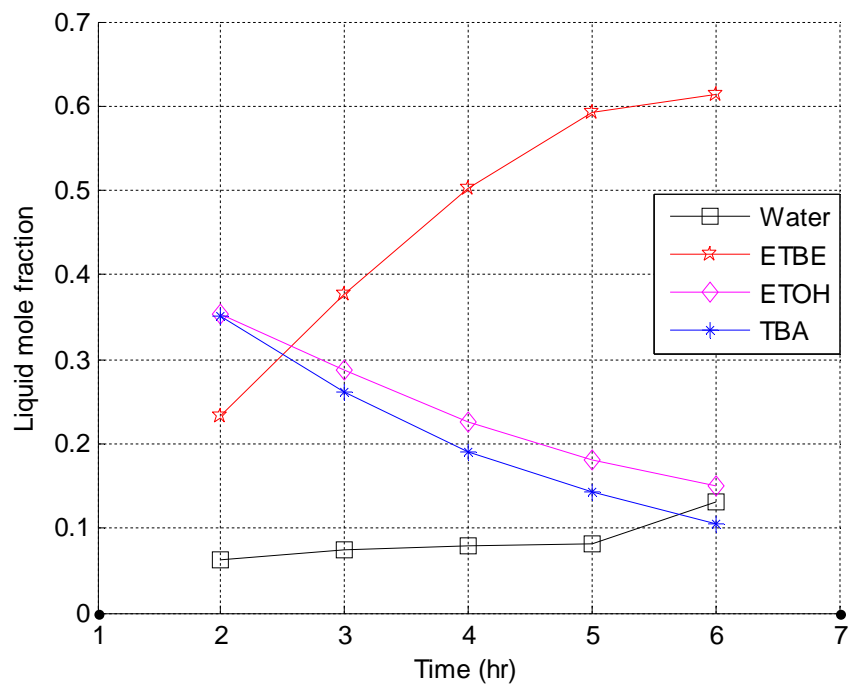


**Figure 5-12** Liquid mole fraction profile with 0% water and catalyst  $\text{H}_2\text{SO}_4$



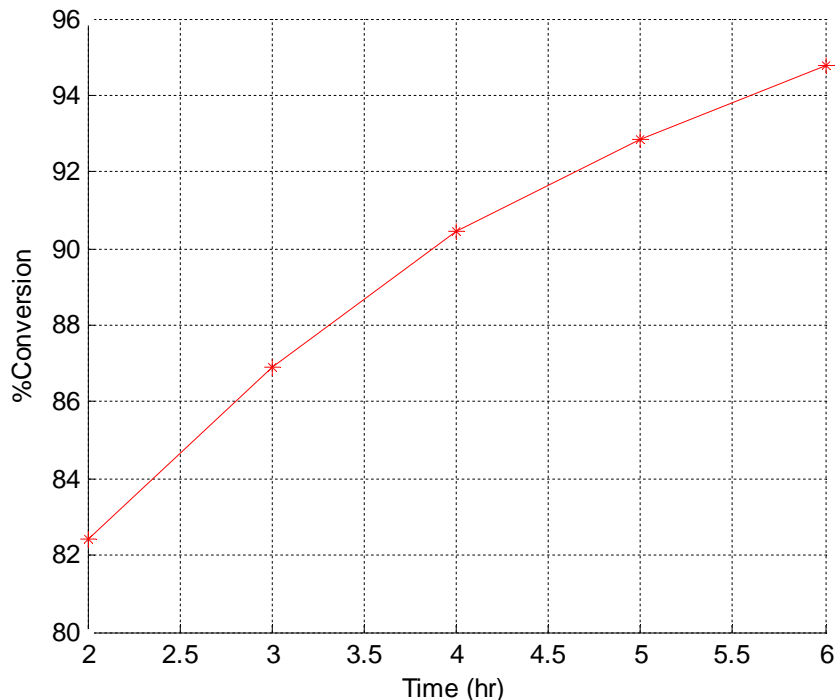


**Figure 5-13** Conversion profile for 0% water and catalyst  $H_2SO_4$

From the previous figures, sulfuric acid gives ETBE purity higher than that which was given by potassium hydrogen sulfate. For 90% water in the feed,  $KHSO_4$  catalyst the purity of ETBE in the distillate is (0.1487) compared with (0.16615) for sulfuric acid, and for 0% water in the feed the purity is (0.29996) for potassium hydrogen sulfate compared with (0.61317) for sulfuric acid. In the experiments where  $H_2SO_4$  is used the tert-butanol which is the limited reactant is almost consumed, while when using potassium hydrogen sulfate with the same batch time amount of tert-butanol is still unreacted even it is higher than the amount of ETBE when using 90% water and nearly equal to the amount of ETBE when no water is used for the same amount of catalyst used, this is due to that sulfuric acid is a strong acid causes the tert-butanol and ethanol to react faster and therefore, increases the conversion of tert-butanol, so for 0% water in the feed the conversion is (85.5775%) when using potassium hydrogen sulfate compared with (94.789%) for sulfuric acid. Higher amount of  $KHSO_4$  catalyst

are required to increase the purity of ETBE and the conversion. Therefore, an experiment with higher amount of  $\text{KHSO}_4$  has been performed.

### 5.3.5 Effect of Changing the Catalyst Amount

$\text{KHSO}_4$  catalyst has been used with three times its amount in the previous experiments in order to increase the purity of ETBE and the % conversion of TBA. Figures 5-14 and 5-15 show the liquid mole fraction profile and conversion profile using feed molar ratio of 1:1, reflux ratio 5, boiler heat duty 146W, and 0.12 kg catalyst/1kg bulk reactant. All experimental results of increasing the catalyst amount are given in Appendix (D.5).

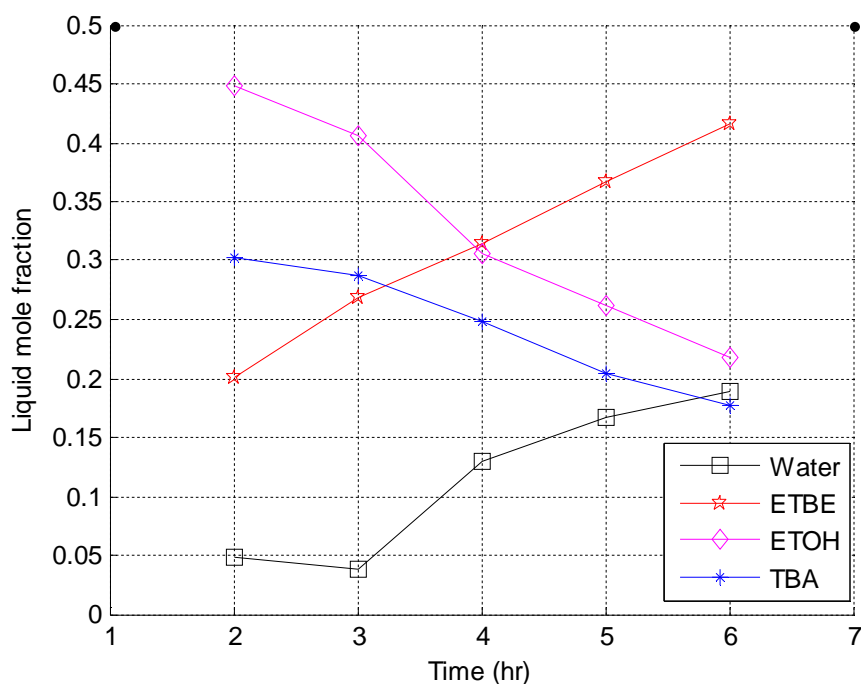


**Figure 5-14** Liquid mole fraction profile with 0% water and 3\* $\text{KHSO}_4$

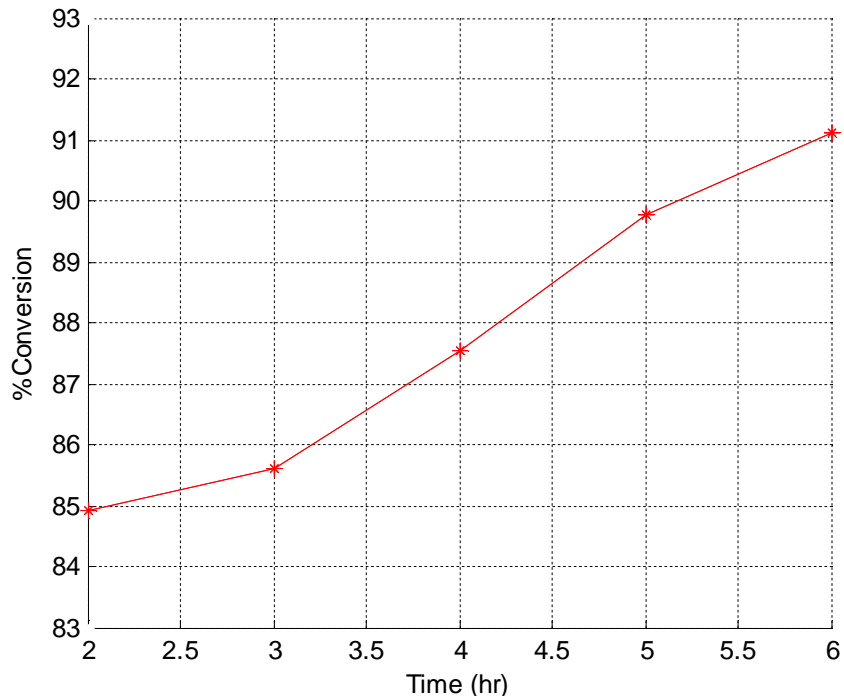


**Figure 5-15** Conversion profile for 0% water and 3\*KHSO<sub>4</sub>

From the previous figures it is clear that the purity of ETBE and conversion of TBA increase with increasing the amount of KHSO<sub>4</sub>. The purity of ETBE changed from (0.29996) to (0.41622) when increasing the catalyst amount due to more tert-butanol and ethanol reacts to produce ETBE and therefore, the conversion increased.

#### 5.4 Experimental Results of the Intermediate Reactive Section

The reaction section has been changed to an intermediate section, where the catalyst KHSO<sub>4</sub> is placed in the middle section and the reactants have been introduced to the still, samples were taken every hour for 6h starting from the second hour. The operating conditions of the present experiment are feed molar ratio 1:1, reflux ratio 5, and boiler heat duty 146W, with 160 g amount of catalyst. Figures 5-16 and 5-17 show the liquid mole fraction of components in the distillate and the %conversion of TBA using the intermediate reactive section, respectively. Experimental results are given in Appendix (D.6).

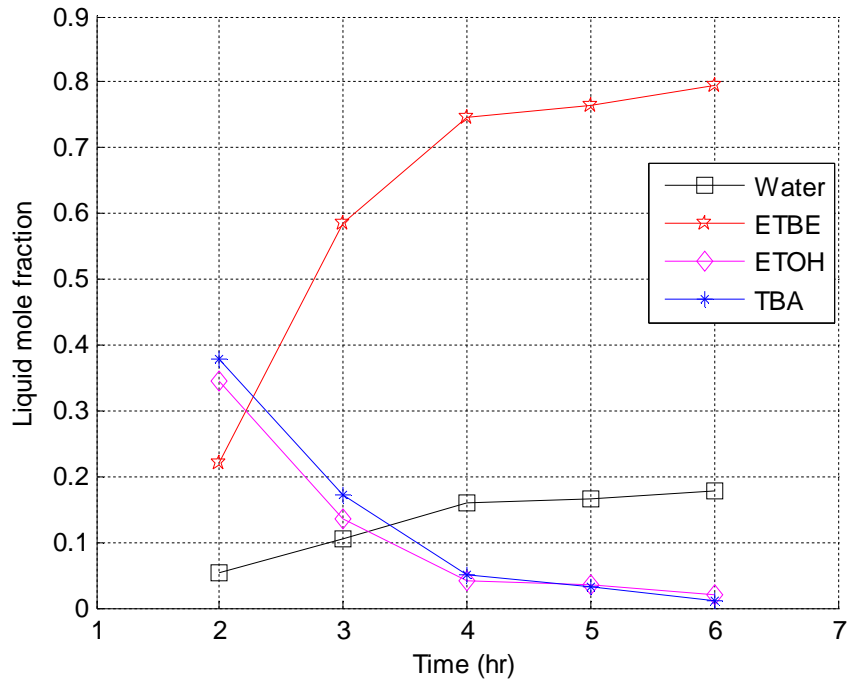


**Figure 5-16** Liquid mole fraction profile using intermediate reactive section

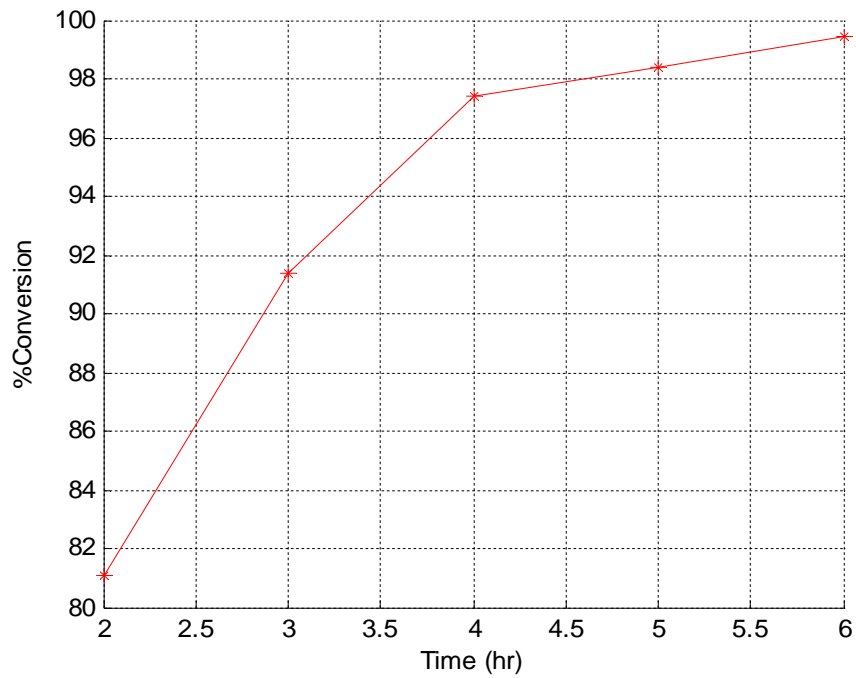


**Figure 5-17** Conversion profile using intermediate reactive section

Figures (5.16) and (5.16) show the purity of ETBE in the distillate and % conversion increased to (0.79407) and (99.465%), when intermediate reactive section has been used. This is due to the availability of large amount of catalyst.

## 5.5 Results of Purification Experiments

In this section the purification results are presented. In the separation of alcohol or hydrocarbons from compounds like ethers, extraction with water is an effective technique (Yang et al., 2001). Results of purification (mole fraction) of the experiment when 0% water in feed used and catalyst  $\text{KHSO}_4$  are given in Table 5-2 for 1:1 volume fraction of water to distillate, and 2:1. The upper layer consists almost of ETBE and its fraction increases with increasing the amount of water added. Results of other purification experiments for 0% water in feed used with catalyst  $\text{H}_2\text{SO}_4$ , three times catalyst  $\text{KHSO}_4$ , and experiment when the intermediate reactive section used are given in Fig. 5-18, 5-19, and 5-20, respectively, when ratios of water to distillate used are 1:1, 2:1, and 4:1, and the experimental results are given in Appendix D.7.

**Table 5-2** Results of 0% Water in Feed and Catalyst  $\text{KHSO}_4$

Component	1:1	2:1
Water	15.97	12.565
ETBE	45.506	69.397
Ethanol	15.754	6.243
Tert-butanol	13.782	11.795

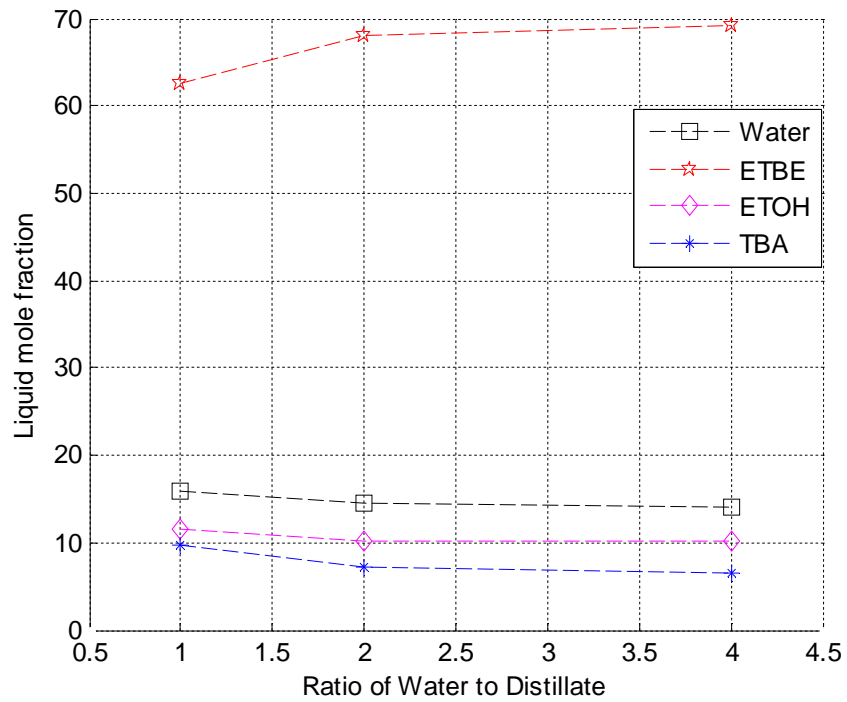


**Figure 5-18** Liquid Composition Profile in the Upper Layer, 0% Water in Feed H<sub>2</sub>SO<sub>4</sub>

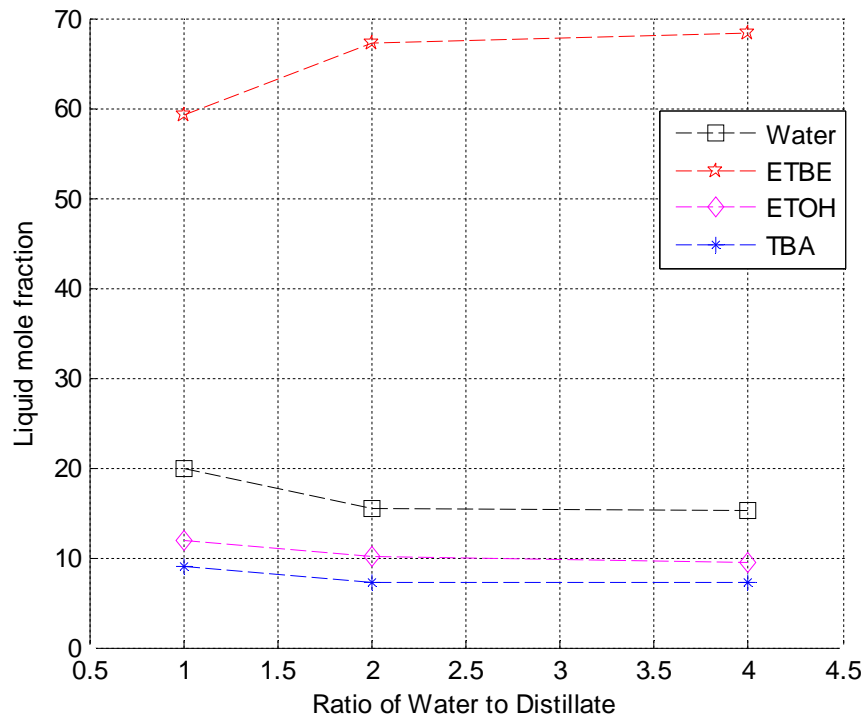


**Figure 5-19** Liquid Composition Profile in the Upper Layer, Three Times Catalyst KHSO<sub>4</sub>

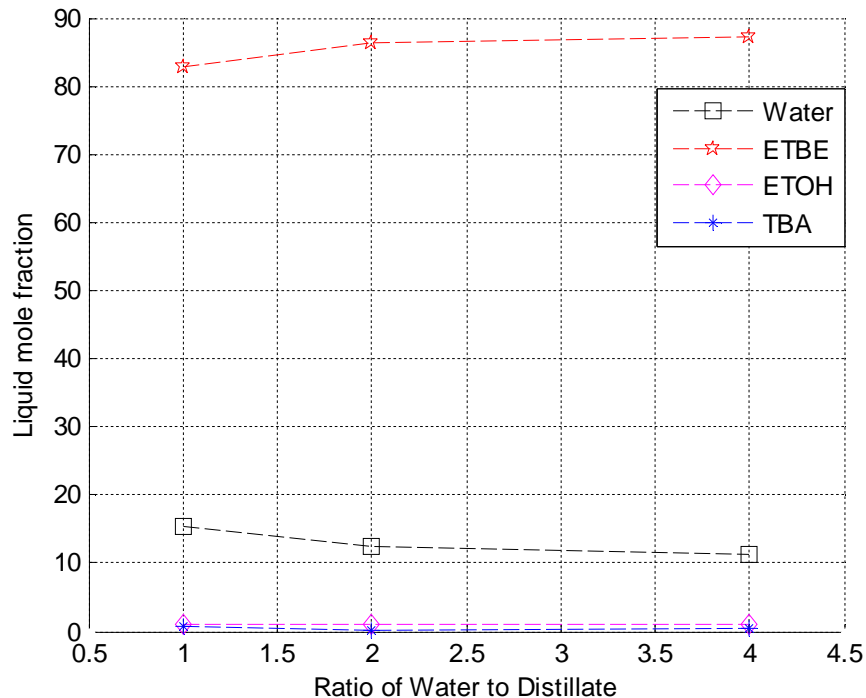


**Figure 5-20** Liquid Composition Profile in the Upper Layer, Intermediate Reactive Section

From the previous figures, increasing the ratio of water from 2:1 to 4:1 has no significant effect on the purity of ETBE. For 0% water in feed used with catalyst  $\text{KHSO}_4$  ETBE fraction increased from 29.996 to 69.397, and for 0% water in feed used with catalyst  $\text{H}_2\text{SO}_4$  ETBE fraction increased from 61.317 to 69.128, for three times catalyst  $\text{KHSO}_4$  ETBE fraction increased from 41.622 to 68.241, and for intermediate reactive section ETBE fraction increased from 79.407 to 87.142.

## 5.6 Theoretical Results

### 5.6.1 Checking the Validity of the Unsteady State Equilibrium Model

The validity and accuracy of the proposed unsteady state equilibrium model for production of ETBE from ethanol and tert-butanol using MATLAB (R2009b) are checked with Aspen Plus (10.2) program using a rigorous distillation model (RADFRAC) with the same operating conditions in both programs Appendix D.8.

Results of liquid mole fraction in the distillate and bottom with time of the two programs are shown on the same plot for comparison, Fig. 5-21, 5-22, and 5-23. ETBE formed is mostly collected in the distillate because it has the lower boiling point 73C° compared with 78, 83, and 100 C° for ethanol, tert-butanol and water, respectively.

The comparison of the two programs shows good agreement in composition profiles with small deviation which is due to the lack of knowledge in the Aspen Plus data of activity coefficients, Antoine parameters, enthalpy of vapor and liquid coefficients, reaction rate kinetics and amount of catalyst used. Figure 5-24 shows the error between the two programs which is bounded with  $\pm 10\%$  error lines.

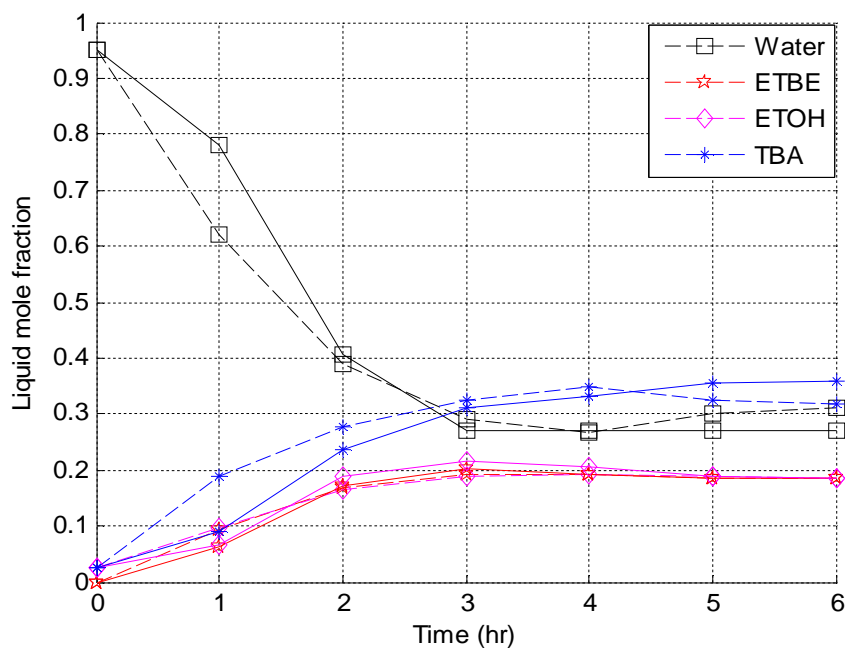


**Figure 5-21** Comparison of the Proposed EQ Program and Aspen Plus, Distillate  
Solid lines: ASPEN PLUS, Dashed Lines: Proposed Program



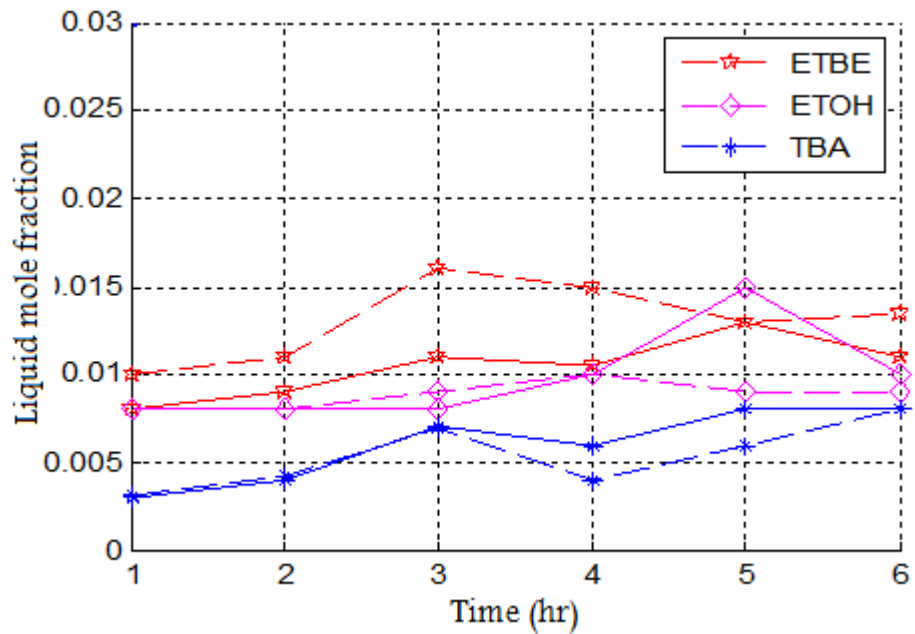


**Figure 5-22** Comparison of the Proposed EQ Program and Aspen Plus, Bottom  
 Solid lines: ASPEN PLUS, Dashed Lines: Proposed Program

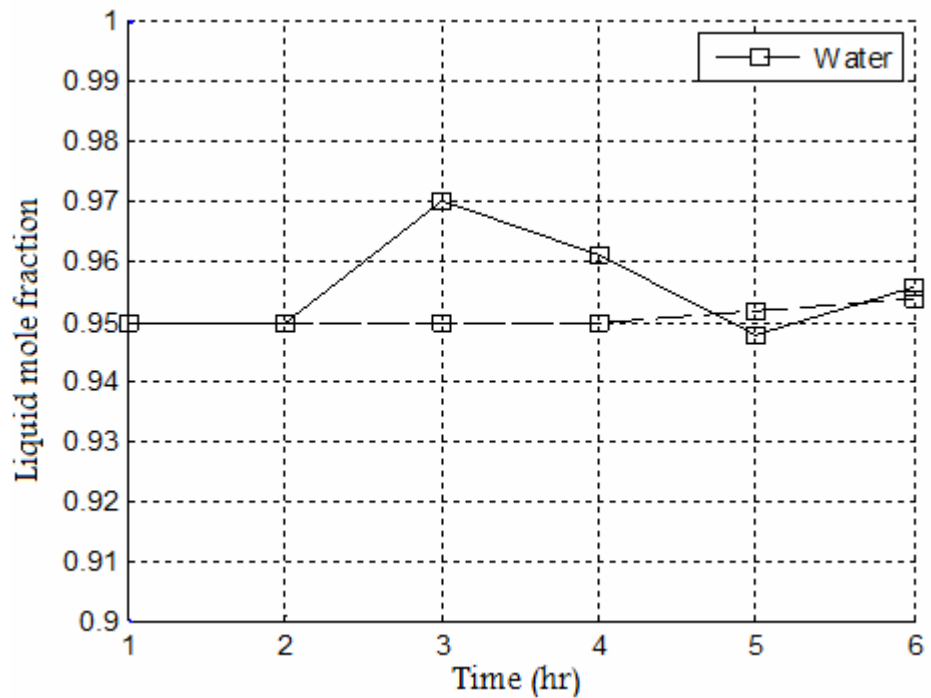


**Figure 5-23** Comparison of the Proposed EQ Program and Aspen Plus, Bottom  
 Solid lines: ASPEN PLUS, Dashed Lines: Proposed Program

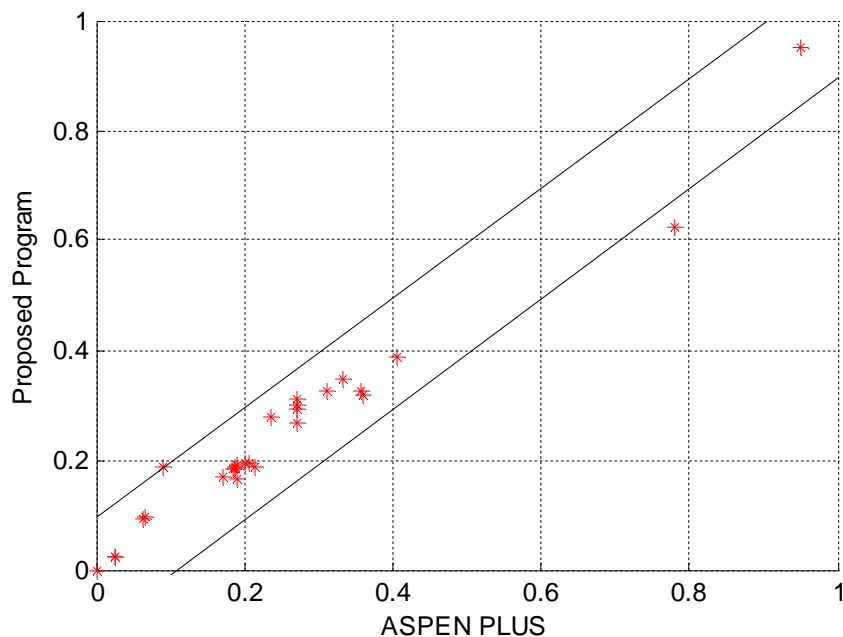


**Figure 5-24** Error between the Two Programs in the Distillate

### 5.6.2 Comparison of Experimental and Equilibrium Model Results

After checking the validity of equilibrium model in section 5-6-1, different variables have been studied such as feed molar ratio, reflux ratio, and heat duty and the results were compared with the present experimental work. Figures 5-25 to 5-27 show the results of liquid composition profile with time in the distillate for experimental and theoretical equilibrium model for reflux ratios of 3, 4 and 5, FMR of 1:1 and boiler heat duty 146W. Figures 5-28 and 5-29 give the comparison in heat duty and Figures 5-30 and 5-31 show the comparison between experimental and theoretical model where no water used in the feed for 0.04 kg catalyst/kg reactant and 0.12 kg catalyst/kg reactant, respectively. When intermediate reactive section has been used Fig. 5-32 shows the comparison between theoretical and experimental results, Appendix D.9 gives the equilibrium model results.

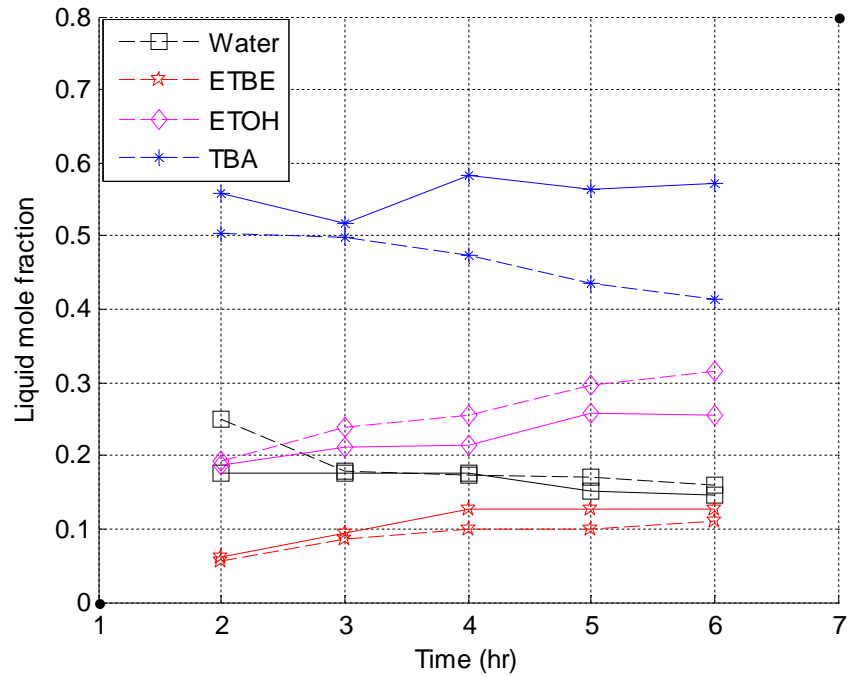


**Figure 5-25** Experimental and EQ Model Composition profile in the Distillate for  $R_r=3$ , Heat Duty=146W, Solid Lines  $\equiv$  EQ Model, Dashed Lines  $\equiv$  Experimental

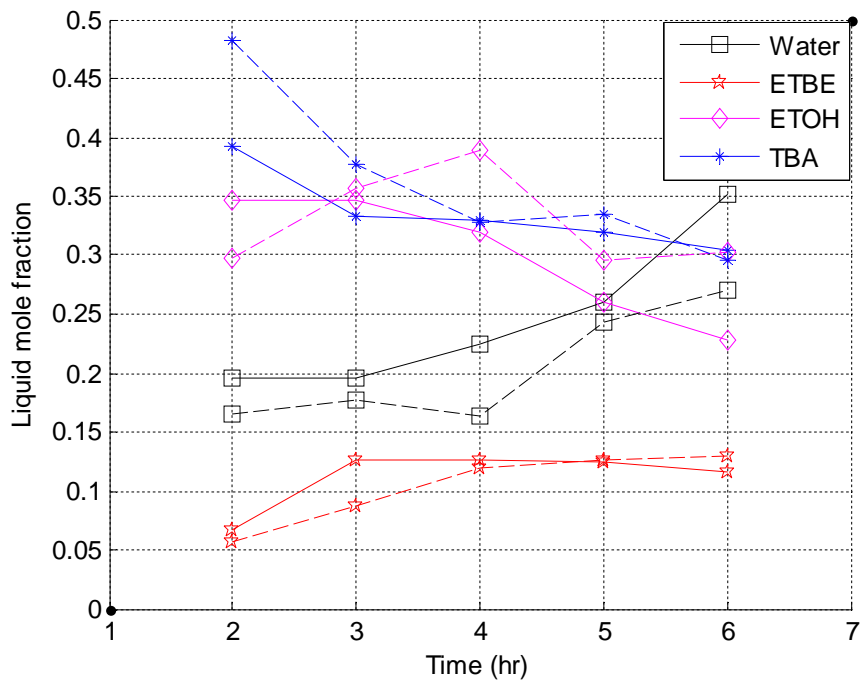


**Figure 5-26** Solid Lines  $\equiv$  EQ, Dashed Lines  $\equiv$  Experimental,  $R_r=4$ , Heat Duty=146W

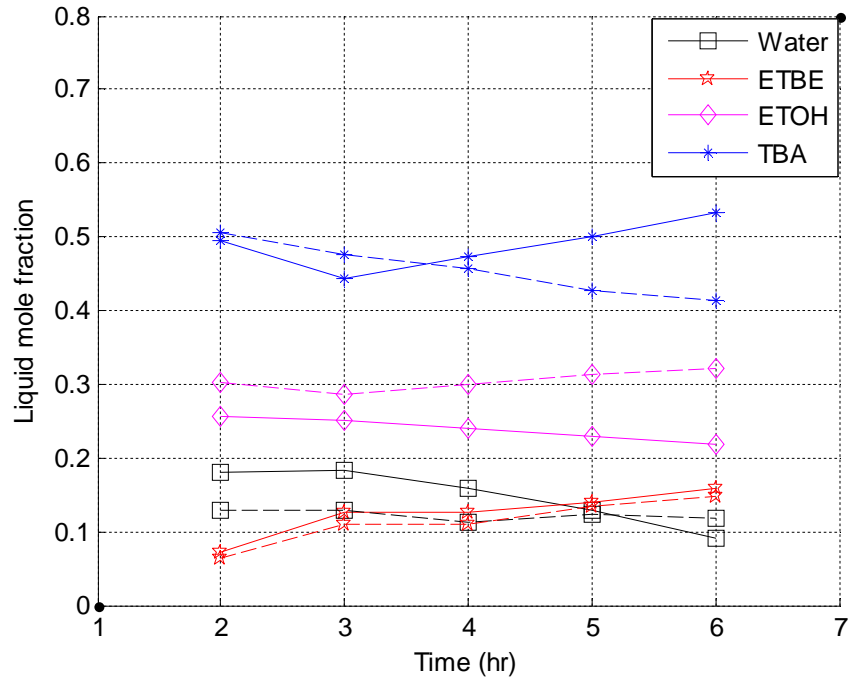


Figure 5-27 Solid Lines  $\equiv$  EQ, Dashed Lines  $\equiv$  Experimental,  $R_r=5$ , Heat Duty=146W

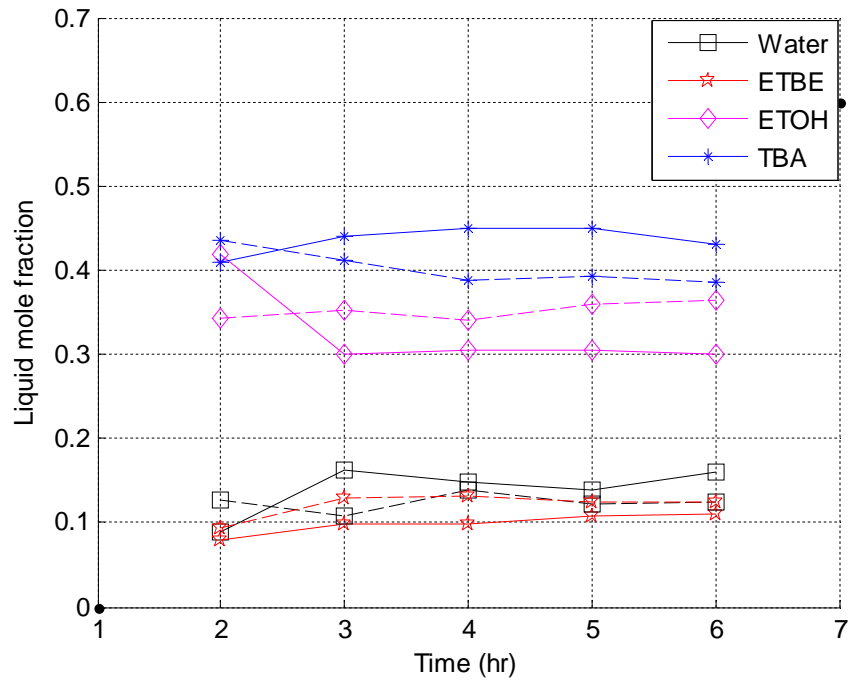


Figure 5-28 Solid Lines  $\equiv$  EQ, Dashed Lines  $\equiv$  Experimental, Heat Duty=65W

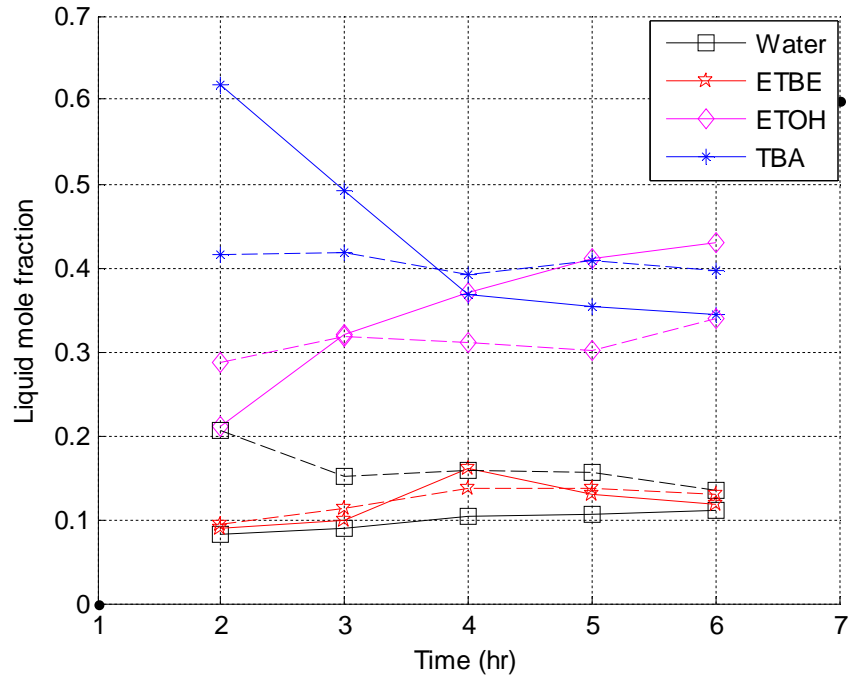


Figure 5-29 Solid Lines  $\equiv$  EQ, Dashed Lines  $\equiv$  Experimental, Heat Duty=90W

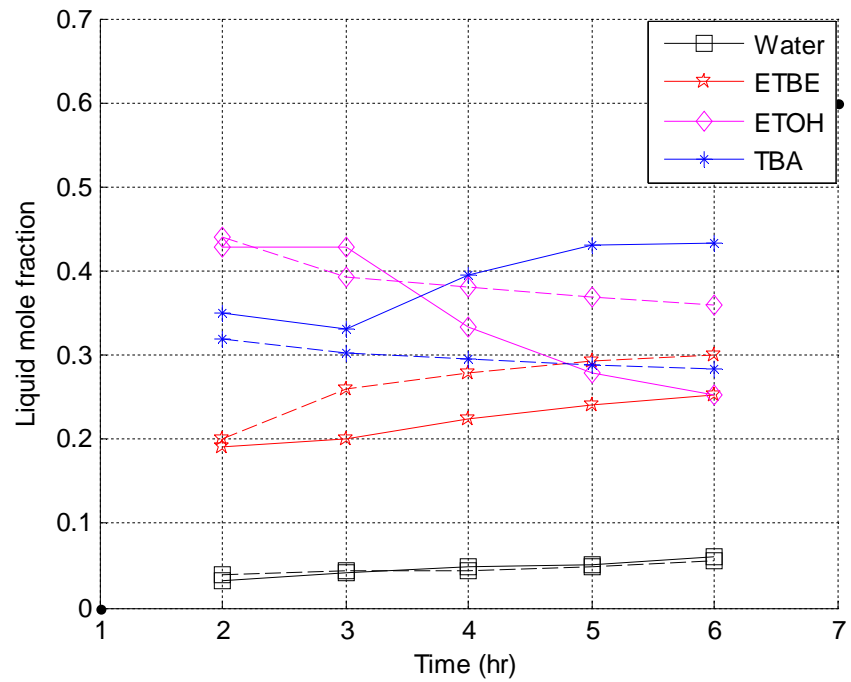
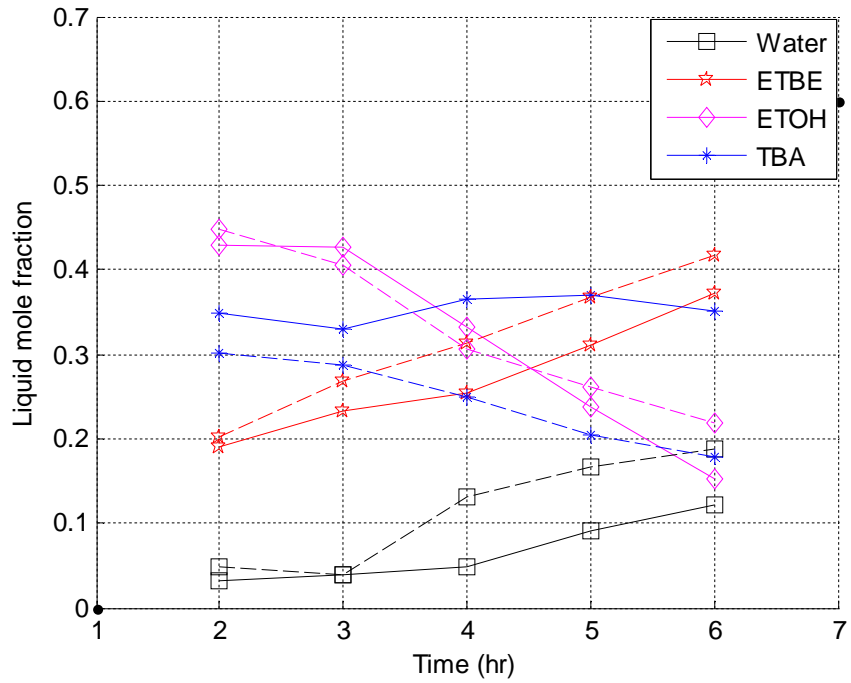
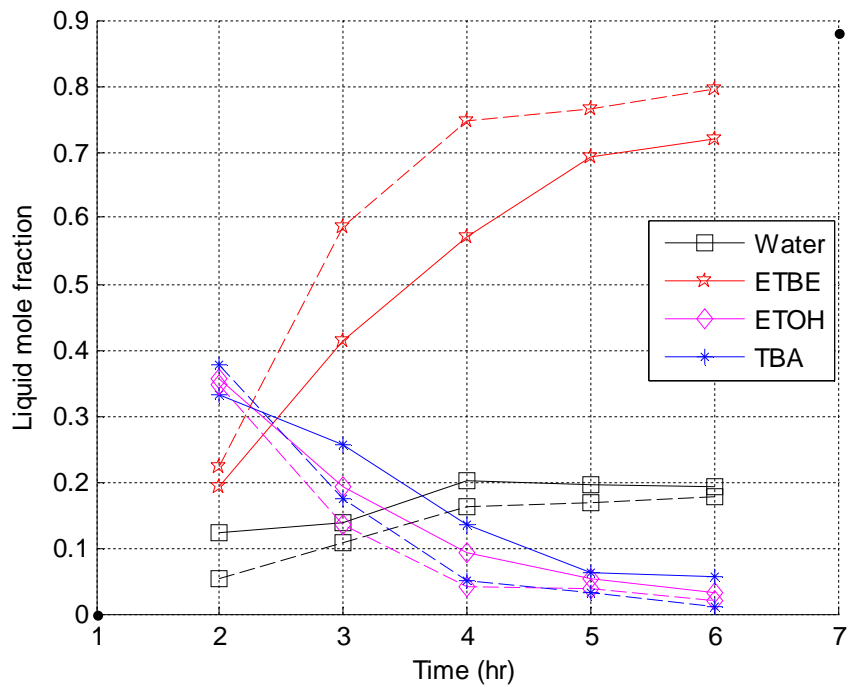


Figure 5-30 Solid Lines  $\equiv$  EQ, Dashed Lines  $\equiv$  Experimental, 0% Water in Feed



**Figure 5-31** Solid Lines  $\equiv$  EQ, Dashed Lines  $\equiv$  Experimental, 0% Water in Feed with Three Times Catalyst  $\text{KHSO}_4$



**Figure 5-32** Solid Lines  $\equiv$  EQ, Dashed Lines  $\equiv$  Experimental, Intermediate Reactive Section

All the above figures show good agreement between experimental and theoretical results within  $\pm 10\%$  errors Figures 5-33 to 5-40. Such deviations may be attributed to the little difference in the size and shape of packings and the manual operation of the distillation column when the reflux ratio and heat duty were being set.

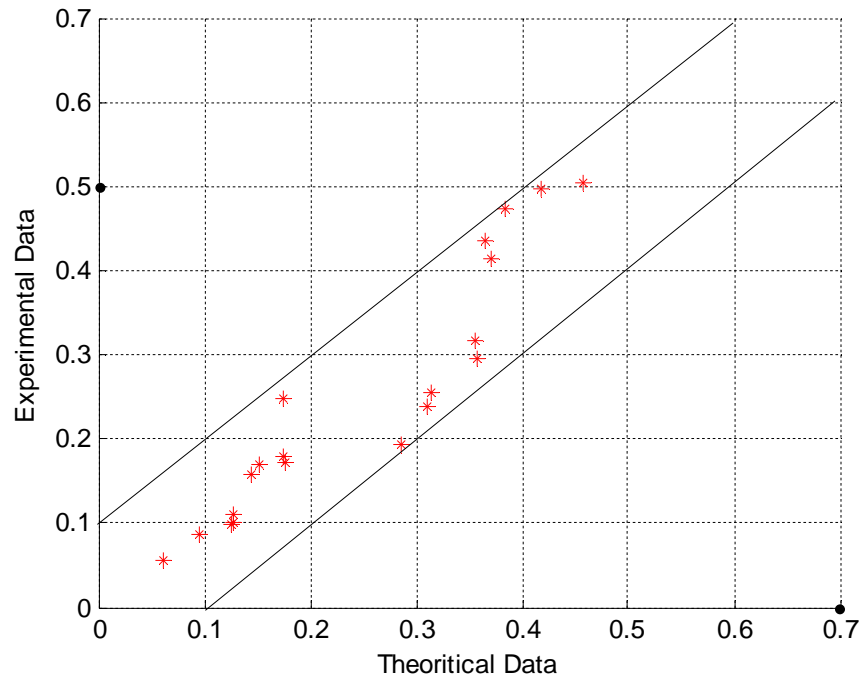


**Figure 5-33** Error between Experimental and EQ Model for  $Rr=3$

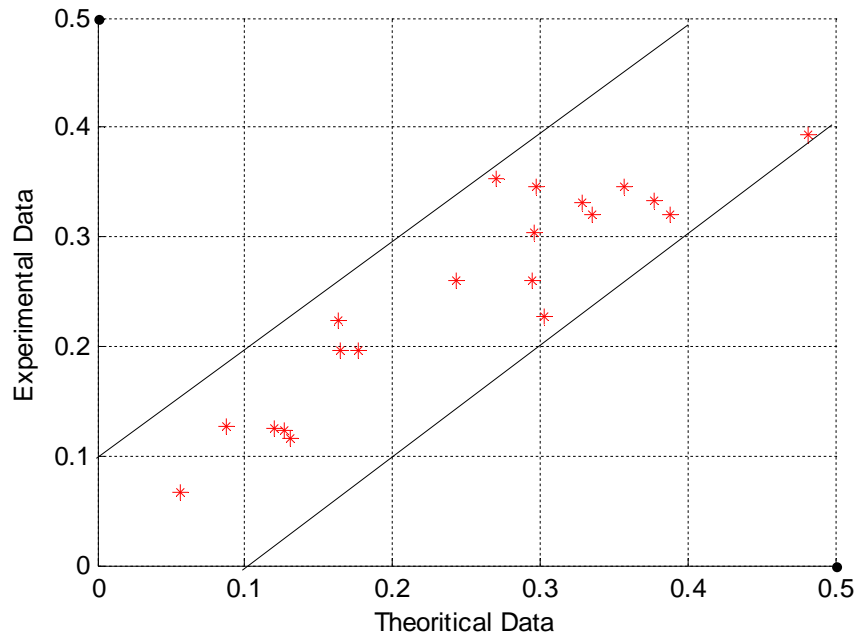


**Figure 5-34** Error between Experimental and EQ Model for  $Rr=4$

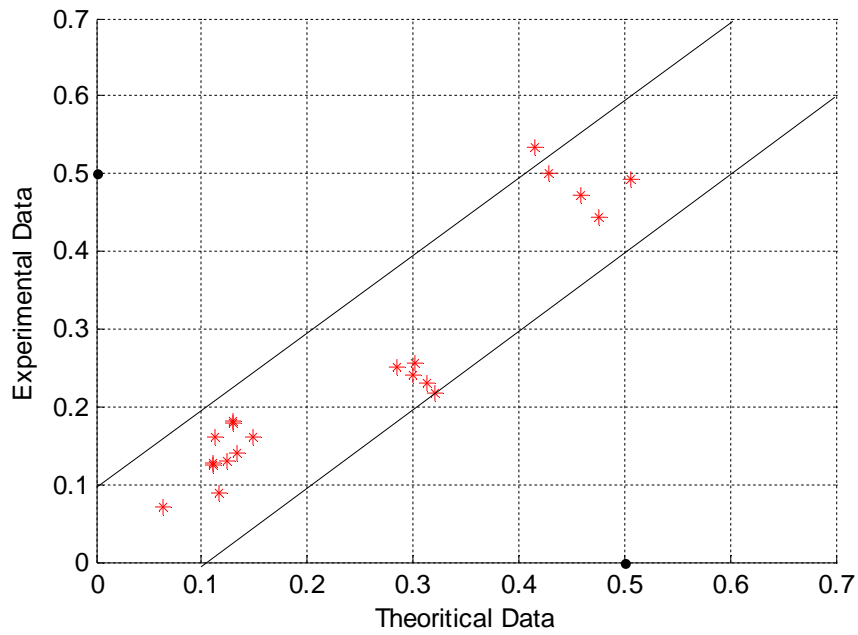


**Figure 5-35** Error between Experimental and EQ Model for  $Rr=5$



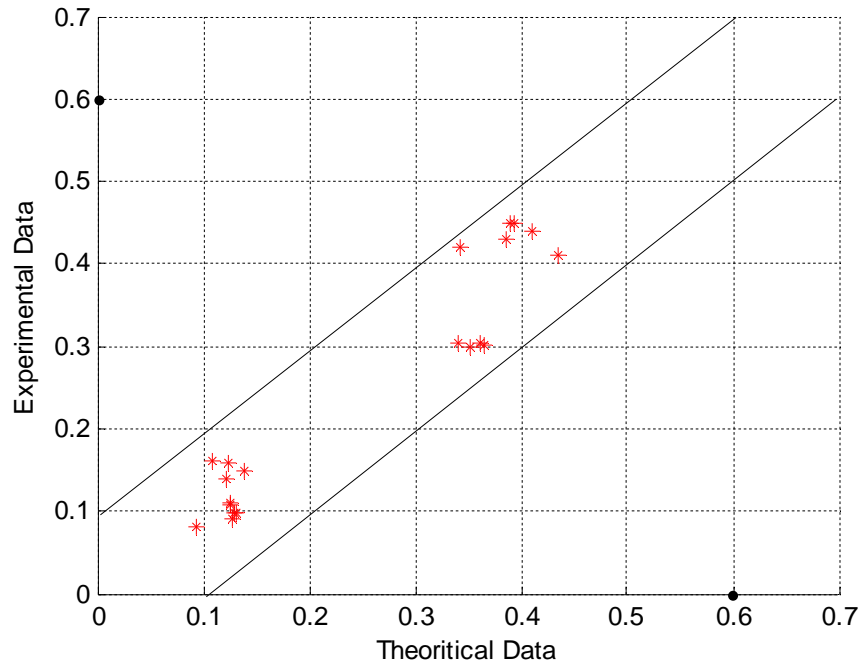


**Figure 5-36** Error between Experimental and EQ Model for Heat Duty=65W

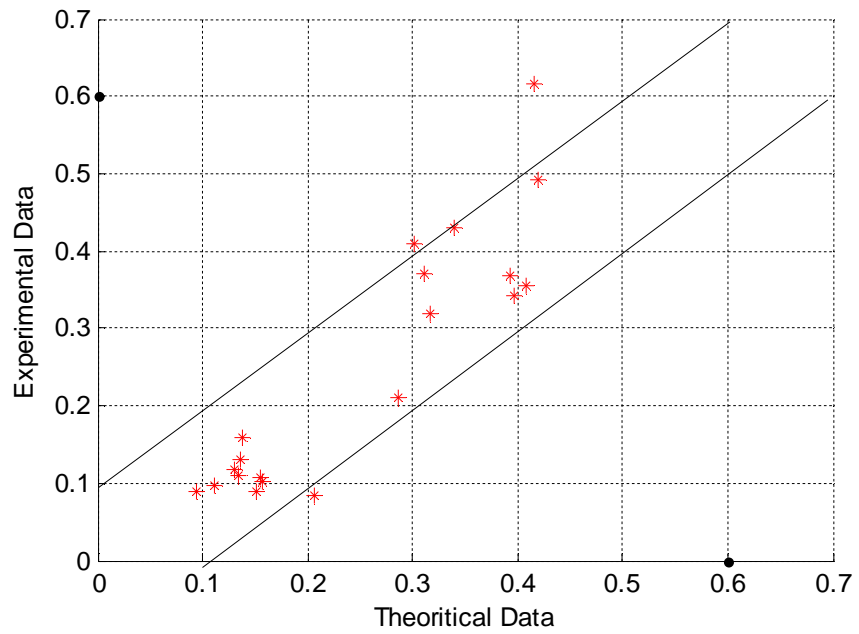


**Figure 5-37** Error between Experimental and EQ Model for Heat Duty=90W

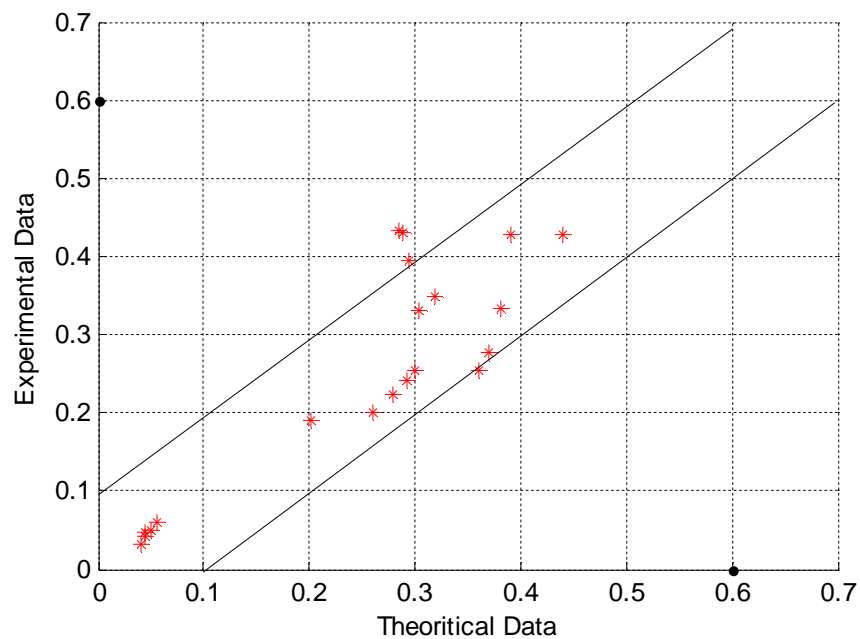


**Figure 5-38** Error between Experimental and EQ Model for 0% Water in Feed  
Catalyst KHSO<sub>4</sub>

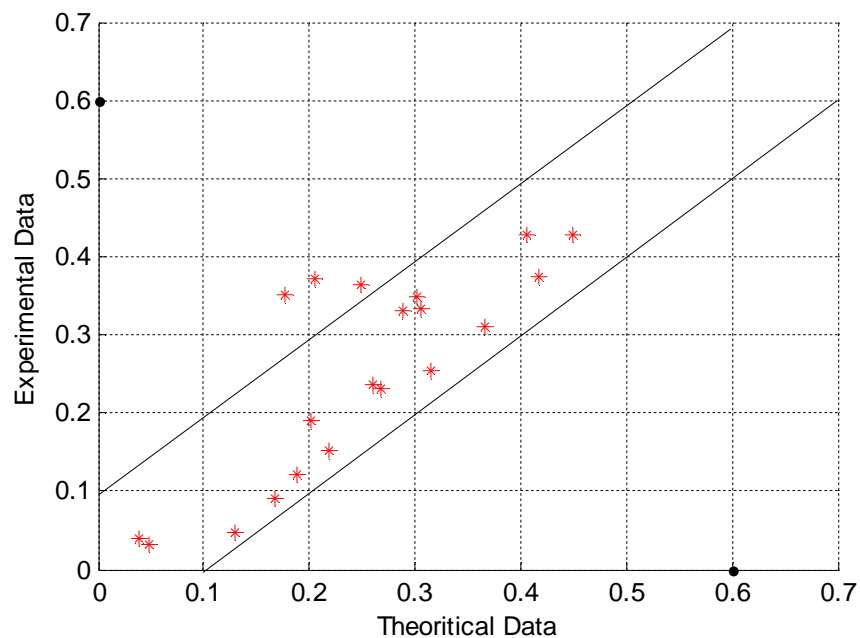


**Figure 5-39** Error between Experimental and EQ Model for 0% Water in Feed with Three  
Times Catalyst KHSO<sub>4</sub>

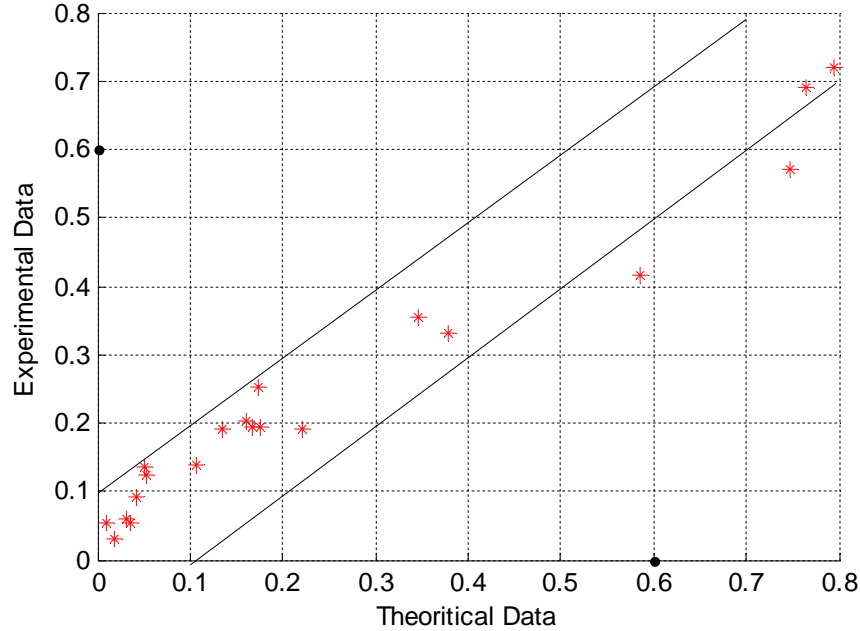


**Figure 5-40** Error between Experimental and EQ Model for Intermediate Reactive Section

### 5.6.3 Comparison of Experimental and Non-Equilibrium Model Results

For the same operating conditions of experimental work studied previously as well as the dimensions of distillation column and packing are used in rate-based model program in order to compare the results with the experimental work. Figures 5-41 to 5-43 show the comparison of experimental results with the results predicted from non-equilibrium model for variable reflux ratio 3, 4, and 5, Figures 5-44 and 5-45 show the comparison for variable boiler heat duty of 65, and 90W, Figures 5-46 and 5-47 show the comparison when no water used in feed for 0.04 kg catalyst/kg reactant and for 0.12 kg catalyst/ kg reactant, respectively, and finally Fig. 5-48 shows the comparison when the intermediate reactive section used. Theoretical results of non-equilibrium model are given in Appendix D.10.

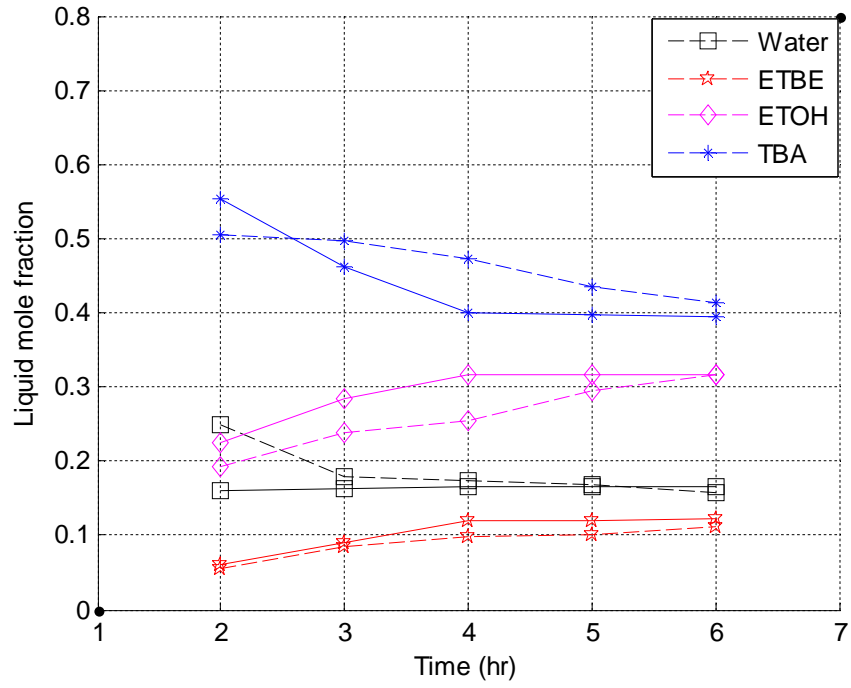


**Figure 5-41** Experimental and EQ Model Composition profile in the Distillate for  $Rr=3$   
 Solid Lines  $\equiv$  NEQ Model, Dashed Lines  $\equiv$  Experimental

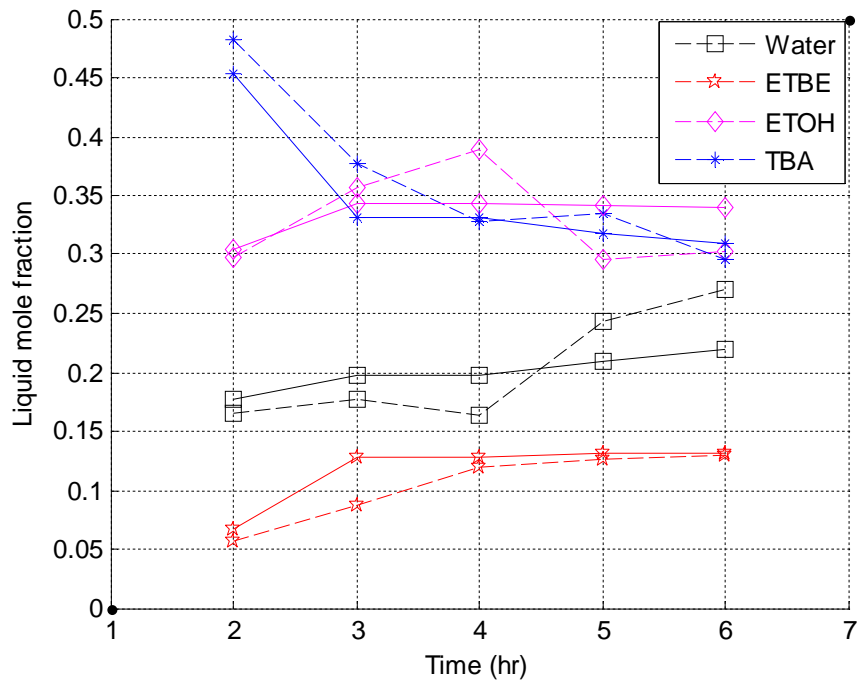


**Figure 5-42** Solid Lines  $\equiv$  NEQ Model, Dashed Lines  $\equiv$  Experimental,  $Rr=4$

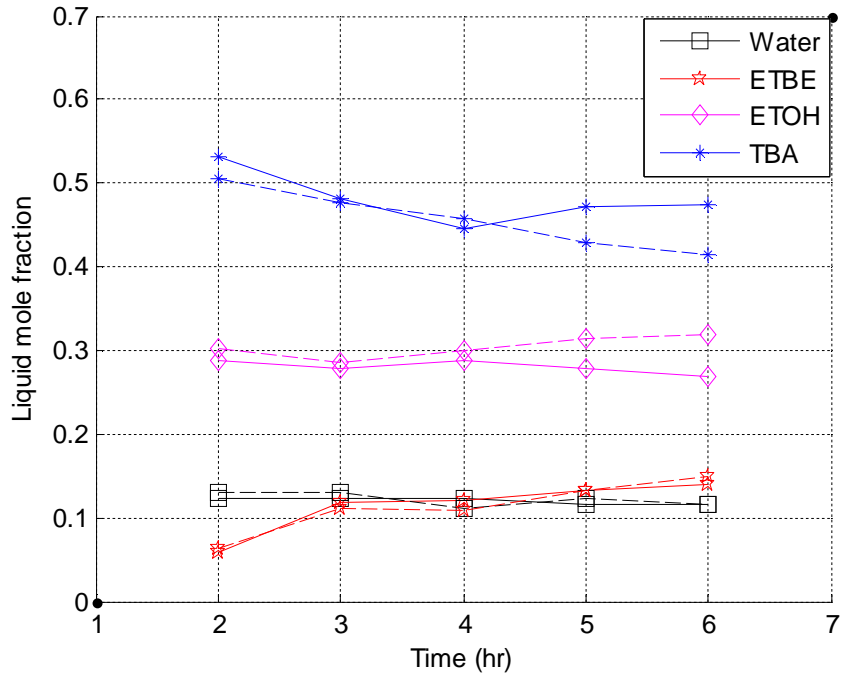


**Figure 5-43** Solid Lines = NEQ Model, Dashed Lines = Experimental,  $Rr=5$

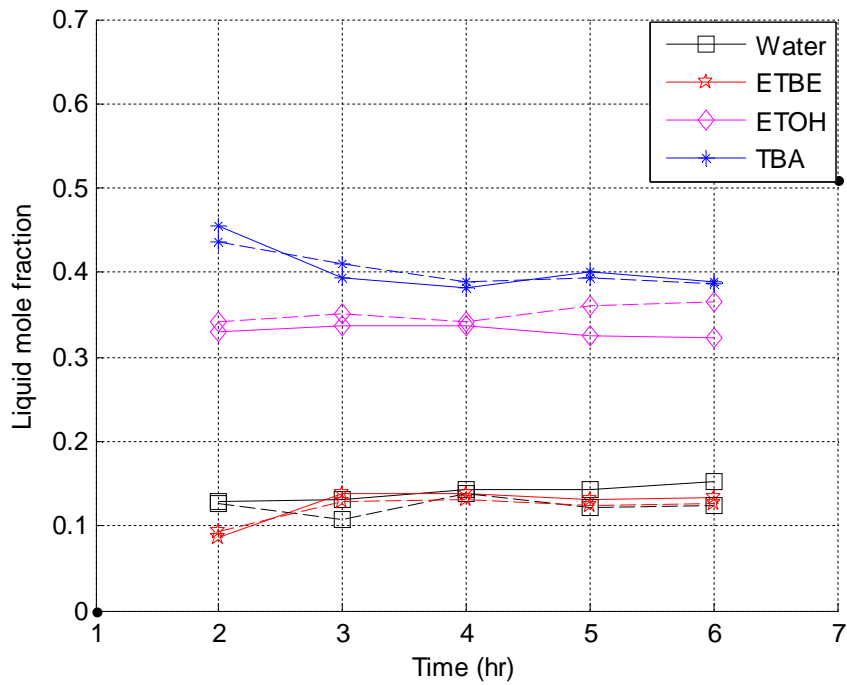


**Figure 5-44** Solid Lines = NEQ Model, Dashed Lines = Experimental, for Heat Duty=65W

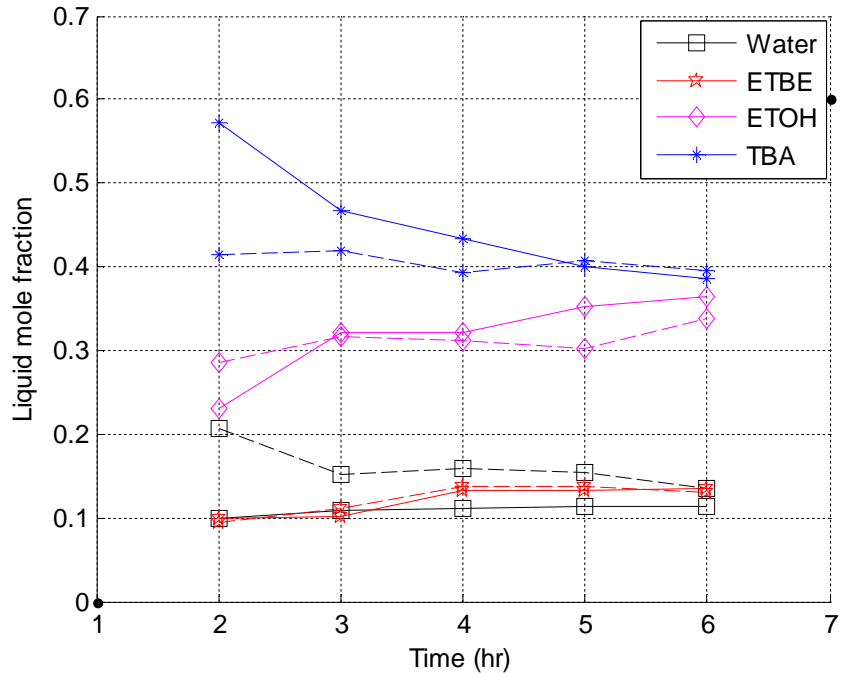


**Figure 5-45** Solid Lines  $\equiv$  NEQ Model, Dashed Lines  $\equiv$  Experimental, for Heat Duty=90W

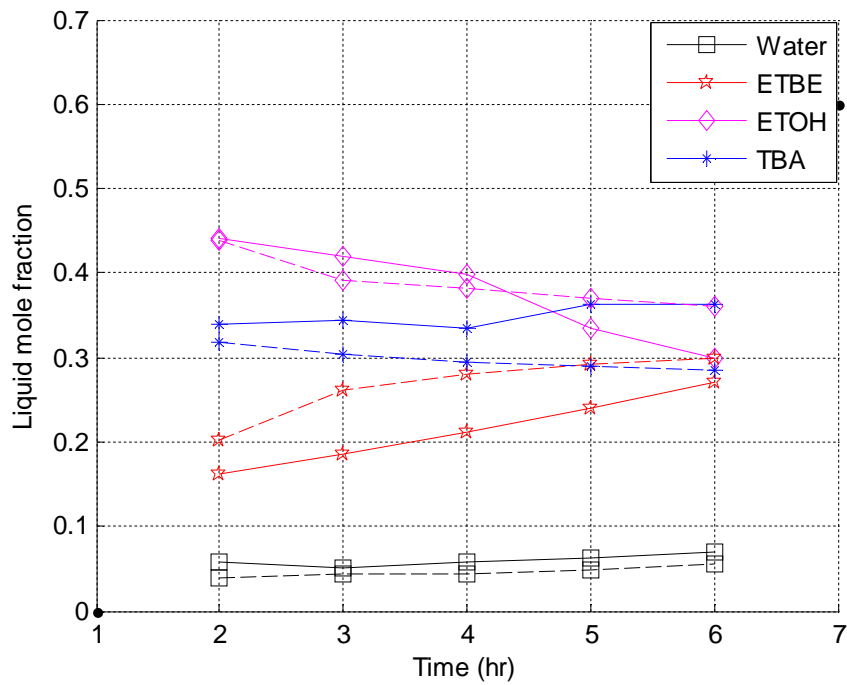


**Figure 5-46** Solid Lines  $\equiv$  NEQ Model, Dashed Lines  $\equiv$  Experimental, 0% Water in feed, Catalyst KHSO<sub>4</sub>

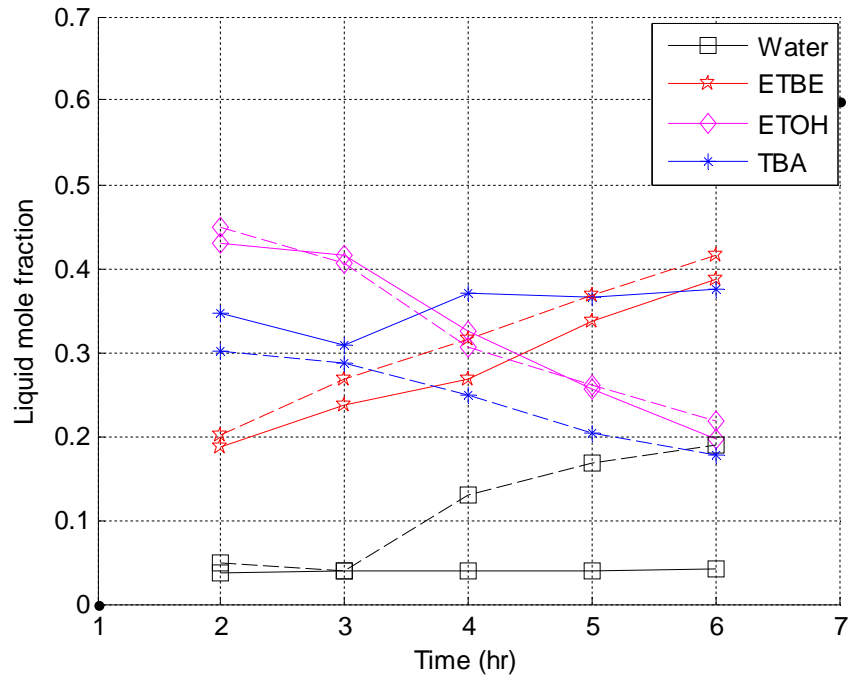


**Figure 5-47** Solid Lines  $\equiv$  NEQ Model, Dashed Lines  $\equiv$  Experimental, 0% Water in feed, Three Times Catalyst  $\text{KHSO}_4$

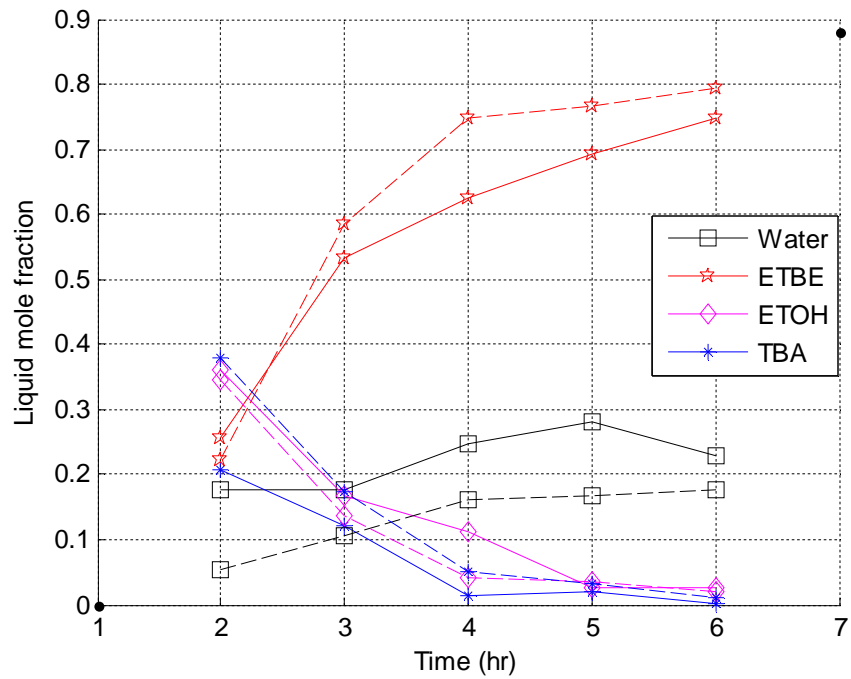


**Figure 5-48** Solid Lines  $\equiv$  NEQ Model, Dashed Lines  $\equiv$  Experimental, Intermediate Reactive Section

From the above figures the liquid mole fraction profiles of each components in the distillate predicted from the rate-based or non-equilibrium model are nearly equal to the experimental profiles more than the liquid fraction profiles obtained from equilibrium model Figures 5-25 to 5-32. i.e. the deviation of non equilibrium model from experimental data is less than the deviation of equilibrium model from experimental data. The errors between the experimental and the non-equilibrium model results are plotted in Figures 5-49 to 5-56 which are bounded within  $\pm 10\%$  lines.

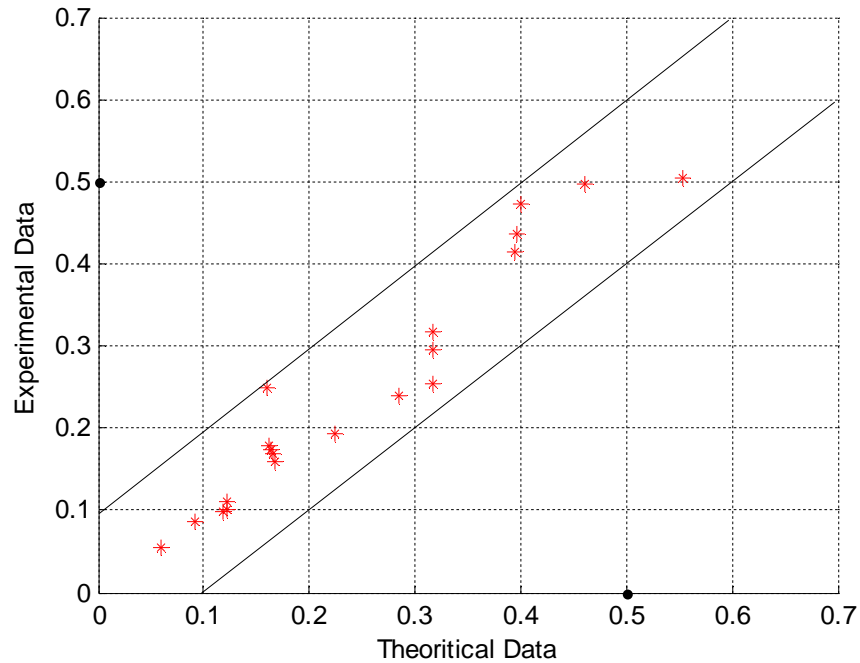


**Figure 5-49** Error between Experimental and NEQ Model for  $Rr=3$



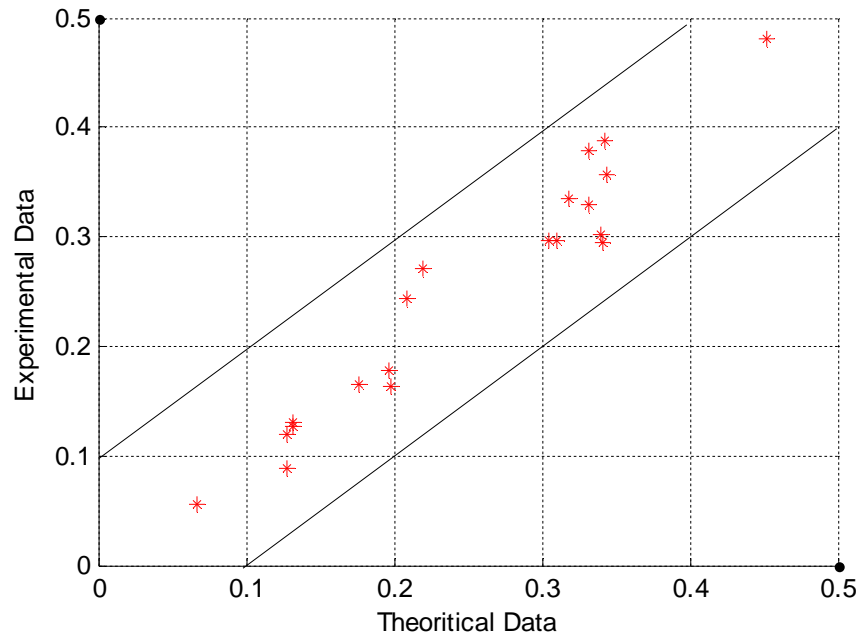


**Figure 5-50** Error between Experimental and NEQ Model for  $Rr=4$

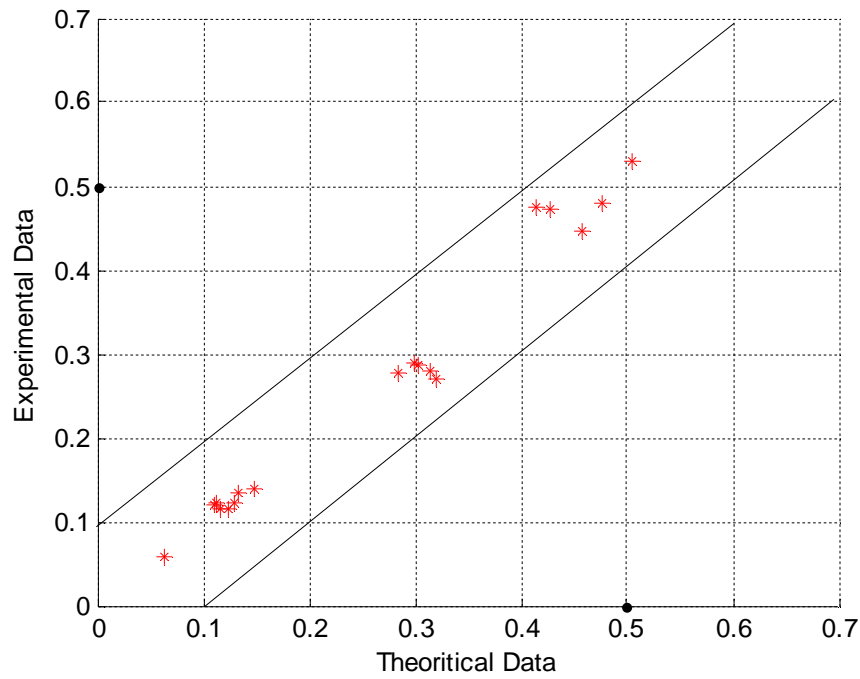


**Figure 5-51** Error between Experimental and NEQ Model for  $Rr=5$

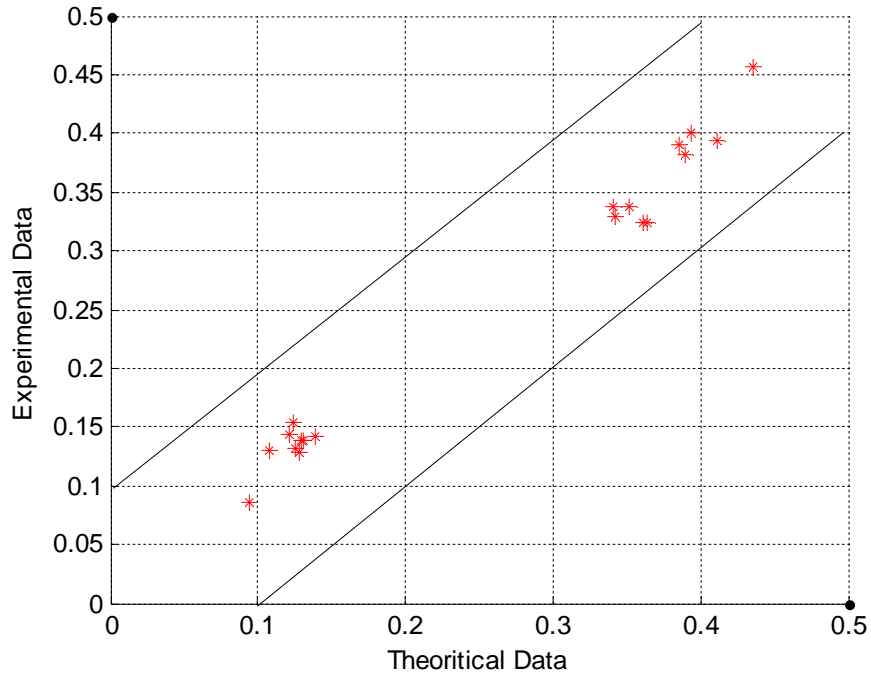


**Figure 5-52** Error between Experimental and NEQ Model for Heat Duty=65W

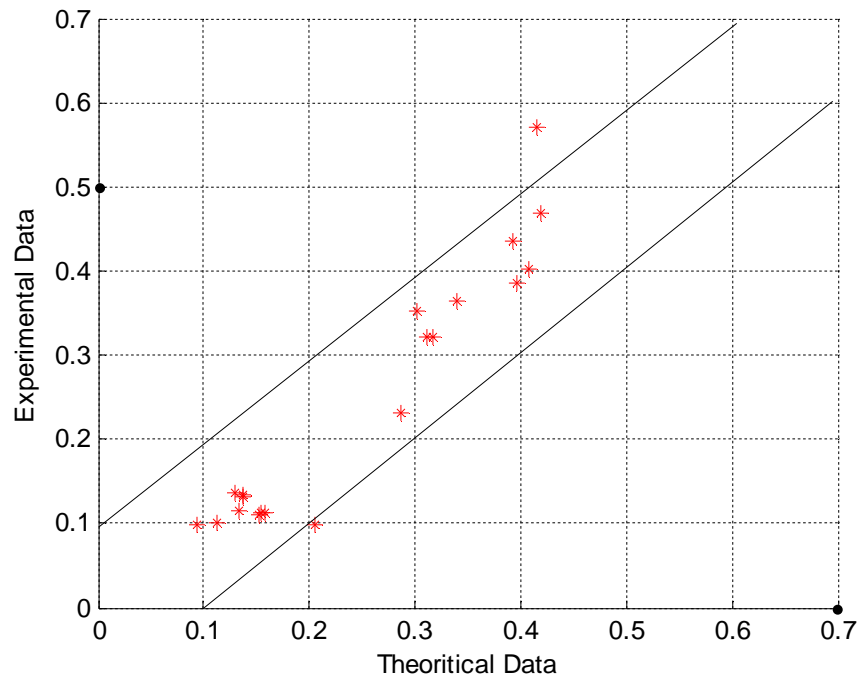


**Figure 5-53** Error between Experimental and NEQ Model for Heat Duty=90W

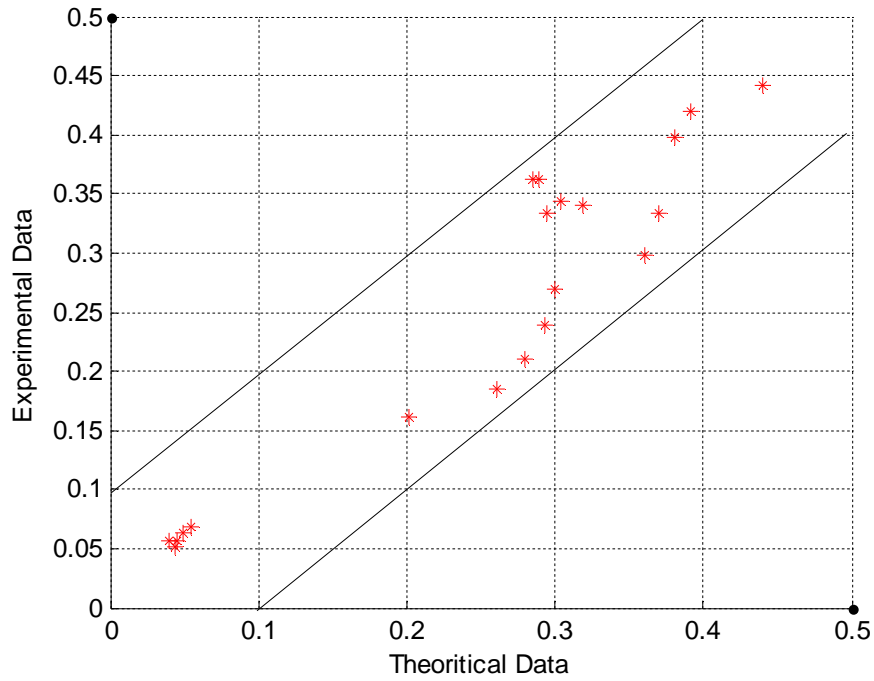


**Figure 5-54** Error between Experimental and NEQ Model for 0% Water in Feed, KHSO<sub>4</sub>

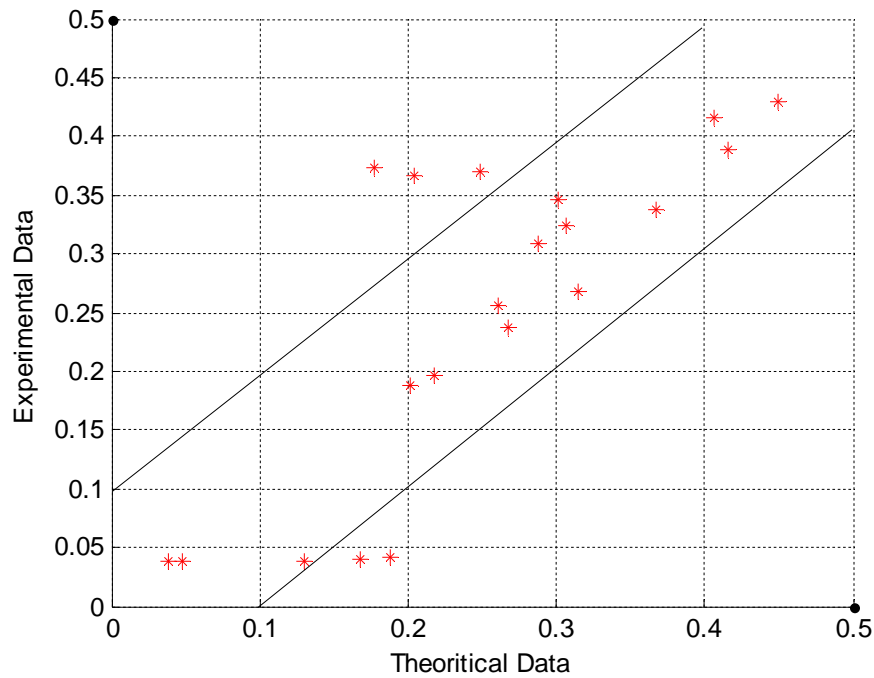


**Figure 5-55** Error between Experimental and NEQ Model for 0% Water in Feed Three Times Catalyst KHSO<sub>4</sub>

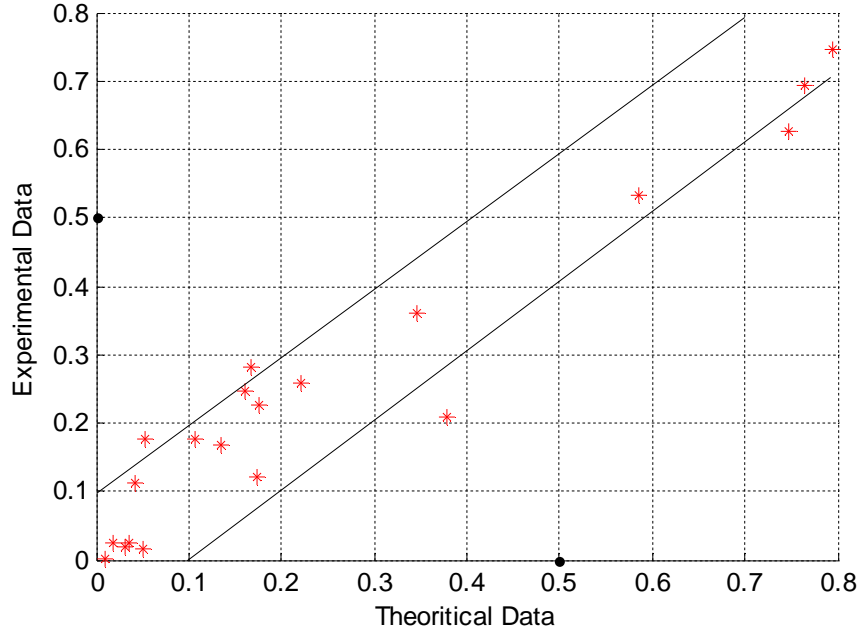


**Figure 5-56** Error between Experimental and NEQ Model for 0% Water in Feed Intermediate Reactive Section

### 5.6.4 Comparison of Equilibrium and Non-Equilibrium Model Results

In this section, the difference between the unsteady state results of equilibrium and non equilibrium models were explored. For the studied variables of experimental part the two models were compared. Figures 5-57 to 5-59 show the comparison of EQ and NEQ results for changing the reflux ratio, Figures 5-60 and 5-61 show the comparison for changing the boiler heat duty, Figures 5-62 and 5-63 show the comparison when no water used in feed for 0.04 kg catalyst/kg reactant and for 0.12 kg catalyst/ kg reactant, respectively, and Fig. 5-64 shows the comparison when the intermediate reactive section is used. From the results it can be observed that there is a small difference between the EQ and NEQ model, and the difference vary in nonlinear form with time. This is because in the non-equilibrium model the effect of mass and heat transfer on the process is taken into account, while, in equilibrium model it is neglected. Also, the consideration of a Murphee vapor efficiency of 1 in the equilibrium model.

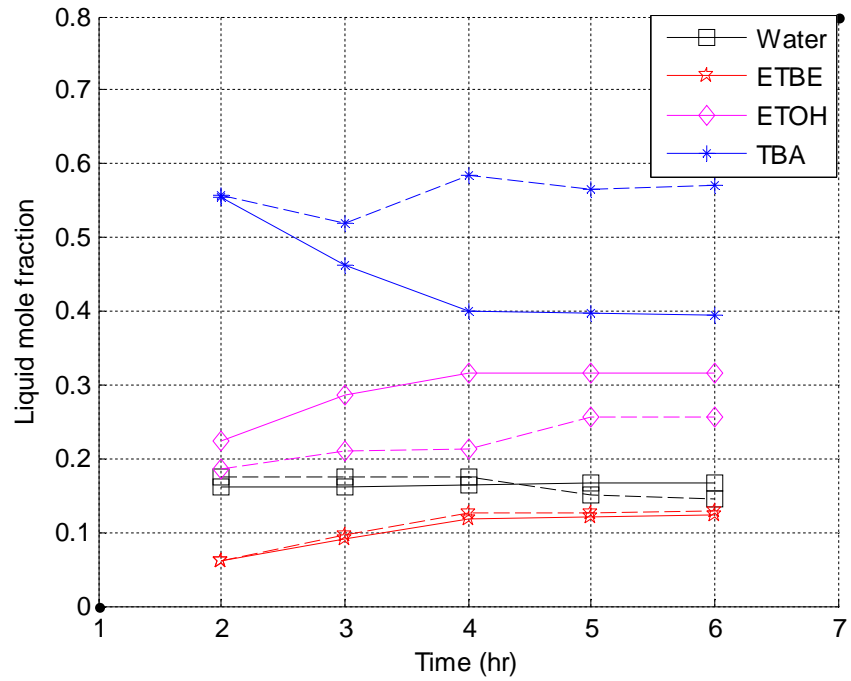


**Figure 5-57** Solid Lines  $\equiv$  NEQ Model, Dashed Lines  $\equiv$  EQ, for Rr=3

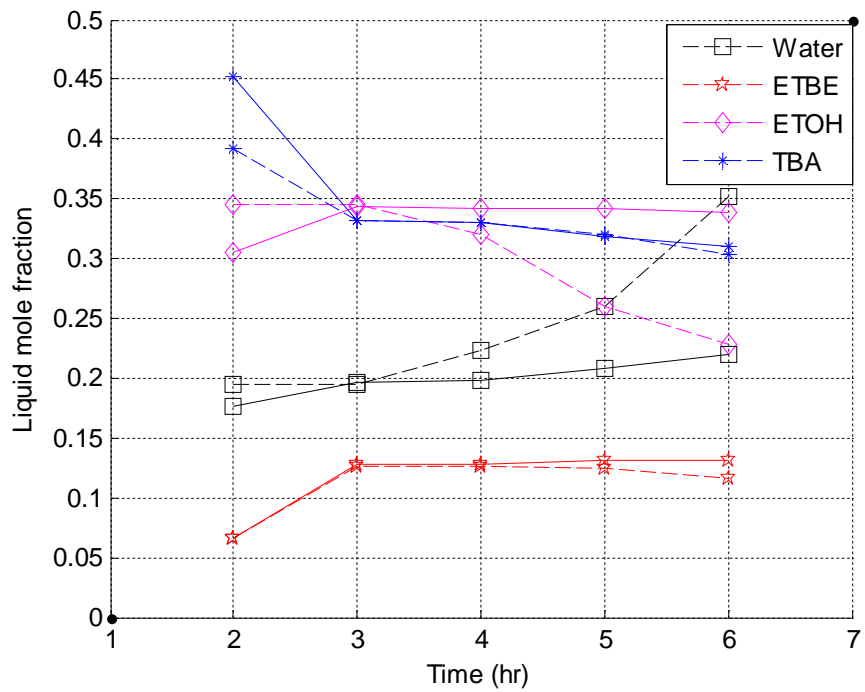


**Figure 5-58** Solid Lines  $\equiv$  NEQ Model, Dashed Lines  $\equiv$  EQ, for Rr=4

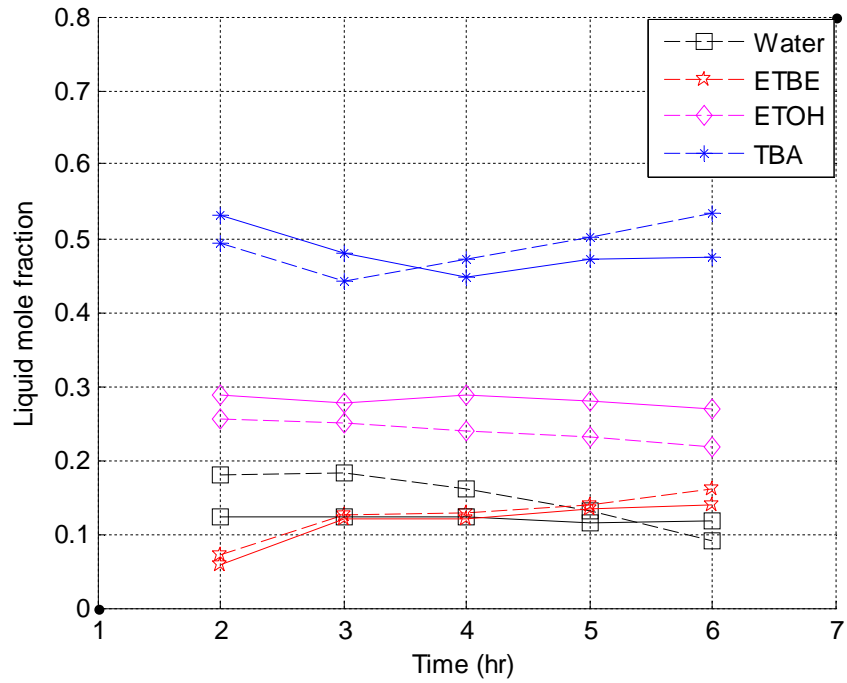


**Figure 5-59** Solid Lines  $\equiv$  NEQ Model, Dashed Lines  $\equiv$  EQ, for  $Rr=5$

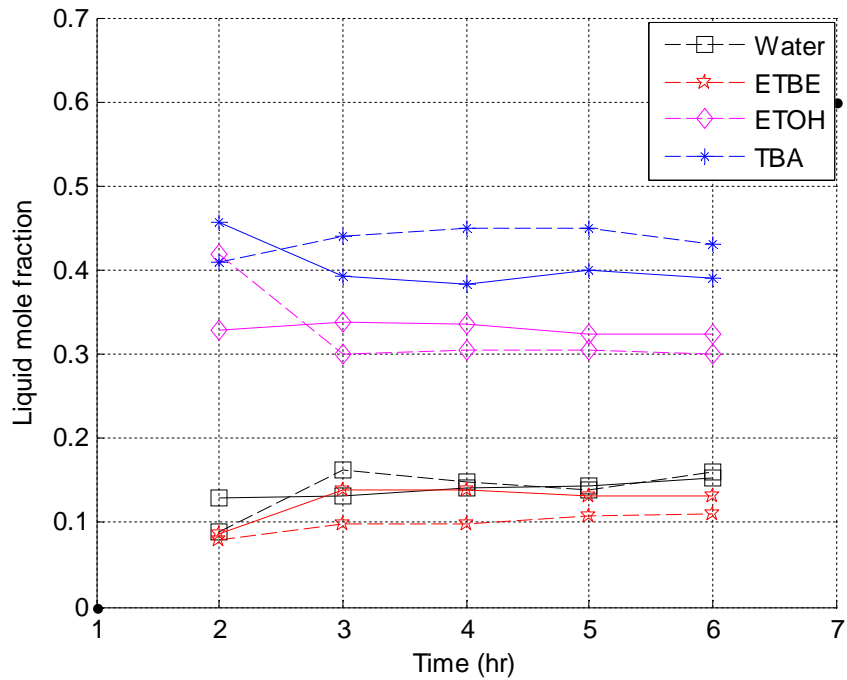


**Figure 5-60** Solid Lines  $\equiv$  NEQ Model, Dashed Lines  $\equiv$  EQ, for Heat Duty=65W

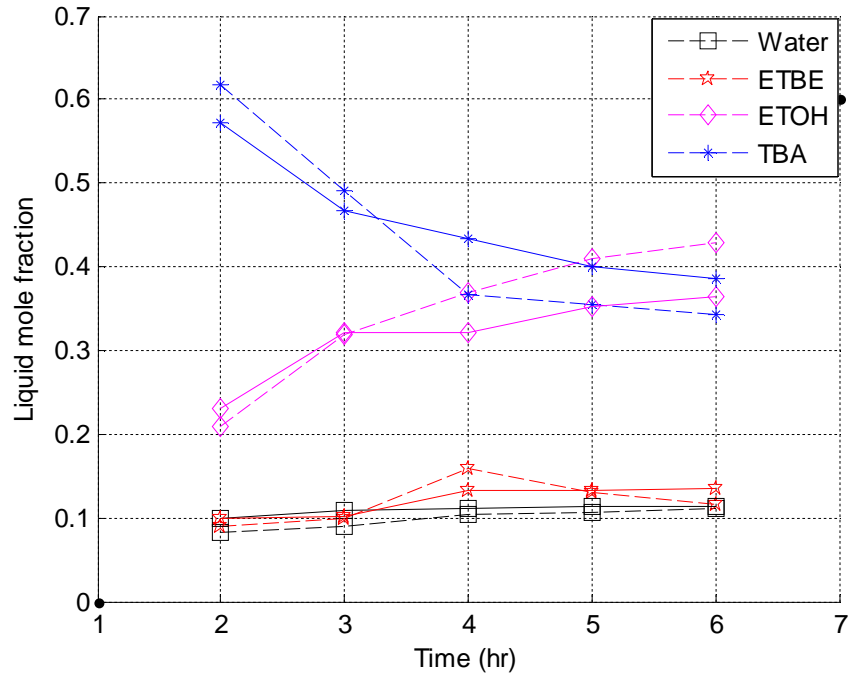


Figure 5-61 Solid Lines  $\equiv$  NEQ Model, Dashed Lines  $\equiv$  EQ, for Heat Duty=90W

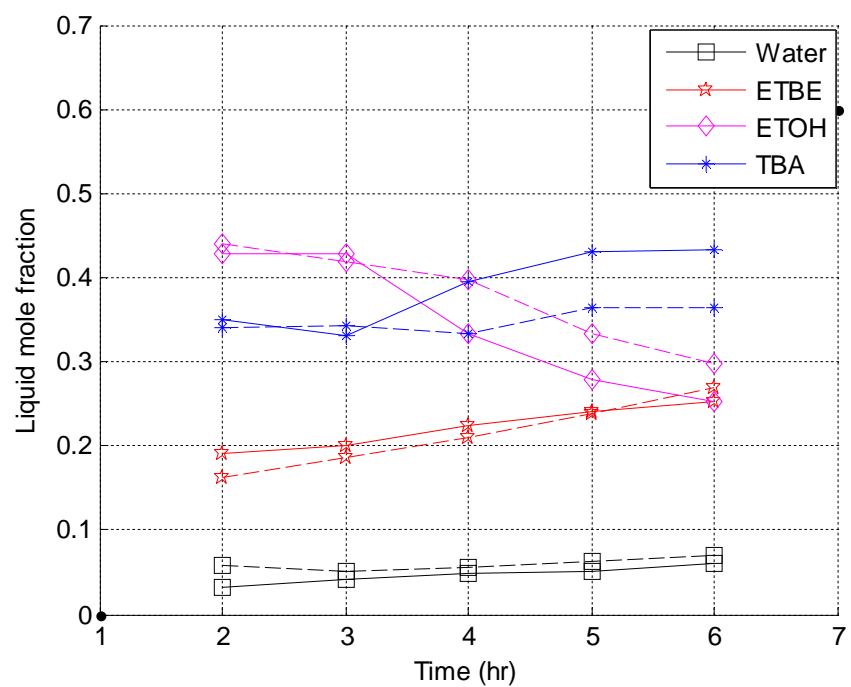
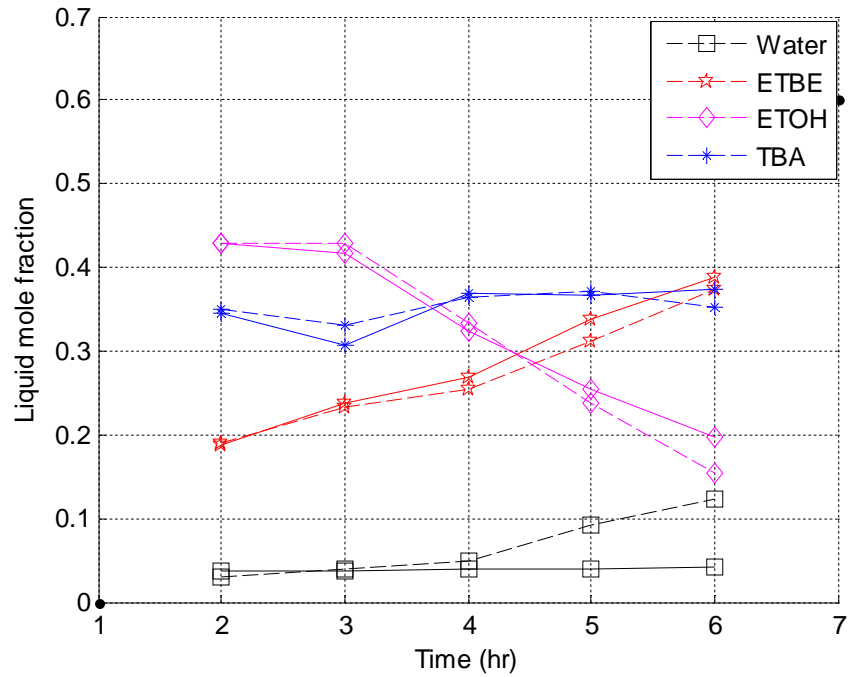
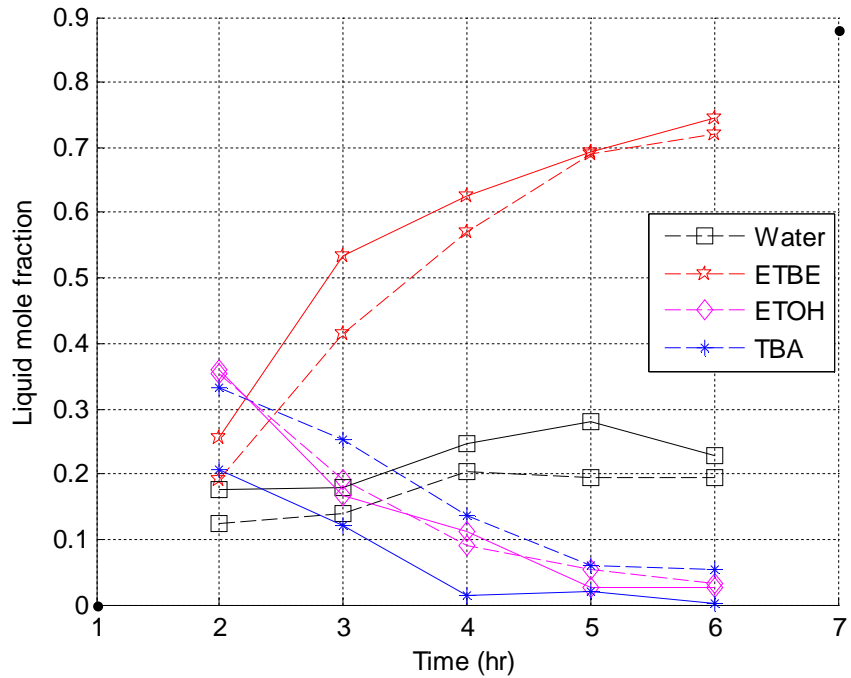


Figure 5-62 Solid Lines  $\equiv$  NEQ Model, Dashed Lines  $\equiv$  EQ, for 0% Water in Feed Catalyst KHSO<sub>4</sub>



**Figure 5-63** Solid Lines  $\equiv$  NEQ Model, Dashed Lines  $\equiv$  EQ, for 0% Water in Feed  
Three Times Catalyst  $\text{KHSO}_4$



**Figure 5-64** Solid Lines  $\equiv$  NEQ Model, Dashed Lines  $\equiv$  EQ,  
Intermediate Reactive Section



From the above figures all liquid compositions are in distillate. The liquid mole fraction of each component on stage with time is obtained from the NEQ program. Figures 5-65 to 5-68 show the liquid compositions profiles along stages for ethanol, tert-butanol, ethyl tert-butyl ether, and water with time, respectively, for reflux ratio of 5 and heat duty of 146W. Figures 5-69 to 5-72 show the liquid composition profiles with time for ETBE when reflux ratio 3, reflux ratio 4, heat duty 65W, and heat duty 90W, respectively, where the profiles of other components are nearly the same as for reflux ratio 5 and heat duty 146W. Figures 5-73 to 5-75 show the liquid composition profiles for ETBE for 0% water in feed with 0.04 kg catalyst / kg reactant, for 0% water in feed with 0.12 kg catalyst / kg reactant, and for the intermediate reactive section, respectively. These figures show that the composition of ETBE increases with time at the top of distillation column because ETBE has the lowest boiling point among other components. While, the concentrations of ETOH and TBA decrease with time, since they react to produce ETBE, and increase toward the top of the column because their lower boiling point in the system, and finally the composition of water increases towards the bottom of tower since it is the heaviest component.

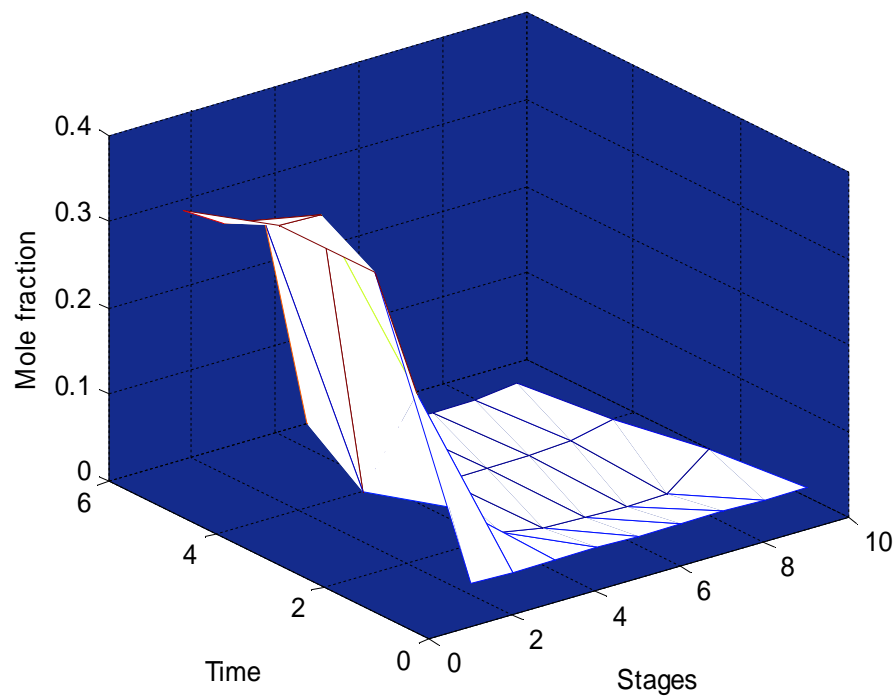


**Figure 5-65** ETOH Liquid Composition Profile,  $R_r=5$ , Heat Duty=146W

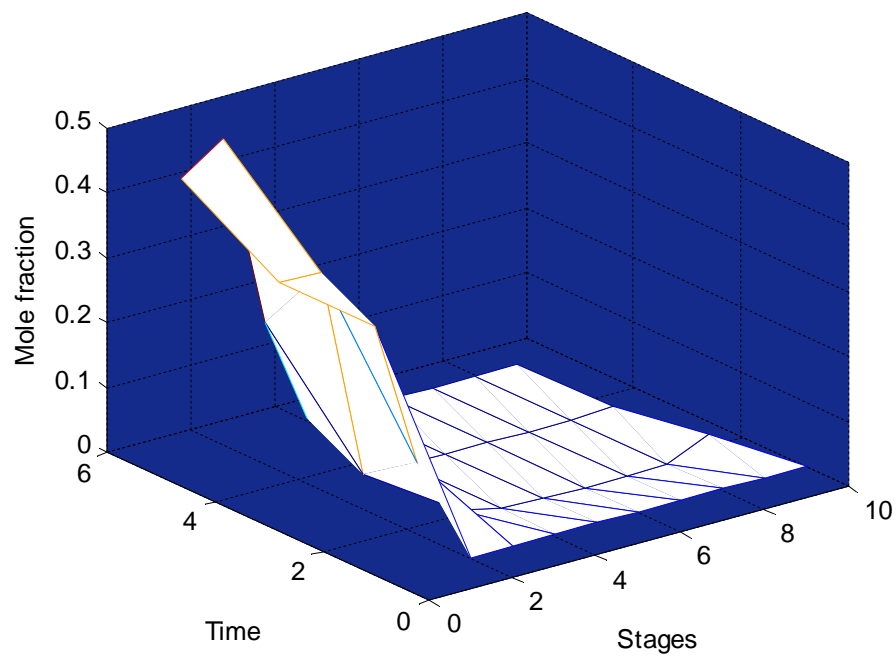


**Figure 5-66** TBA Liquid Composition Profile,  $R_r=5$ , Heat Duty=146W

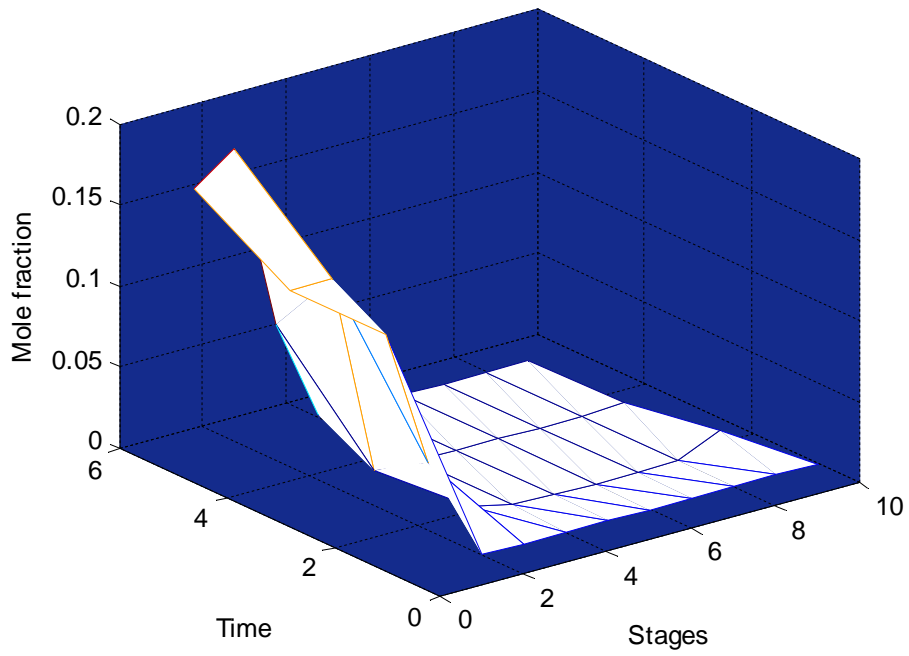


**Figure 5-67** ETBE Liquid Composition Profile,  $R_r=5$ , Heat Duty=146W

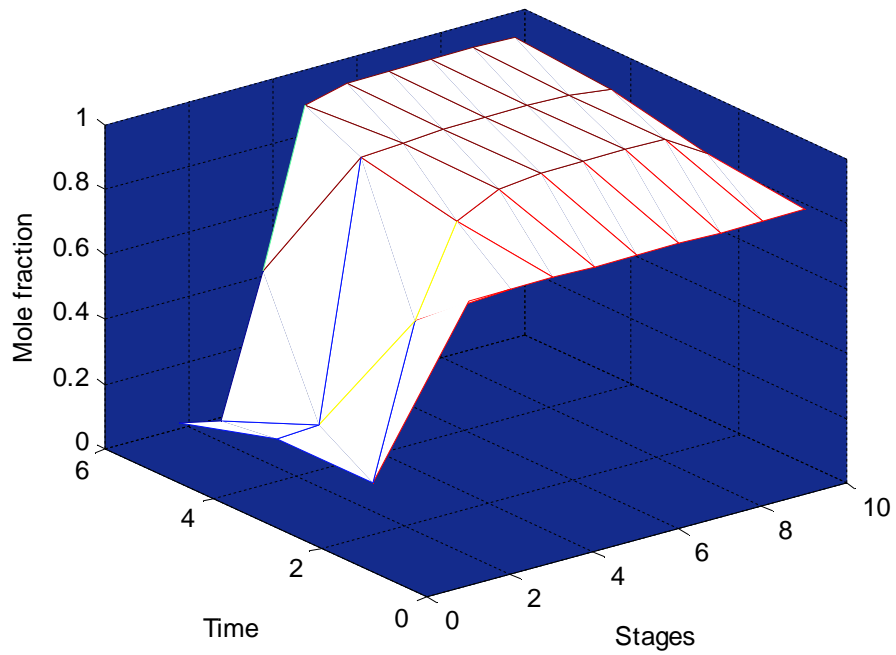


**Figure 5-68** Water Liquid Composition Profile,  $R_r=5$ , Heat Duty=146W

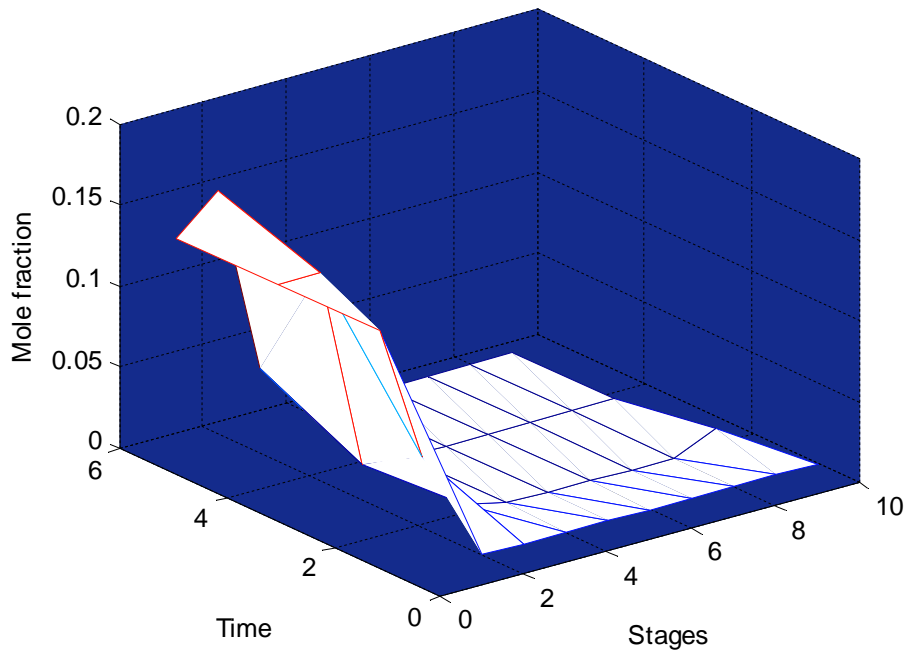


**Figure 5-69** ETBE Liquid Composition Profile,  $R_r=3$ , Heat Duty=146W

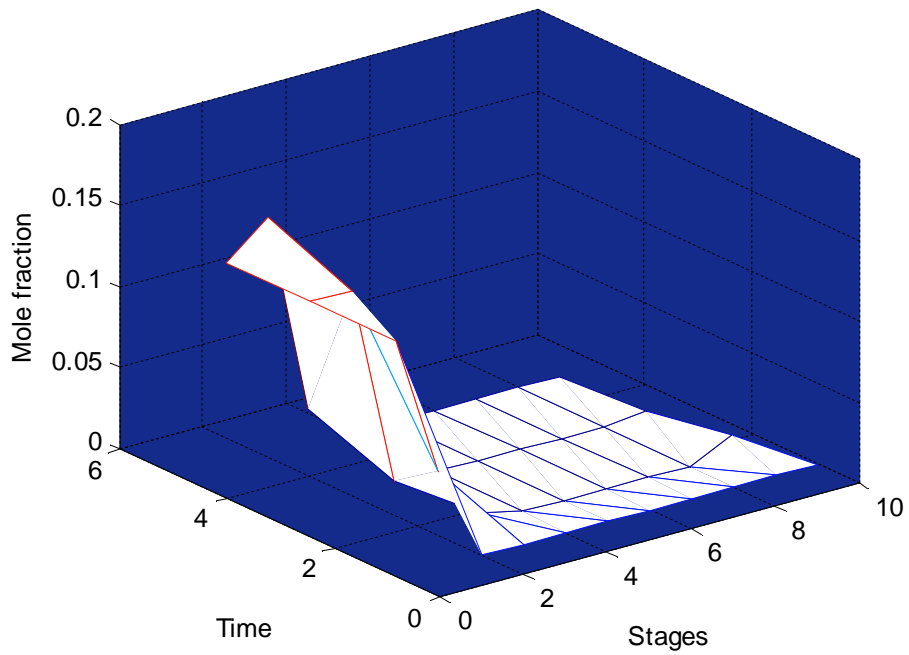


**Figure 5-70** ETBE Liquid Composition Profile,  $R_r=4$ , Heat Duty=146W

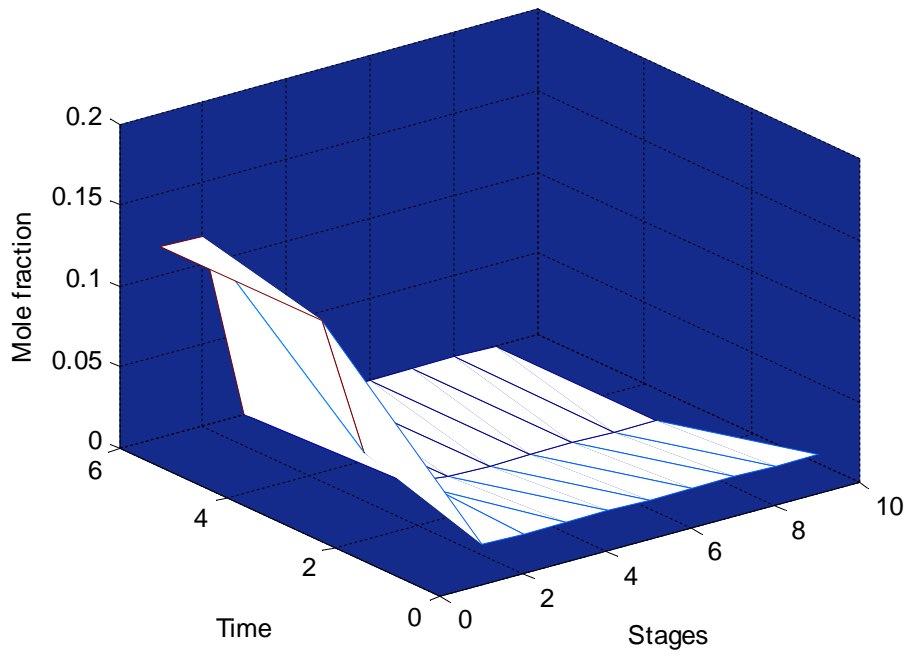


**Figure 5-71** ETBE Liquid Composition Profile,  $R_r=5$ , Heat Duty=65W

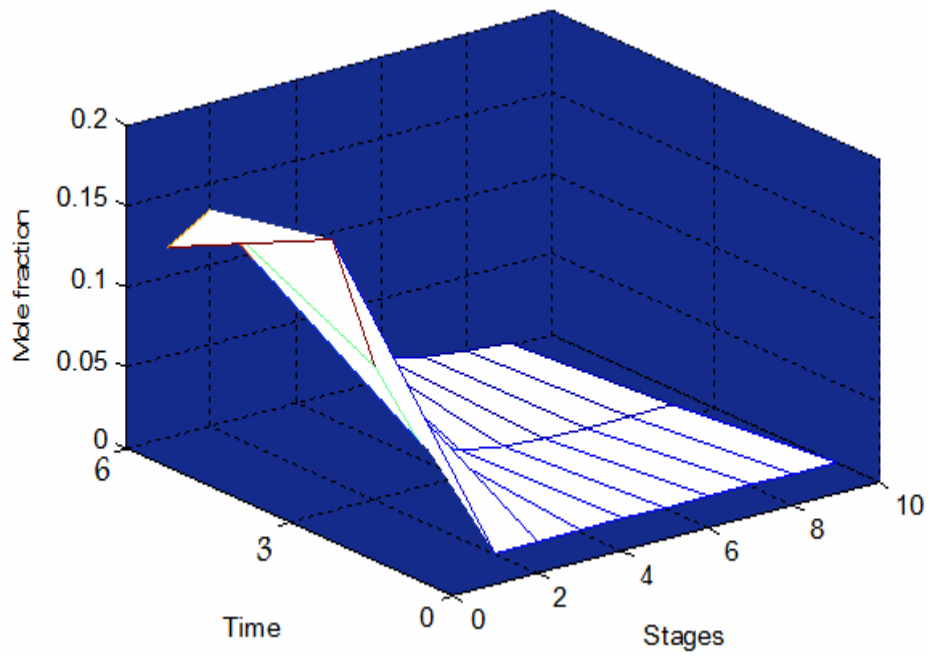


**Figure 5-72** ETBE Liquid Composition Profile,  $R_r=5$ , Heat Duty=90W

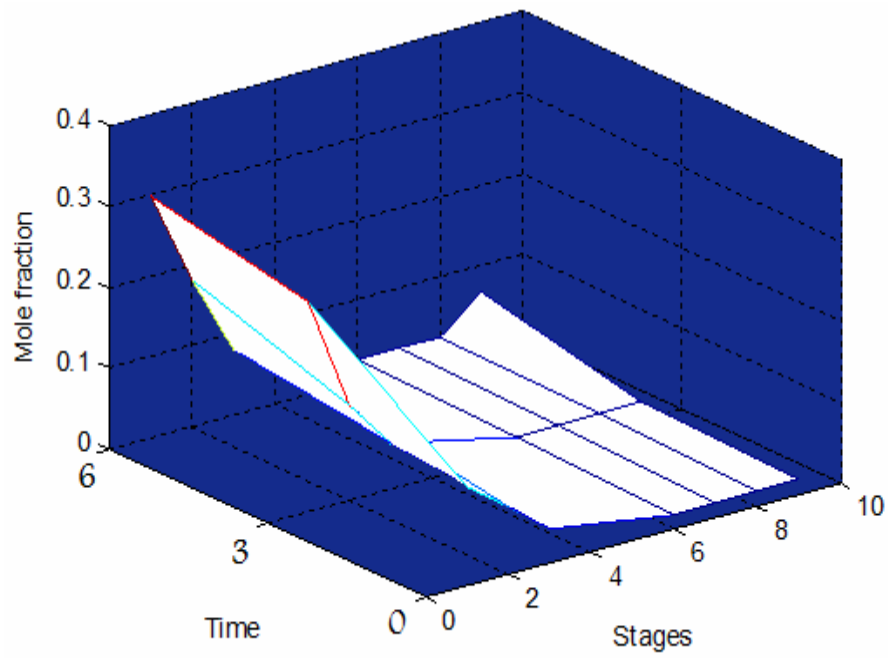


**Figure 5-73** ETBE Liquid Composition Profile, for 0% Water in Feed with 0.04 kg Catalyst / kg Reactant

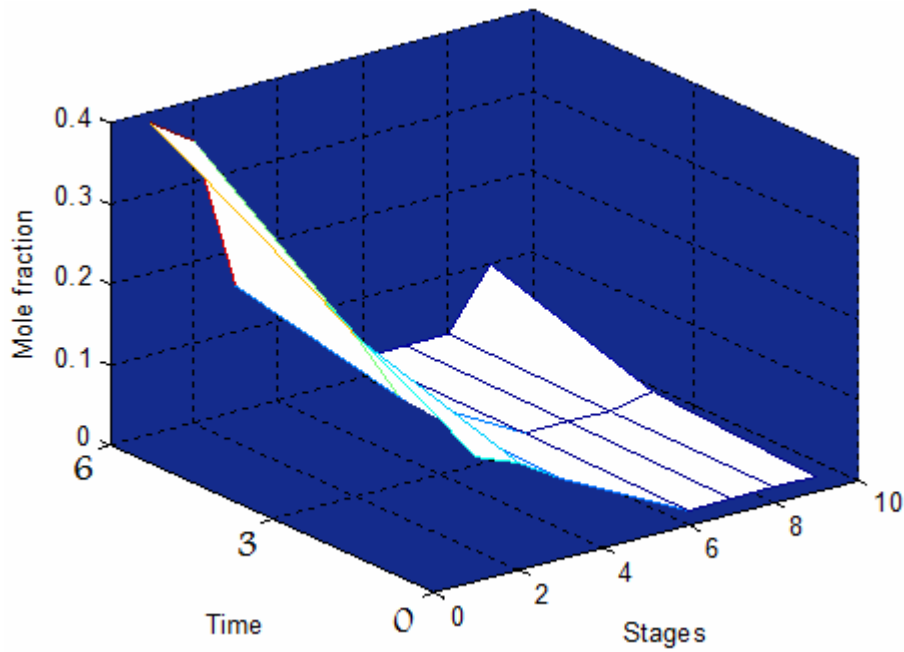


**Figure 5-74** ETBE Liquid Composition Profile, for 0% Water in Feed with 0.12 kg Catalyst / kg Reactant

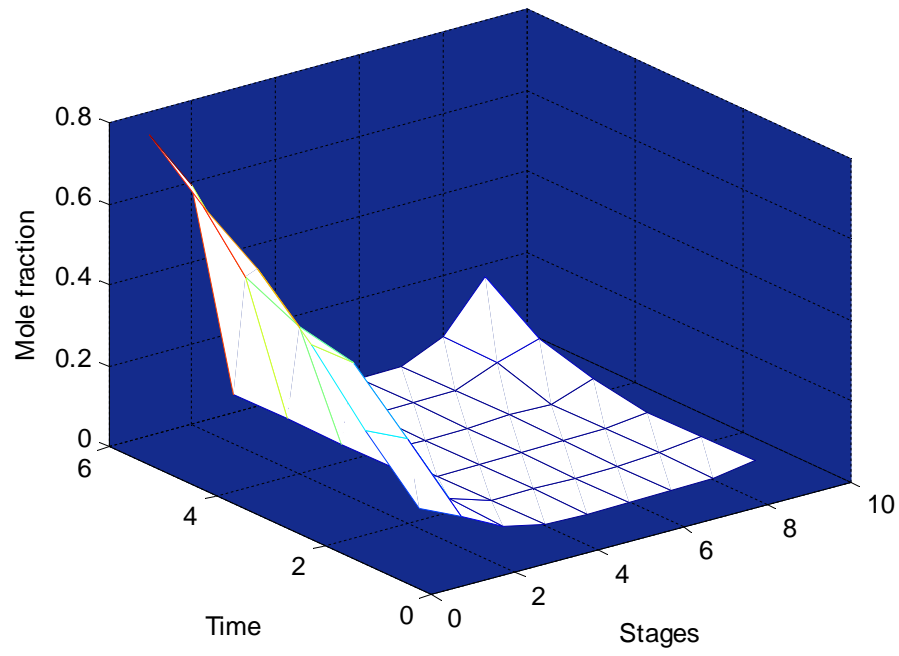


**Figure 5-75** ETBE Liquid Composition Profile, for Intermediate Reactive Section

## Chapter Six

### Conclusions and Recommendations

#### 6.1 Conclusions

Several conclusions have been extracted from the present work:

1. As the feed molar ratio of ethanol to tert-butanol increases, the purity of ethyl tert-butyl ether in the distillate decreases, and the best FMR was 1.
2. For the reflux ratio studied in the present work, increasing the reflux ratio cause the purity of ETBE in the distillate to increase, and the best reflux ratio was 5.
3. Changing the heat duty of still affects the composition where the increase of heat duty increases the purity of ETBE at the top.
4. When sulfuric acid was used as a catalyst purity of ETBE in the distillate and TBA conversion is higher than that when potassium hydrogen sulfate was used as a catalyst. The purity of ETBE was (0.29996) for potassium hydrogen sulfate compared with (0.61317) for sulfuric acid and % conversion was (85.5775%) when using potassium hydrogen sulfate while, % conversion for sulfuric acid was (94.789%).
5. The purity of ETBE can be improved by increasing the amount of catalyst, but it is also augment the cost of the process, it was changed from (0.29996) to (0.41622) when increasing the catalyst amount from 0.04 kg catalyst/kg reactant to 0.12 kg catalyst/kg reactant.
6. Intermediate reactive section gives better results (purity of ETBE, and conversion of TBA) than the reactive still, but this type of process needed higher amount of catalyst.
7. UNIFAC liquid phase activity coefficient model is the most appropriate model to describe the non ideality of ETOH-TBA-ETBE-H<sub>2</sub>O system.
8. Both equilibrium model program profiles and the rate-based model program profiles agreed with profiles of components from the experimental work. The



NEQ model profiles are near to the experimental profiles more than the EQ model.

9. Purification of ETBE by adding water to extract the alcohols present with ETBE in the distillate can vary with the variation of the amount of water added. Increasing the ratio of water to distillate (from 1:1 to 2:1 and 4:1) results in more purified ETBE, but increasing the water ratio from 2:1 to 4:1 has little significance on increasing purity of ETBE.

## **6.2 Recommendations for the Future Work**

The following suggestions for future work can be considered:

1. Studying a reactive distillation unit with tray column experimentally to produce ETBE.
2. Reactive distillation catalyzed with heterogeneous catalyst such as Amberlyst 15 or  $\beta$ -Zeolite to produce ETBE, which needs to take the geometry of catalyst particles and their distribution in consideration especially in the rate-based model.
3. Using continuous mode of reactive distillation to produce ETBE where the steady state operation is considered.

## References

- Abrams, D. S. and J. M. Prausnitz, *AIChE J.*, 21, 116-128 (1975), cited in Seader and Henley (1998).
- Al-Arfaj, M. A. and W. L. Luyben, "Effect of number of fractionating trays on reactive distillation performance", *AIChE Journal*, Vol. 46, No. 12, December (2000).
- Al-Arfaj, M. A. and W. L. Luyben, "Control study of ethyl tert-butyl ether reactive distillation", *Ind. Eng. Chem. Res.*, 41, 3784-3796, (2002).
- Al-Harhi, F. S., A. E. Abasaheed, and I. S. Al-Mutaz "Modeling and simulation of a reactive distillation unit for production of MTBE", M. Sc. Thesis, King Saud university, Kingdom Saudia Arabia, June (2008).
- Al-Zaidi, M. D., and A. Al-Hemiri, "Estimation of mass transfer coefficient in a packed bed distillation column using batch mode", Ph. D. Thesis, University of Baghdad, Baghdad, Iraq (2009).
- ASPEN PLUS, version 10.2.1, Aspen Technology, Inc., Cambridge, MA. (2000).
- Assabumrungrat, S., D. Wangwattanasate, V. Pavarajarau, P. Praserttham, A. Arpornwichanop, and S. Goto "Production of ethyl tert-butyl ether from tert-butanol and ethanol catalyzed by  $\beta$ -Zeolite in reactive distillation", *Korean J. Chem. Eng.*, 21(6), 1139-1146 (2004).
- Bahar, A., and C. Ozgen "State estimation for a reactive batch distillation column", The International Federation of Automatic Control, Seoul, Korea, July 6-11, (2008).
- Baur, R., A. Higler, R. Taylor, and R. Krishna "Comparison of equilibrium stage and non equilibrium stage models for reactive distillation", *Chem. Eng. Journal*, 76, 33-47 (2000a).

- Baur, R., R. Taylor, and R. Krishna “Development of a dynamic non equilibrium cell model for reactive distillation tray columns”, Chem. Eng. Sci., 55, 6139-6154 (2000b).
- Baur, R., R. Taylor, and R. Krishna “Dynamic behavior of reactive distillation tray columns described with a non equilibrium cell model” Chem. Eng. Sci., 56, 1721-1729 (2001a).
- Baur, R., R. Taylor, and R. Krishna “Dynamic behavior of reactive distillation columns described by a non equilibrium stage model” Chem. Eng. Sci., 56, 2085-2102 (2001b).
- Billet, R., and M. Schultes “Advantage in correlating packed column performance”, IChem. E. Symp., No. 128, B129 (1992).
- Bisowarno B. H., and M. O. Tade “Dynamic simulation of startup in ethyl tert-butyl ether reactive distillation with input multiplicity”, Ind. Eng. Chem. Res., 39, 1950-1954 (2000).
- Bolun X., W. Jiang, Z. Guosheng, W. Huajun, and L. Shiqing “Multiplicity analysis in reactive distillation column using ASPEN PLUS” Chinese J. Chem. Eng., 14 (3), 301-308 (2006).
- Bravo, J. L., and J. R. Fair “Generalized correlation for mass transfer in packed distillation columns”, Ind. Eng. Chem. Processes Des. Dev., 21,162-170 (1982).
- Budi, H., Y. Tian, and M. O. Tade “Introduction of separation and reactive stages on ETBE reactive distillation columns, AIChE, 50, 646-653 (2004).
- Frednslund , A., R. L. Jones, and J. M. Prausnitz, AIChE J., 21, 1086-1099 (1975) sited in Seader and Henley (1998).
- Gomez, J. M., J. M. Reneaume, M. Roques, M. Meyer, and X. Meyer “A mixed integer nonlinear programming formulation for optimal design of a catalytic distillation column based on a generic non equilibrium model”, Ind. Eng. Chem. Res., 45, 1373-1388 (2006).

- Hamodi, H. M., N. B. Nakkash, and N. Al-Haboobi “Simulation of batch reactive distillation for production of methyl acetate”, M. Sc. Thesis, Al-Nahrain University, Baghdad, Iraq (2004).
- Hamza, T. M., and C. K. Haweel “Study of performance of batch reactive distillation”, M. Sc. Thesis, University of Baghdad, Baghdad, Iraq (2005).
- Harmsen, G. J. “Reactive distillation the front runner of industrial process intensification”, *Chemical Engineering and Processing*, 46, 774-780 (2007).
- Higler, A., R. Taylor, and R. Krishna “Modeling a reactive separation process using a non equilibrium stage model”, *Computers Chem. Engng.*, Vol. 22, Suppl., S111-S118 (1998).
- Higler, A., and R. Taylor “A non equilibrium model for reactive distillation”, Ph. D. Thesis, Clarkson university (1999).
- Higler, A., R. Taylor, and R. Krishna “Non equilibrium modeling of reactive distillation: multiple steady state in MTBE synthesis”, *Chem. Eng. Sci.*, 54, 1389-1395 (1999).
- Jensen, K., and R. Datta “Equilibrium thermodynamic analysis of the liquid- phase ethyl tert-butyl ether (ETBE) reaction”, *Ind. Eng. Chem. Res.*, (1994).
- Jhon, Y. H., and T. Lee “Dynamic simulation for reactive distillation with ETBE synthesis”, *Separation and Purification Technology*, 31, 301-317 (2003).
- Kenig, E. Y., A. Gorak, A. Pahalahti, K. Jakobsson, J. A. Ittamaa, and K. Sunmacher “Advanced rate-based simulation tool for reactive distillation”, *AIChE Journal*, Vol. 50, No. 2, 322-342, February (2004).
- Kister, H. Z. “Distillation design”, McGraw-Hill, Inc., New York (1992).
- Kooijman, H. A., and R. Taylor “Dynamic non equilibrium column simulation”, Ph.D. Thesis, Clarkson University (1995).
- Kooijman, H. A., and R. Taylor “The ChemSep book, technical document”, ChemSep user manual, October (1995).

- Kotora, M., Z. Svandova, and J. Markos “A three-phase non equilibrium model for catalytic distillation”, *Chemical Papers*, 63 (2), 197-204 (2009).
- Krishnamurthy, R., and R. Taylor “A non equilibrium stage model of multicomponent separation processes. Part I: Model description and method of solution”, *AIChE Journal*, Vol. 31, No. 3 (1985).
- Lei, Z., B. Chen, and Z. Ding “Special distillation processes”, Elsevier, China (2005).
- Li, Y., X. Yung, and S. Wu “Zeolite film packing: Application to synthesis of ETBE in a catalytic distillation column”, *Fuel Chemistry Division Preprints*, 48 (1), 439-440 (2003).
- Matouq M., A. T. Quitain, K. Takahashi, and S. Goto “Reactive distillation for synthesizing ethyl tert-butyl ether from low grade alcohol catalyzed by potassium hydrogen sulfate”, *Ind. Eng. Chem. Res.*, 35,982-984 (1996).
- Mohammed Z. M., and A. M. Shakoor “Mathematical modeling and simulation for production of MTBE by reactive distillation”, M. Sc. Thesis, University of Technology, Baghdad, Iraq, February (2009).
- Murat, M.N., A. R. Muhamed, and S. Bhatia “Modeling of a reactive distillation column: Methyl tert-butyl ether (MTBE) simulation studies, *IIUM Engineering Journal*, Vol. 4, No. 2 (2003).
- Nakkash, N. B., and A. H. Al-Zhazraji “Simulation of continuous reactive distillation”, *Jordan International Chemical Conference V (IICE05)*, 14, September (2005).
- Nakkash, N. B., N. Al-Habobi, and H. M. Hamodee “Simulation of batch reactive distillation for methyl acetate production”, *Spring National Meeting AIChE, T8000. Advances in distillation and absorption*, 23-March (2010).
- Onda, K., H. Takenchi, and Y. Okumoto “Mass transfer coefficients between gas and liquid phases in packed columns”, *Journal of Chemical Engineering of Japan*, Vol. 1, No. 1, 56-62 (1968).

- Orbey H., and S. Sandler “Modeling vapor-liquid equilibria, cubic equation of state and their mixing rules”, Cambridge series in chemical engineering, Cambridge, USA. (1998).
- Ozbay, N., and N. Oktar “Thermodynamic study of liquid phase synthesis of ethyl tert-butyl ether using tert-butanol and ethanol”, J. Chem. Eng. Data, 54, 3208-3214 (2009).
- Peng, D.Y., and D. B. Robinson “A new two-constant equation of state” Ind. Eng. Chem. Fundamentals, 15, 59-64 (1976).
- Peng, J., S. Lextrait, T. Edgar, and R. B. Eldridge “A comparison of steady state equilibrium and rate-based models for packed reactive distillation columns”, Ind. Eng. Chem. Res., 41, 2735-2744 (2002).
- Peng, J., T. Edgar, and R. B. Eldridge “Dynamic rate-based and equilibrium models for a packed reactive distillation columns”, Chem. Eng. Sci., 58, 2671-2680 (2003).
- Podrebarac, G. G., F.T. Ng, and G. L. Rempel “The production of diacetone alcohol with catalytic distillation Part II: A rate-based catalytic distillation model for the reaction zone”, Chem. Eng. Sci., Vol. 35, No. 5, 1077-1088 (1998).
- Perry, R. H., and D. W. Green “Perry’s chemical engineer’s handbook”, McGraw-Hill Companies, Inc. (1997).
- Quitain, A. T., and S. Goto “Liquid-liquid equilibrium of ternary ETBE-ETOH-H<sub>2</sub>O and quaternary ETBE-ETOH-H<sub>2</sub>O-TBA mixtures” The Canadian Journal of Chemical Engineering, Vol. 76, August (1998).
- Quitain, A. T., H. Itoh, and S. Goto “Industrial scale simulation of proposed process for synthesizing ethyl tert-butyl ether from bioethanol”, Journal of Chemical Engineering of Japan, Vol. 32, No. 4, 539-543 (1999a).
- Quitain, A. T., H. Itoh, and S. Goto “Reactive distillation for synthesizing ethyl tert-butyl ether from bioethanol”, Journal of Chemical Engineering of Japan, Vol. 3, No. 3, 280-287 (1999b).

- Reid, R. C., J. M. Prausnitz, and B. E. Poling “The properties of gases and liquids”, fourth edition, McGraw-Hill, Inc., New York (1987).
- Renon, H. and J. M. Prausnitz, *AIChE J.*, 14, pp. 135. Sited in Bouneb N., A-H Meniai, and W. Louaer “Introduction of the group contribution concept into the NRTL model”, *ESCAPE20*, Elsevier B. V. (2010).
- Seader, J.D., and E. J. Henley “Separation process principles”, John Wiley and Sons, Inc., New York (1998).
- Singh, A. P., J. C. Thompson, and B. B. He “A continuous-flow reactive distillation reactor for biodiesel preparation from seed oils”, *ASAE/CSAE Meeting Presentation*, 1-4 August (2004).
- Sinnott, R. K. “Coulson and Richardson’s chemical engineering, chemical engineering design Vol. 6”, third edition, Butterworth Heinemann (1999).
- Slokiewicz, P. M. “Determination of the Lungmuir-Hinshelwood kinetic equation of synthesis of ethers”, *Applied Catalysis A:General*, 269,33-42 (2004).
- Smith, J. M., H. C. Van ness, and M. M. Abbot “Introduction to chemical engineering thermodynamics”, sixth edition, McGraw-Hill Chemical Engineering Series, USA (2001).
- Sneesby, M. G., M. Tade, R. Datta, and T. N. Smith “ETBE synthesis via reactive distillation 1. Steady state simulation and design aspects”, *Ind. Eng. Chem. Res.*, 36, 1855-1869 (1997a).
- Sneesby, M. G., M. Tade, R. Datta, and T. N. Smith “ETBE synthesis via reactive distillation 1. Dynamic simulation and control aspects”, *Ind. Eng. Chem. Res.*, 36, 1870-1881 (1997b).
- Soave, G. “Equilibrium constants from a modified Redlich-Kowng equation of state”, *Chem. Eng. Sci.*, 27, 1197-1203 (1972).
- Sundmacher, K., and U. Hoffmann “Development of a new catalytic distillation process for fuel ethers via a detailed non equilibrium model”, *Chem. Eng. Sci.*, Vol.51, No. 10, 2359-2368 (1996).

- Sundmacher, K., and A. Kienle “Reactive distillation status and future directions”, Wiley-VHC (2002).
- Tade, M. O., and Y. Tian “Conversion influence for ETBE reactive distillation”, Separation and Purification Technology, 19, 85-91 (2000).
- Taylor, R. and R. Krishna “Review modeling reactive distillation”, Chem. Eng. Sci., 55, 5183-5229 (2000).
- Toichigi, K., and K. Kojima, “The determination of group Wilson parameters to activity coefficients by ebulliometer”, Journal of Chemical Engineering of Japan, vol. 9, No. 4 (1976).
- Umar, M., R. Saleemi, N. Feroz, and S. Qaiser “Synthesis of ETBE in packed reactive distillation column using macroporous ion exchange resin catalyst”, World Congress on Engineering and Computer Science (WCECS), San Francisco, USA, 22-24 October (2008).
- Umar, M., A. R. Saleemi, and B. Saha “Liquid phase synthesis of ETBE from ethanol and tert-butyl alcohol using macroporous and gelular ion exchange resin catalyst”, The Nucleus, 46 (3), 101-107 (2009a).
- Umar, M., D. Patel, and B. Saha “Kinetic studies of liquid phase ethyl tert-butyl ether (ETBE) synthesis using macroporous and gelular ion exchange resin catalyst”, Chem. Eng. Sci., 46, 4424-4432 (2009b).
- Valsenko, N., Y. Nochkina, A. Topka, and P. E. Strizhak “Liquid phase synthesis of ethyl tert-butyl ether over acid cation-exchange inorganic-organic resins”, Applied Catalysis A: General, 362, 82-87 (2009).
- Varsili, D., and T. Dogn “Simultaneous production of tert-amyl ethyl ether and tert-amyl alcohol from isoamylene-ethanol-water mixtures in a batch reactive distillation column”, Ind. Eng. Chem. Res., 44, 5227-5232 (2005).
- Wagner, I., J. Stichlmair, and J. R. Fair “Mass transfer in beds of modern, high efficiency random packings”, Ind. Eng. Chem. Res., 36, 227-237 (1997).



- Walas, S. M. "Phase equilibria in chemical engineering", Butterworth Publications, London (1985).
- Yang, B., S. Yang, and H. Wang "Simulation for the reactive distillation process to synthesize ethyl tert-butyl ether", J. Chem. Eng. Of Japan, 34, 1165-1170 (2001).
- Yang, B. and H. Wang "Vapor-liquid equilibrium for mixtures of water, alcohols, and ethers", J. Chem. Eng. Data, 47, 1324-1329 (2002).

## Appendix A

### Equilibrium model properties

#### A.1 Heat of Formation (Reid et al., 1987).

Table A-1 Heat of Formation

Component	Heat of formation (J/mol)
Ethanol	$-276.6 \times 10^3$
Tert-butanol	$-359.01 \times 10^3$
ETBE	$-348.93 \times 10^3$
Water	$-287.91 \times 10^3$

#### A.2 Heat Capacity Constants of Liquid Phase in J/mol .K

Table A-2 Liquid Heat Capacity Coefficients (Jensen and Datta, 1994)

Component	a	B	c	D
Ethanol	-386.058	3.4299	-0.0081	$7.379 \times 10^{-6}$
Tert-butanol	-2971.14	24.47	-0.0637	$-6,5.543 \times 10^{-5}$
ETBE	18.79	1.251	$-3.015 \times 10^{-3}$	$3.637 \times 10^{-6}$
Water	44.56	0.45	$1.64 \times 10^{-3}$	$1.786 \times 10^{-6}$

#### A.3 Heat Capacity Constants of Vapor Phase in J/mol .K (Reid et al., 1987).

Table A-3 Vapor Heat Capacity Coefficients

Component	$a_v$	$b_v$	$c_v$	$d_v$
Ethanol	9.014	$2.141 \times 10^{-1}$	$-8.39 \times 10^{-5}$	$1.373 \times 10^{-9}$
Tert-butanol	$-4.861 \times 10^1$	$7.172e \times 10^{-1}$	$-7.084 \times 10^{-4}$	$2.92 \times 10^{-7}$
ETBE	7.5	$6.293 \times 10^{-1}$	$-3.69e \times 10^{-4}$	$7.072 \times 10^{-9}$
Water	$3.224 \times 10^1$	$1.92e \times 10^{-3}$	$1.055 \times 10^{-5}$	$-3.596 \times 10^{-9}$

## A.4 UNIFAC Model Parameters

**Table A-4** Group Number for Each Component

Component	Molecular Formula	Group Number
Ethanol	C <sub>6</sub> H <sub>14</sub> O	4CH <sub>3</sub> 1C 1CH <sub>2</sub> O
Tert-butanol	C <sub>4</sub> H <sub>10</sub> O	3CH <sub>3</sub> 1OH 1C
ETBE	C <sub>2</sub> H <sub>6</sub> O	1CH <sub>3</sub> 1CH <sub>2</sub> 1OH
Water	H <sub>2</sub> O	1H <sub>2</sub> O

**Table A-5** Group Parameters for Each Component (Reid et al., 1987)

	CH <sub>3</sub>	CH <sub>2</sub>	C	OH	H <sub>2</sub> O	CH <sub>2</sub> O
R <sub>k</sub>	0.9011	0.6744	0.2195	1.0000	0.9200	0.9183
Q <sub>k</sub>	0.8480	0.5400	0.0000	1.2000	1.4000	0.7800

**Table A-6** Group Interaction Parameter a<sub>mk</sub> in (K<sup>-1</sup>) (Reid et al., 1987)

	n					
m	CH <sub>3</sub>	CH <sub>2</sub>	C	OH	H <sub>2</sub> O	CH <sub>2</sub> O
CH <sub>3</sub>	0.0	0.0	0.0	986.5	1318.0	251.5
CH <sub>2</sub>	0.0	0.0	0.0	986.5	1318.0	251.5
C	0.0	0.0	0.0	986.5	1318.0	251.5
OH	156.4	156.4	156.4	0.0	353.5	28.06
H <sub>2</sub> O	300.0	300.0	300.0	-229.1	0.0	540.0
CH <sub>2</sub> O	83.36	83.36	83.36	237.7	-314.7	0.0

## A.5 Comparison of Wilson and UNIFAC with Yang and Wang 2002

### 1. Wilson Method

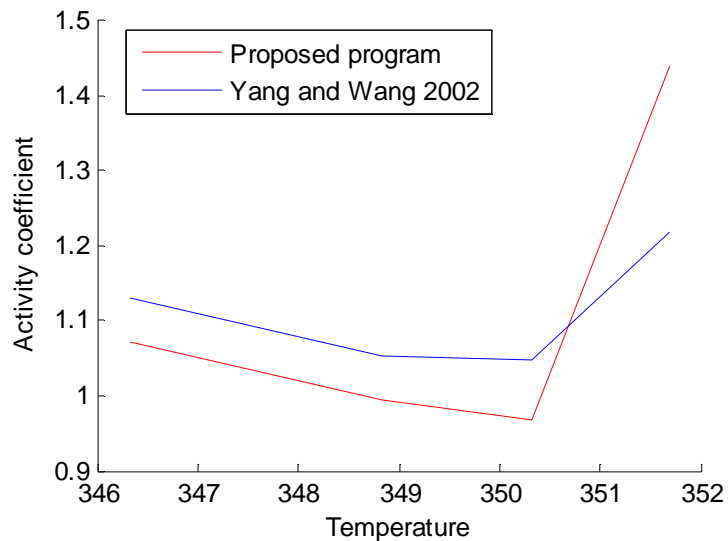


Figure A-1  $\gamma$  of ETOH, Wilson

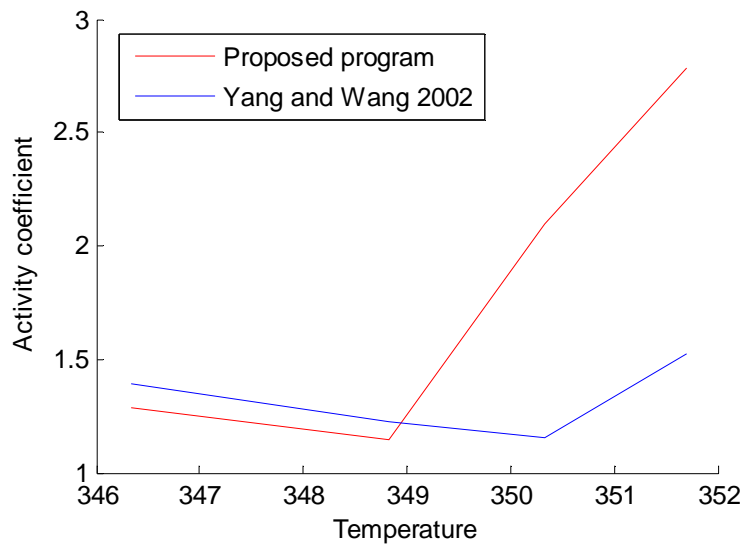
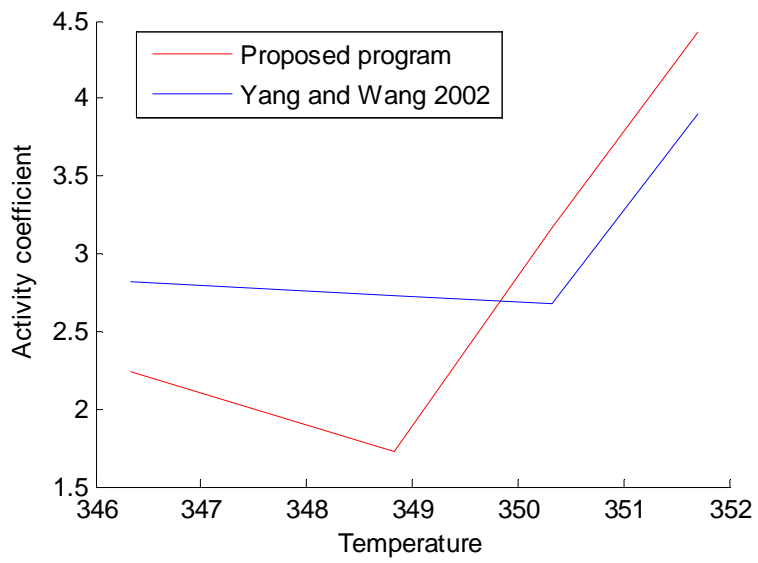
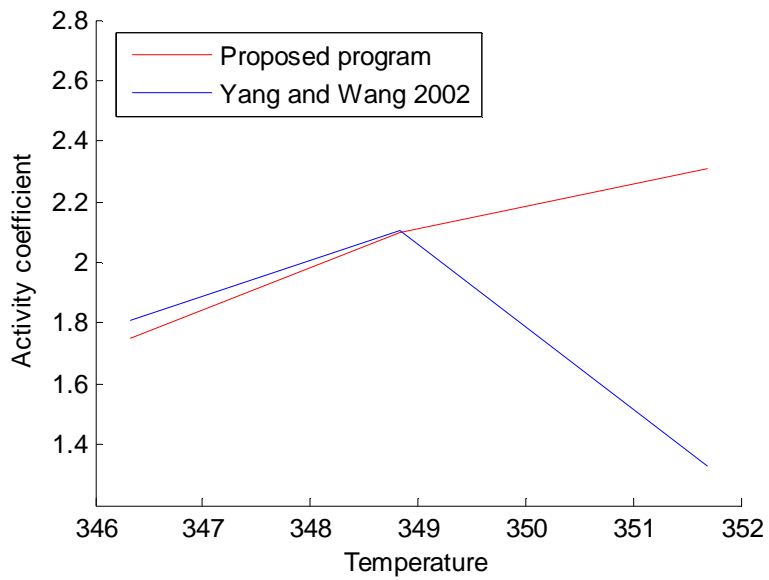


Figure A-2  $\gamma$  of TBA, Wilson



**Figure A-3**  $\gamma$  of ETBE, Wilson



**Figure A-4**  $\gamma$  of H<sub>2</sub>O, Wilson

## 2. UNIFAC Method

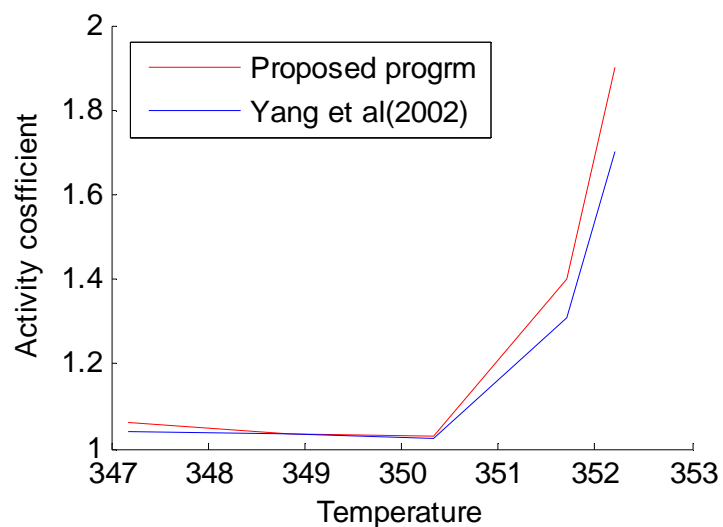


**Figure A-5**  $\gamma$  of ETOH, UNIFAC

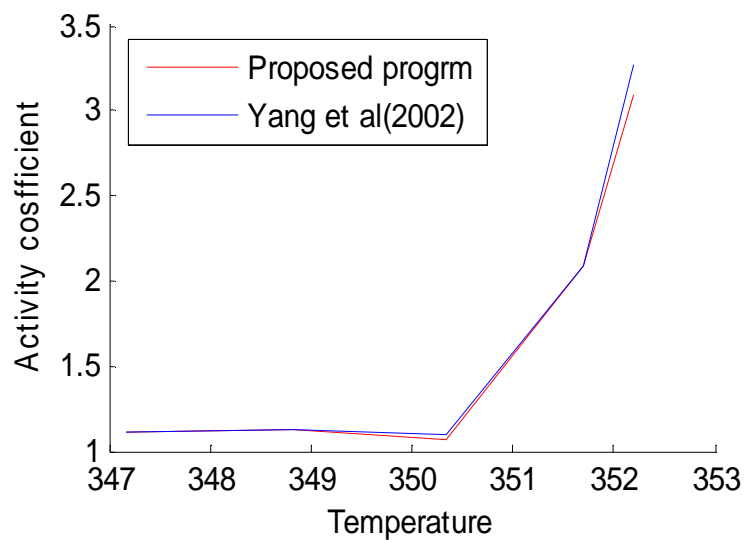


**Figure A-6**  $\gamma$  of TBA, UNIFAC

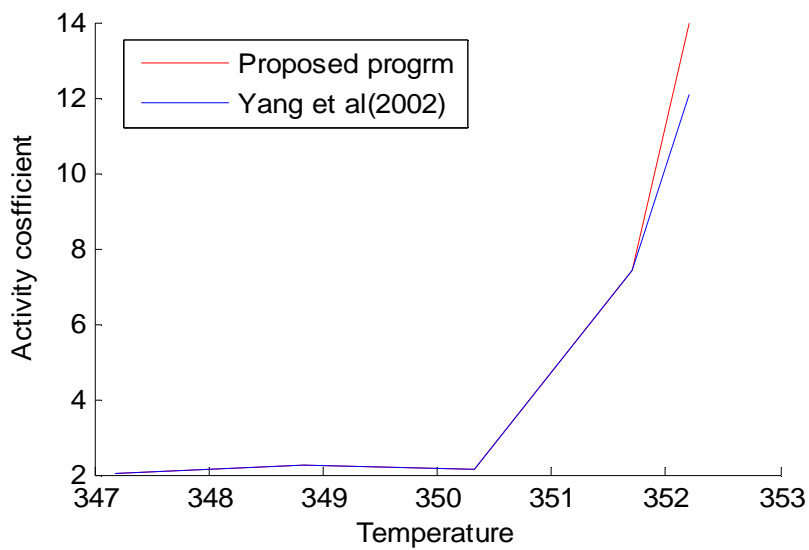


**Figure A-7**  $\gamma$  of E TBE, UNIFAC

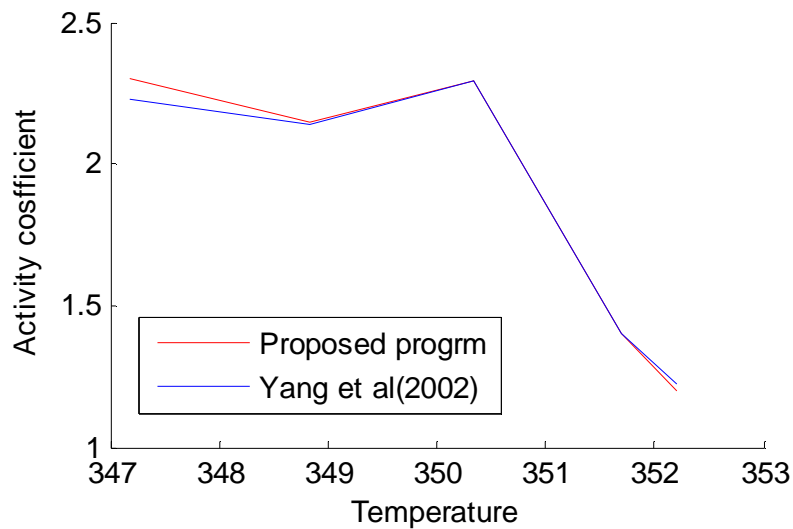


**Figure A-8**  $\gamma$  of H<sub>2</sub>O, UNIFAC

## A.6 Activity Coefficient Programs

### 1. Wilson Program

```
clc
clear
%%% WILSON METHOD
% #1 ETHANOL, #2 TERT-BUTANOL, #3 ETBE, #4 H2O
T=input('INPUT THE TEMPERATURE IN KELVIN THEN PRESS ENTER>> ');
%MOLE FRACTION X
%X1=.3305;X2=.1569;X3=.1015;X4=.4111;
%T=350.33 K
X10=0.3782;
X20=0.3501;
X30=0.0405;
X40=0.2312;
X1=X10;X2=X20;X3=X30;X4=X40;
R=8.314;
%MOLAR VOLUME IN KMOLE/m3
A=[0.057131,.094221,.131618,.018003];
B=[.00006,-.000075,.000706,-.000001];
C=[0.000000064,.000004,-.000023,.000000118];
V(1)=(A(1)+B(1)*(T-273)+C(1)*((T-273)^2))/1000;
V(2)=(A(2)+B(2)*(T-273)+C(2)*((T-273)^2))/1000;
V(3)=(A(3)+B(3)*(T-273)+C(3)*((T-273)^2))/1000;
V(4)=(A(4)+B(4)*(T-273)+C(4)*((T-273)^2))/1000;
%LAMDA= Y
U12=3954.1;U21=-3470.4;
U13=5286.5;U31=-1034.8;
U14=1046.8;U41=3975.0;
U23=2366.5;U32=230.5;
U24=-358.8;U42=7944.9;
U34=12923.1;U43=8780.1;
%WILSON PARAMETER U
Y11=1;Y22=1;Y33=1;Y44=1;
Y12=(V(2)/V(1))*exp(-U12/(R*T));Y21=(V(1)/V(2))*exp(-U21/(R*T));
Y13=(V(3)/V(1))*exp(-U13/(R*T));Y31=(V(1)/V(3))*exp(-U31/(R*T));
Y14=(V(4)/V(1))*exp(-U14/(R*T));Y41=(V(1)/V(4))*exp(-U41/(R*T));
Y23=(V(3)/V(2))*exp(-U23/(R*T));Y32=(V(2)/V(3))*exp(-U32/(R*T));
Y24=(V(4)/V(2))*exp(-U24/(R*T));Y42=(V(2)/V(4))*exp(-U42/(R*T));
Y34=(V(4)/V(3))*exp(-U34/(R*T));Y43=(V(3)/V(4))*exp(-U43/(R*T));
%GAMMA O
O1=exp((-log(X1*Y11+X2*Y12+X3*Y13+X4*Y14))+1-
((X1*Y11/(X1*Y11+X2*Y12+X3*Y13+X4*Y14))+(X2*Y21/(X1*Y21+X2*Y22+X3*Y23+X4*Y24))+(X3*Y31/(X1*Y31+X2*Y32+X3*Y33+X4*Y34))+(X4*Y41/(X1*Y41+X2*Y42+X3*Y43+X4*Y44)))));
O2=exp((-log(X1*Y21+X2*Y22+X3*Y23+X4*Y24))+1-
((X1*Y12/(X1*Y11+X2*Y12+X3*Y13+X4*Y14))+(X2*Y22/(X1*Y21+X2*Y22+X3*Y23+X4*Y24))+(X3*Y32/(X1*Y31+X2*Y32+X3*Y33+X4*Y34))+(X4*Y42/(X1*Y41+X2*Y42+X3*Y43+X4*Y44)))));
O3=exp((-log(X1*Y31+X2*Y32+X3*Y33+X4*Y34))+1-
((X1*Y13/(X1*Y11+X2*Y12+X3*Y13+X4*Y14))+(X2*Y23/(X1*Y21+X2*Y22+X3*Y23+X4*Y24))+(X3*Y33/(X1*Y31+X2*Y32+X3*Y33+X4*Y34))+(X4*Y43/(X1*Y41+X2*Y42+X3*Y43+X4*Y44)))));
```



```

4))+(X3*Y33/(X1*Y31+X2*Y32+X3*Y33+X4*Y34))+(X4*Y43/(X1*Y41+X2*Y42+X3*Y43+X4
*Y44)))
O4=exp((-log(X1*Y41+X2*Y42+X3*Y43+X4*Y44))+1-
((X1*Y14/(X1*Y11+X2*Y12+X3*Y13+X4*Y14))+(X2*Y24/(X1*Y21+X2*Y22+X3*Y23+X4*Y2
4))+(X3*Y34/(X1*Y31+X2*Y32+X3*Y33+X4*Y34))+(X4*Y44/(X1*Y41+X2*Y42+X3*Y43+X4
*Y44))))

```

## 2. UNIQUAC Program

```

%%%%%%%%%   UNIQUAC
clc
clear
% input temperature in kelvin
T=input('Temperature(K):')
%Ethanol #1
%TBA #2
%ETBE #3
%Water #4
% Initial composition of each component in the column
%T=348.83 For temperature=348.83 K, xETOH=0.4034 , xTBA=0.2547 ,
%xETBE=0.0612 , xH2O=0.2807.
X10=0.4034;
X20=0.2547;
X30=0.0612;
X40=0.2807;
X1=X10;X2=X20;X3=X30;X4=X40;
%%% 1: COMBINATORIAL TERM
r=[2.7755,3.9228,5.0501,.92];
q=[2.588,3.744,4.572,1.4];

J1=r(1)/(r(1)*X1+r(2)*X2+r(3)*X3+r(4)*X4);
J2=r(2)/(r(1)*X1+r(2)*X2+r(3)*X3+r(4)*X4);
J3=r(3)/(r(1)*X1+r(2)*X2+r(3)*X3+r(4)*X4);
J4=r(4)/(r(1)*X1+r(2)*X2+r(3)*X3+r(4)*X4);

L1=q(1)/(q(1)*X1+q(2)*X2+q(3)*X3+q(4)*X4);
L2=q(2)/(q(1)*X1+q(2)*X2+q(3)*X3+q(4)*X4);
L3=q(3)/(q(1)*X1+q(2)*X2+q(3)*X3+q(4)*X4);
L4=q(4)/(q(1)*X1+q(2)*X2+q(3)*X3+q(4)*X4);

% uic=ln Oc
u1c=exp(1-J1+log(J1)-5*q(1)*(1-(J1/L1)+log(J1/L1)));
u2c=exp(1-J2+log(J2)-5*q(2)*(1-(J2/L2)+log(J2/L2)));
u3c=exp(1-J3+log(J3)-5*q(3)*(1-(J3/L3)+log(J3/L3)));
u4c=exp(1-J4+log(J4)-5*q(4)*(1-(J4/L4)+log(J4/L4)));

%%% 2:RESIDUAL TERM
R=8.314;
%CRITICAL PROPERTIES
Tc=[513.9,506,531,647.3];
Pc=[61.4,39.7,30.4,221.2];
%NORMAL BOILING POINT TB

```

```

TB=[78+273,83+273,73+273,100+273];
TBR=[TB(1)/Tc(1),TB(2)/Tc(2),TB(3)/Tc(3),TB(4)/Tc(4)];
%VETERE EQUATION
HVB(1)=R*Tc(1)*TBR(1)*((0.4343*log(Pc(1))-0.69431+0.89584*TBR(1))/(0.37691-
0.37306*TBR(1)+0.15075*((Pc(1))^(-1))*((TBR(1))^(-2))));%J/mol
HVB(2)=R*Tc(2)*TBR(2)*((0.4343*log(Pc(2))-0.69431+0.89584*TBR(2))/(0.37691-
0.37306*TBR(2)+0.15075*((Pc(2))^(-1))*((TBR(2))^(-2))));
HVB(3)=R*Tc(3)*TBR(3)*((0.4343*log(Pc(3))-0.69431+0.89584*TBR(3))/(0.37691-
0.37306*TBR(3)+0.15075*((Pc(3))^(-1))*((TBR(3))^(-2))));
HVB(4)=R*Tc(4)*TBR(4)*((0.4343*log(Pc(4))-0.69431+0.89584*TBR(4))/(0.37691-
0.37306*TBR(4)+0.15075*((Pc(4))^(-1))*((TBR(4))^(-2))));
%REDUCED TEMPERATURE
TR=[T/Tc(1),T/Tc(2),T/Tc(3),T/Tc(4)];
%HEAT OF VAPORIZATION
HV(1)=HVB(1)*(((1-TR(1))/(1-TBR(1)))^0.38);
HV(2)=HVB(2)*(((1-TR(2))/(1-TBR(2)))^0.38);
HV(3)=HVB(3)*(((1-TR(3))/(1-TBR(3)))^0.38);
HV(4)=HVB(4)*(((1-TR(4))/(1-TBR(4)))^0.38);
%%INTERNAL ENERGY
DU(1)=HV(1)-R*T;
DU(2)=HV(2)-R*T;
DU(3)=HV(3)-R*T;
DU(4)=HV(4)-R*T;
%%%%UNIQUAC PARAMETERS U
%MOLAR VOLUME IN KMOLE/m3
A=[0.057131,.094221,.131618,.018003];
B=[.00006,-.000075,.000706,-.000001];
C=[0.000000064,.000004,-.000023,.000000118];
V(1)=(A(1)+B(1)*(T-273)+C(1)*((T-273)^2))/1000;%m3/mol
V(2)=(A(2)+B(2)*(T-273)+C(2)*((T-273)^2))/1000;
V(3)=(A(3)+B(3)*(T-273)+C(3)*((T-273)^2))/1000;
V(4)=(A(4)+B(4)*(T-273)+C(4)*((T-273)^2))/1000;
%%
C11=DU(1)/V(1);C22=DU(2)/V(2);C33=DU(3)/V(3);C44=DU(4)/V(4);
C12=((C11*C22)^0.5);C13=((C11*C33)^0.5);C14=((C11*C44)^0.5);
C21=((C11*C22)^0.5);C23=((C22*C33)^0.5);C24=((C22*C44)^0.5);
C31=((C11*C33)^0.5);C32=((C22*C33)^0.5);C34=((C33*C44)^0.5);
C41=((C11*C44)^0.5);C42=((C22*C44)^0.5);C34=((C33*C44)^0.5);

U11=-DU(1)/q(1);U22=-DU(2)/q(2);U33=-DU(3)/q(3);U44=-DU(4)/q(4);
U12=((U11*U22)^0.5)*(1-C12);U21=((U11*U22)^0.5)*(1-C12);
U13=((U11*U33)^0.5)*(1-C13);U31=((U11*U33)^0.5)*(1-C13);
U14=((U11*U44)^0.5)*(1-C14);U41=((U11*U44)^0.5)*(1-C14);
U23=((U22*U33)^0.5)*(1-C23);U32=((U22*U33)^0.5)*(1-C23);
U24=((U22*U44)^0.5)*(1-C24);U42=((U22*U44)^0.5)*(1-C24);
U34=((U33*U44)^0.5)*(1-C34);U43=((U33*U44)^0.5)*(1-C34);
%%%%
T11=0;T22=0;T33=0;T44=0;
T12=-((U12-U22)/(R*T));T21=-((U12-U11)/(R*T));
T13=-((U13-U33)/(R*T));T31=-((U13-U11)/(R*T));
T14=-((U14-U44)/(R*T));T41=-((U14-U11)/(R*T));
T23=-((U23-U33)/(R*T));T32=-((U23-U22)/(R*T));
T24=-((U24-U44)/(R*T));T42=-((U24-U22)/(R*T));
T34=-((U34-U44)/(R*T));T43=-((U34-U33)/(R*T));

```

```

%%%%%
U1R=exp(q(1)*(1-log(L1*T11+L2*T21+L3*T31+L4*T41)-
((L1*T11/(L1+L2*T21+L3*T31+L4*T41))+(L2*T12/(L1*T12+L2+L3*T32+L4*T42))+(L3*
T13/(L1*T13+L2*T23+L3+L4*T43))+(L4*T14/(L1*T14+L2*T24+L3*T34+L4)))));
U2R=exp(q(2)*(1-log(L1*T12+L2*T22+L3*T32+L4*T42)-
((L1*T21/(L1+L2*T21+L3*T31+L4*T41))+(L2*T22/(L1*T12+L2+L3*T32+L4*T42))+(L3*
T23/(L1*T13+L2*T23+L3+L4*T43))+(L4*T24/(L1*T14+L2*T24+L3*T34+L4)))));
U3R=exp(q(3)*(1-log(L1*T13+L2*T23+L3*T33+L4*T43)-
((L1*T31/(L1+L2*T21+L3*T31+L4*T41))+(L2*T32/(L1*T12+L2+L3*T32+L4*T42))+(L3*
T33/(L1*T13+L2*T23+L3+L4*T43))+(L4*T34/(L1*T14+L2*T24+L3*T34+L4)))));
U4R=exp(q(4)*(1-log(L1*T14+L2*T24+L3*T34+L4*T44)-
((L1*T41/(L1+L2*T21+L3*T31+L4*T41))+(L2*T42/(L1*T12+L2+L3*T32+L4*T42))+(L3*
T43/(L1*T13+L2*T23+L3+L4*T43))+(L4*T44/(L1*T14+L2*T24+L3*T34+L4)))));
%%%%%
O1=(u1c+U1R)
O2=(u2c+U2R)
O3=(u3c+U3R)
O4=(u4c+U4R)

```

### 3. UNIFAC Program

```

clc
clear
% input temperature in kelvin
T=input('Temperature(K):')
Nt=10;
%Ethanol #1
%TBA #2
%ETBE #3
%Water #4
% Initial composition of each component in the column
%T=348.83 For temperature=348.83 K, xETOH=0.4034 , xTBA=0.2547 ,
%xETBE=0.0612 , xH2O=0.2807.
X10=0.4034;
X20=0.2547;
X30=0.0612;
X40=0.2807;
X1=X10;X2=X20;X3=X30;X4=X40;
%%% 1: COMBINATORIAL TERM
r=[2.7755,3.9228,5.0501,.92];
q=[2.588,3.744,4.572,1.4];
J1=r(1)/(r(1)*X1+r(2)*X2+r(3)*X3+r(4)*X4);
J2=r(2)/(r(1)*X1+r(2)*X2+r(3)*X3+r(4)*X4);
J3=r(3)/(r(1)*X1+r(2)*X2+r(3)*X3+r(4)*X4);
J4=r(4)/(r(1)*X1+r(2)*X2+r(3)*X3+r(4)*X4);

L1=q(1)/(q(1)*X1+q(2)*X2+q(3)*X3+q(4)*X4);
L2=q(2)/(q(1)*X1+q(2)*X2+q(3)*X3+q(4)*X4);
L3=q(3)/(q(1)*X1+q(2)*X2+q(3)*X3+q(4)*X4);
L4=q(4)/(q(1)*X1+q(2)*X2+q(3)*X3+q(4)*X4);

% uic=ln Oc
ulc=1-J1+log(J1)-5*q(1)*(1-(J1/L1)+log(J1/L1));

```

```

u2c=1-J2+log(J2)-5*q(2)*(1-(J2/L2)+log(J2/L2));
u3c=1-J3+log(J3)-5*q(3)*(1-(J3/L3)+log(J3/L3));
u4c=1-J4+log(J4)-5*q(4)*(1-(J4/L4)+log(J4/L4));

%%% 2:RESIDUAL TERM

%%%% eki
e11=.3277;e21=.2087;e31=.4637;e41=0;e51=0;e61=0;
e12=.6795;e22=0;e32=.3205;e42=0;e52=0;e62=0;
e13=.7419;e23=0;e33=0;e43=0;e53=.258;e63=0;
e14=0;e24=0;e34=0;e44=0;e54=0;e64=1;

% t=exp(-amk/T)
t11=1;t12=1;t13=exp(-986.5/T);t14=1;t15=exp(-476.4/T);t16=exp(-1318/T);
t21=1;t22=1;t23=exp(-986.5/T);t24=1;t25=exp(-476.4/T);t26=exp(-1318/T);
t31=exp(-156.4/T);t32=exp(-156.4/T);t33=1;t34=exp(-156.4/T);t35=exp(-
84/T);t36=exp(-353.5/T);
t41=1;t42=1;t43=exp(-986.5/T);t44=1;t45=exp(-251.5/T);t46=exp(-1318/T);
t51=exp(-26.76/T);t52=exp(-26.76/T);t53=exp(-164.5/T);t54=exp(-
26.76/T);t55=1;t56=exp(-472.5/T);
t61=exp(-300/T);t62=exp(-300/T);t63=exp(229.1/T);t64=exp(-
300/T);t65=exp(195.4/T);t66=1;

%B ik
B11=e11*t11+e21*t21+e31*t31+e41*t41+e51*t51+e61*t61;
B21=e12*t11+e22*t21+e32*t31+e42*t41+e52*t51+e62*t61;
B31=e13*t11+e23*t21+e33*t31+e43*t41+e53*t51+e63*t61;
B41=e14*t11+e24*t21+e34*t31+e44*t41+e54*t51+e64*t61;
B12=e11*t12+e21*t22+e31*t32+e41*t42+e51*t52+e61*t62;
B22=e12*t12+e22*t22+e32*t32+e42*t42+e52*t52+e62*t62;
B32=e13*t12+e23*t22+e33*t32+e43*t42+e53*t52+e63*t62;
B42=e14*t12+e24*t22+e34*t32+e44*t42+e54*t52+e64*t62;
B13=e11*t13+e21*t23+e31*t33+e41*t43+e51*t53+e61*t63;
B23=e12*t13+e22*t23+e32*t33+e42*t43+e52*t53+e62*t63;
B33=e13*t13+e23*t23+e33*t33+e43*t43+e53*t53+e63*t63;
B43=e14*t13+e24*t23+e34*t33+e44*t43+e54*t53+e64*t63;
B14=e11*t14+e21*t24+e31*t34+e41*t44+e51*t54+e61*t64;
B24=e12*t14+e22*t24+e32*t34+e42*t44+e52*t54+e62*t64;
B34=e13*t14+e23*t24+e33*t34+e43*t44+e53*t54+e63*t64;
B44=e14*t14+e24*t24+e34*t34+e44*t44+e54*t54+e64*t64;
B15=e11*t15+e21*t25+e31*t35+e41*t45+e51*t55+e61*t65;
B25=e12*t15+e22*t25+e32*t35+e42*t45+e52*t55+e62*t65;
B35=e13*t15+e23*t25+e33*t35+e43*t45+e53*t55+e63*t65;
B45=e14*t15+e24*t25+e34*t35+e44*t45+e54*t55+e64*t65;
B16=e11*t16+e21*t26+e31*t36+e41*t46+e51*t56+e61*t66;
B26=e12*t16+e22*t26+e32*t36+e42*t46+e52*t56+e62*t66;
B36=e13*t16+e23*t26+e33*t36+e43*t46+e53*t56+e63*t66;
B46=e14*t16+e24*t26+e34*t36+e44*t46+e54*t56+e64*t66;
% Q= fi
% k=1
Q1=((X1*q(1)*e11)+(X2*q(2)*e12)+(X3*q(3)*e13)+(X4*q(4)*e14))/(q(1)*X1+q(2)*
X2+q(3)*X3+q(4)*X4);
% k=2

```

```

Q2=( (X1*q(1)*e21)+(X2*q(2)*e22)+(X3*q(3)*e23)+(X4*q(4)*e24))/(q(1)*X1+q(2)*
X2+q(3)*X3+q(4)*X4);
%      k=3
Q3=( (X1*q(1)*e31)+(X2*q(2)*e32)+(X3*q(3)*e33)+(X4*q(4)*e34))/(q(1)*X1+q(2)*
X2+q(3)*X3+q(4)*X4);
%      k=4
Q4=( (X1*q(1)*e41)+(X2*q(2)*e42)+(X3*q(3)*e43)+(X4*q(4)*e44))/(q(1)*X1+q(2)*
X2+q(3)*X3+q(4)*X4);
%      k=5
Q5=( (X1*q(1)*e51)+(X2*q(2)*e52)+(X3*q(3)*e53)+(X4*q(4)*e54))/(q(1)*X1+q(2)*
X2+q(3)*X3+q(4)*X4);
%      k=2
Q6=( (X1*q(1)*e61)+(X2*q(2)*e62)+(X3*q(3)*e63)+(X4*q(4)*e64))/(q(1)*X1+q(2)*
X2+q(3)*X3+q(4)*X4);

%      s
s1=Q1*t11+Q2*t21+Q3*t31+Q4*t41+Q5*t51+Q6*t61;
s2=Q1*t12+Q2*t22+Q3*t32+Q4*t42+Q5*t52+Q6*t62;
s3=Q1*t13+Q2*t23+Q3*t33+Q4*t43+Q5*t53+Q6*t63;
s4=Q1*t14+Q2*t24+Q3*t34+Q4*t44+Q5*t54+Q6*t64;
s5=Q1*t15+Q2*t25+Q3*t35+Q4*t45+Q5*t55+Q6*t65;
s6=Q1*t16+Q2*t26+Q3*t36+Q4*t46+Q5*t56+Q6*t66;

%UiR
U1R=q(1)*(1-(((Q1*B11/s1)-(e11*log(B11/s1))+((Q2*B12/s2)-
(e21*log(B12/s2)))+(Q3*B13/s3)-(e31*log(B13/s3)))+(Q4*B14/s4)-
(e41*log(B14/s4)))+(Q5*B15/s5)-(e51*log(B15/s5)))+(Q6*B16/s6)-
(e61*log(B16/s6)))));
U2R=q(2)*(1-(((Q1*B21/s1)-e12*log(B21/s1))+((Q2*B22/s2)-
e22*log(B22/s2)))+(Q3*B23/s3)-e32*log(B23/s3)))+(Q4*B24/s4)-
e42*log(B24/s4)))+(Q5*B25/s5)-e52*log(B25/s5)))+(Q6*B26/s6)-
e62*log(B26/s6)))));
U3R=q(3)*(1-(((Q1*B31/s1)-e13*log(B31/s1))+((Q2*B32/s2)-
e23*log(B32/s2))+((Q3*B33/s3)-e33*log(B33/s3)))+(Q4*B34/s4)-
e43*log(B34/s4)))+(Q5*B35/s5)-e53*log(B35/s5)))+(Q6*B36/s6)-
e63*log(B36/s6)))));
U4R=q(4)*(1-(((Q1*B41/s1)-e14*log(B41/s1))+((Q2*B42/s2)-
e24*log(B42/s2))+((Q3*B43/s3)-e34*log(B43/s3)))+(Q4*B44/s4)-
e44*log(B44/s4)))+(Q5*B45/s5)-e54*log(B45/s5)))+(Q6*B46/s6)-
e64*log(B46/s6)))));

O1=exp(u1c+U1R)
O2=exp(u2c+U2R)
O3=exp(u3c+U3R)
O4=exp(u4c+U4R)

```

## A.7 Virial Fugacity coefficient results

**Table A-7** Virial Fugacity Coefficient of Ethanol

Temperature	Fugacity of Components $\phi$			
	Ethanol	Tert-butanol	ETBE	H <sub>2</sub> O
350	0.9722	0.9606	0.9469	0.9850
352	0.9728	0.9615	0.9480	0.9854
354	0.9734	0.9624	0.9490	0.9857
356	0.9740	0.9632	0.9501	0.9860
358	0.9746	0.9640	0.9511	0.9863
360	0.9752	0.9648	0.9521	0.9866
362	0.9757	0.9655	0.9530	0.9868
364	0.9762	0.9663	0.9540	0.9871
366	0.9768	0.9670	0.9549	0.9874
368	0.9773	0.9677	0.9557	0.9876
370	0.9778	0.9684	0.9566	0.9879
372	0.9782	0.9691	0.9575	0.9881
374	0.9787	0.9697	0.9583	0.9884
376	0.9791	0.9703	0.9591	0.9886
378	0.9796	0.9709	0.9599	0.9888
380	0.9800	0.9715	0.9606	0.9890

## A.8 Lee-Kesler Fugacity coefficient results (Smith et al., 2001).

**Table A-8** Fugacity Coefficient of Ethanol

Temperature (K)	$\phi^\circ$	$\phi'$	$\phi$
353	0.9836	0.9827	0.9726
363	0.9846	0.9846	0.9748
373	0.9863	0.9869	0.9780

**Table A-9** Fugacity Coefficient of Tert-butanol

Temperature (K)	$\phi^\circ$	$\phi'$	$\phi$
353	0.9878	0.9855	0.9767
363	0.9856	0.9865	0.9774
373	0.9828	0.9847	0.9736

**Table A-10** Fugacity Coefficient of ETBE

Temperature (K)	$\phi^\circ$	$\phi'$	$\phi$
353	0.9856	0.9539	0.9672
363	0.9869	0.9721	0.9758
373	0.9687	0.9687	0.9565

**Table A-11** Fugacity Coefficient of H<sub>2</sub>O

Temperature (K)	$\phi^\circ$	$\phi'$	$\phi$
353	0.9319	0.8794	0.8917
363	0.9822	0.9724	0.9728
373	0.9829	0.9752	0.9744

## A.9 Antoine Equation Constants in Pa (Yang et al., 2001).

**Table A-11** Antoine Parameters

	ETOH	TBA	H <sub>2</sub> O	ETBE
A1	-75.7609	21.74757	-31.3974	6.67820
A2	-3100.647	-2658.29	-2046.366	-1066.84
A3	-40.50064	-95.5000	-75.40224	208.24
A4	-0.08814077	0	-0.012054	0
A5	20.81208	0	9.165751	0
A6	0.00005045	0	$0.4879195 \cdot 10^{-17}$	0
A7	2.00000	0	6.00000	0

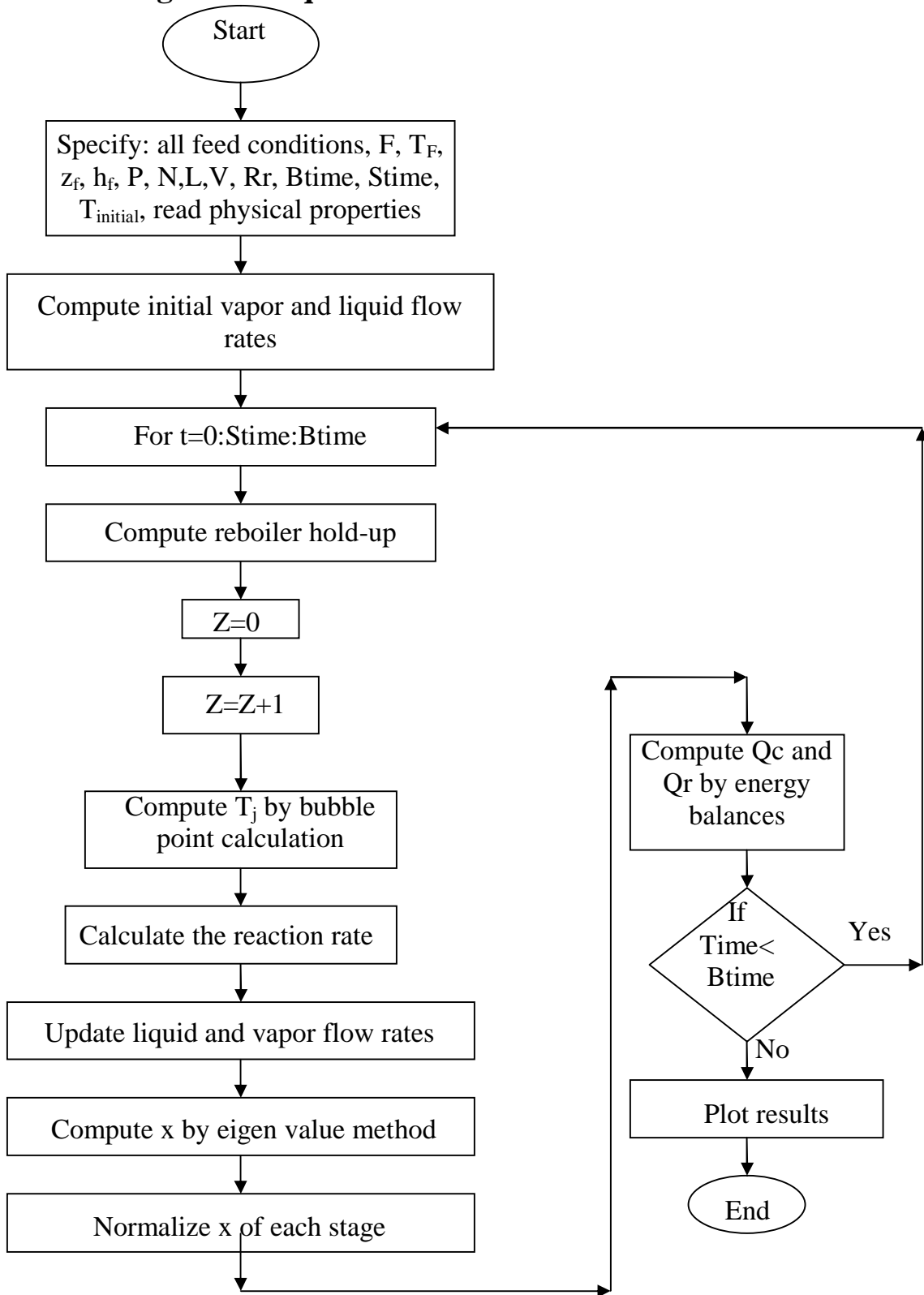
## A.10 Physical Properties (Reid et al., 1987).

**Table A-12** Physical Properties

<b>Component</b>	<b>Density (kg/m<sup>3</sup>)</b>	<b>Latent heat (J/mol)</b>	<b>Molecular weight (g/mol)</b>	<b>Critical temperature (K)</b>	<b>Critical pressure (bar)</b>	<b>Boiling point (C°)</b>
Ethanol	789	38666.172	46.069	513.9	61.4	78
Tert-butanol	787	46703	74.123	506	39.7	83
ETBE	749	30895.761	102.177	531	30.4	73
Water	993	44733	18.015	647.3	221.2	100



## A.11 Block Diagram of Equilibrium Model



## Appendix B

### Non Equilibrium Model Properties

#### B.1 Viscosity of Vapor (Sinnott, 1999)

$$\mu_i^V \xi_i = 34 * 10^{-5} Tr_i^{0.94} \quad \text{in mPa} \quad (\text{B.1})$$

$$\xi_i = \frac{Tc_i^{1/6}}{M_i^{1/2} Pc_i^{1/2}} \quad (\text{B.2})$$

Viscosity of mixture (Asano, 2006):

$$\mu_{mix}^V \sum_i \frac{y_i \mu_i}{\sum_j y_j \phi_{ij}} \quad (\text{B.3})$$

$$\phi_{ij} = \frac{[1 + (\mu_j / \mu_i)^{1/2} (M_j / M_i)^{1/4}]^2}{2.8284(1 + M_i / M_j)^{1/2}} \quad (\text{B.4})$$

#### B.2 Viscosity of Liquid (Sinnott, 1999)

$$\log \mu_i^L = A_{vis} \left( \frac{1}{T} - \frac{1}{B_{vis}} \right) \quad \text{in mPa} \quad (\text{B.5})$$

**Table B-1** Constants of Liquid Viscosity

<b>Component</b>	<b>A<sub>vis</sub></b>	<b>B<sub>vis</sub></b>
Ethanol	686.64	300.88
Tert-butanol	972.1	363.38
ETBE	443.32	234.68
H <sub>2</sub> O	658.25	283.16

Viscosity of mixture:

$$\mu_{mix}^L \sum_i \frac{M_{mix}}{\sum_{i=1}^c \frac{x_i M_i}{\mu_i^L}} \quad (\text{B.6})$$

### B.3 Surface Tension (Sinnott, 1999)

$$\sigma_i = \left[ \frac{P_{ch}(\rho_L - \rho_V)}{M} \right]^4 * 10^{-12} \quad \text{in (dyne/cm)} \quad (\text{B.7})$$

Where  $P_{ch}$  is the Sugden Parachor constant and it can be calculated from Table (8.7) in Sinnott, Colson and Richardson's Chemical Engineering, 1999 Vol. 6, page 335.

**Table B-2** Sugden Parachor Constant

Component	$P_{ch}$
Ethanol	97.4
Tert-butanol	152.2
ETBE	288.2
Water	54.2

Surface tension of mixture:

$$\sigma_{mix} = \sum_{i=1}^c x_i \sigma_i \quad (\text{B.8})$$

### B.4 Thermal Conductivity of Liquid Phase (Sinnott, 1999) in $\text{W/m}^2 \cdot \text{K}$

$$k_{th}^L = 3.56 * 10^{-5} C p_i^L \left[ \frac{(\rho_i^L)^4}{M_i} \right]^{1/3} \quad (\text{B.9})$$

Thermal conductivity of mixture (Asano, 2006):

$$k_{th,mix}^L = \frac{\sum_i y_i k_{th,i}}{\sum_j y_j \phi_{ij}} \quad (\text{B.10})$$

$$\phi_{ij} = \frac{[1 + (\mu_j / \mu_i)^{1/2} (M_j / M_i)^{1/4}]^2}{2.8284(1 + M_i / M_j)^{1/2}} \quad (\text{B.11})$$

## B.5 Thermal Conductivity of Vapor Phase (Sinnott, 1999) in W/m<sup>2</sup>. K

Thermal conductivity of vapor phase is given by:

$$k_{th}^V = \mu_i^V \left[ Cp_i^V + \frac{10.4}{M_i} \right] \quad (\text{B.12})$$

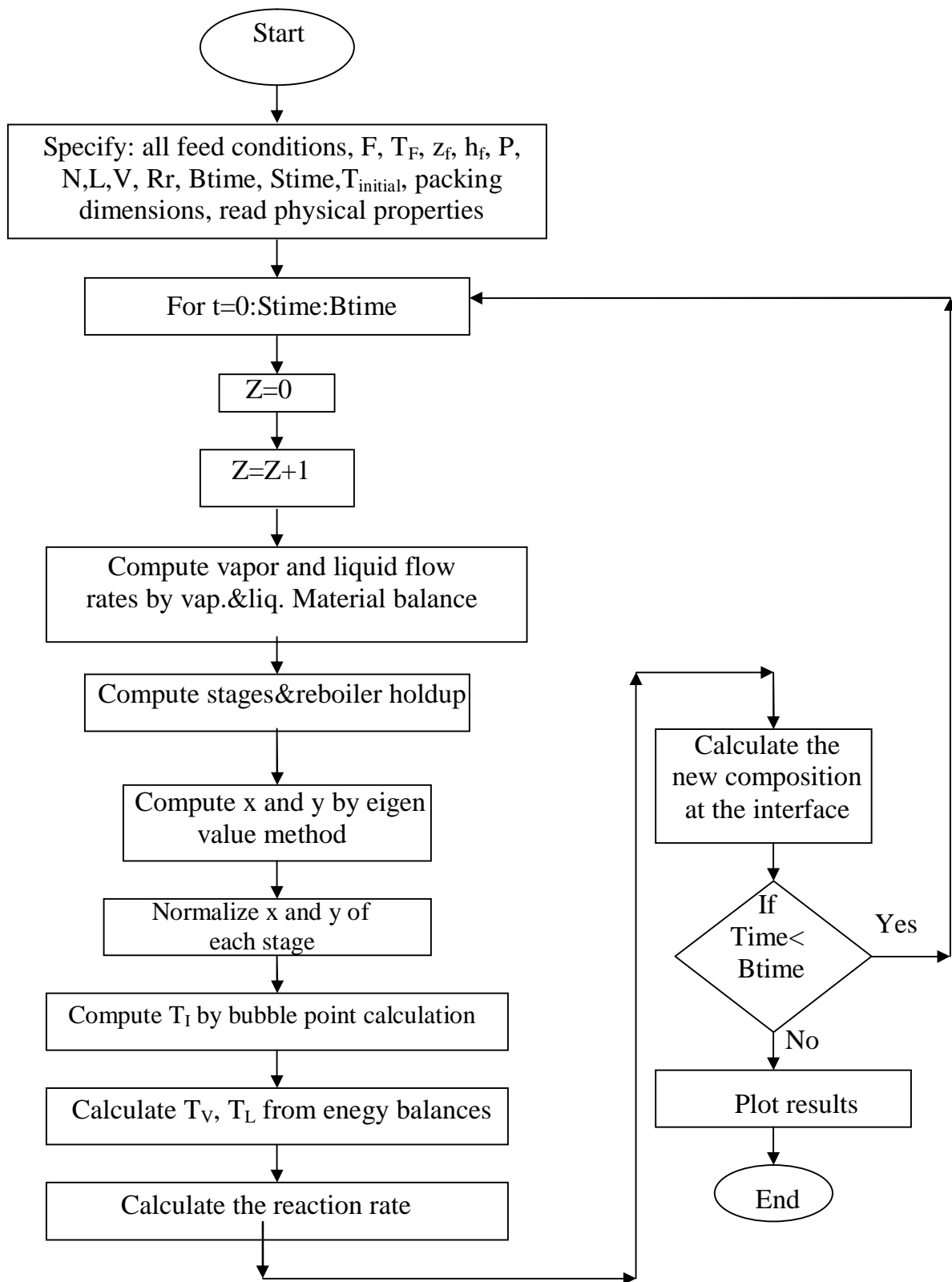
## B.6 Molecular Diffusion Volume of Components (m<sup>3</sup>/kmol)

Molecular diffusion volume of components can be calculated from the atomic volume which is given in Table (11.1), Reid et al., 1987, page 588.

**Table B-3** Molecular Volume

<b>Component</b>	<b>m<sub>v</sub></b>
Ethanol	51.77
Tert-butanol	92.81
ETBE	133.85
Water	10.73

## B.7 Block Diagram of NEQ model



## Appendix (C)

### Experimental Calibrations

#### C.1 Checking the Insulation Efficiency

The column was operated using pure water distillation with zero reflux ratio. The bottom temperature is the boiling point temperature of water 100 C°. The observed top temperature is 99.4 C° after 1 hr. The two temperatures are very close and the efficiency of insulation can be found by:

$$\begin{aligned} \text{Efficiency} &= \frac{\text{Observed}}{\text{Actual}} * 100\% && \text{(C.1)} \\ &= \frac{99.4}{100} * 100\% = 99.4\% \end{aligned}$$

#### C.2 HETP Calculation

Height equivalent to theoretical plates (HETP), for random packing (Seader and Henley, 1998).

$$\text{HETP, ft} = 1.5D_p, \text{in} \quad \text{(C.2)}$$

Where  $D_p$  is the outside diameter of packing.

$$\begin{aligned} \text{HETP, ft} &= 1.5 * 6\text{mm} * \frac{1\text{in}}{2.54 * 10\text{mm}} = 0.354\text{ft} \\ \text{HETP, cm} &= 0.354\text{ft} * \frac{30.48\text{cm}}{1\text{ft}} = 10.78\text{cm} \end{aligned}$$

$$\text{HETP} = \frac{L_T}{N_T} \quad \text{(C.3)}$$

$$N_T = \frac{70\text{cm}}{10.78\text{cm}} = 6.5 \approx 7 \text{ plates}$$

### C.3 Calibration of Heating Rate

The actual heating rates are evaluated by heating distilled water at the different heating power of the electrical heating source.

In order to evaluate the actual power received by the liquid in the still pot, the temperature versus time is plotted for the heating of a known amount of water at these different values of heating rate as in Figure (C.1).

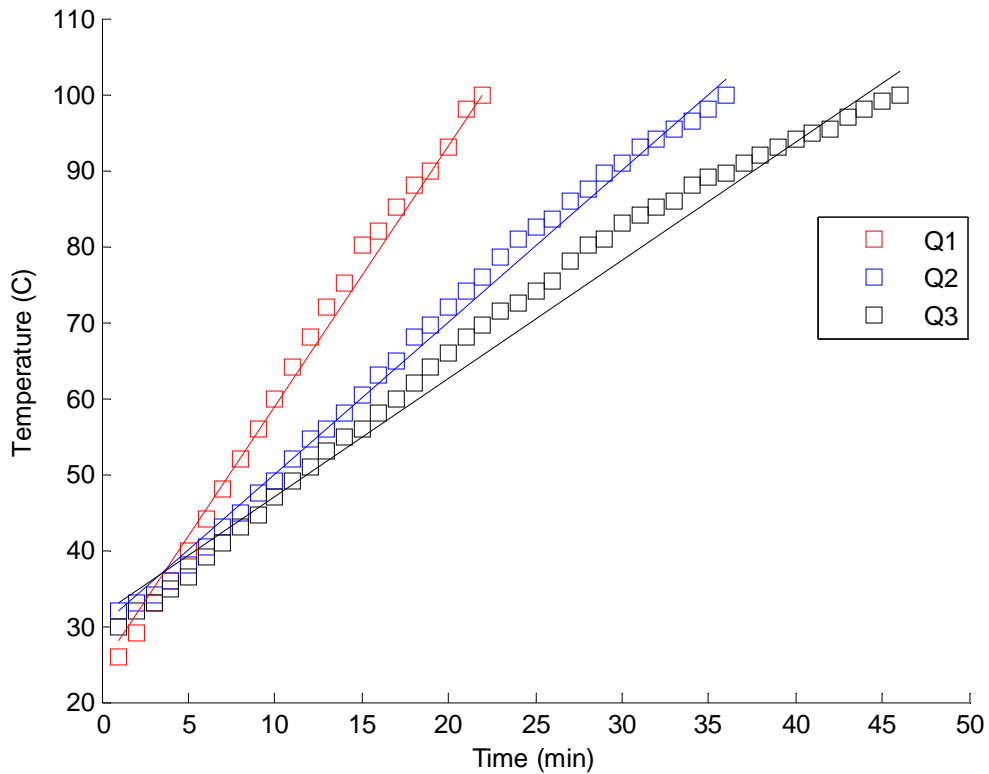


**Figure C-1** Temperature vs. Time at Different Heating Power

The actual heating rate could be evaluated simply by using sensible heat equation of the fluid:

$$Q = mC_p \frac{dT}{dt} \cong mC_p \frac{\Delta T}{\Delta t} \quad (\text{C.4})$$

Q : Rate of heat transfer (Watt)

m : Mass of fluid (kg)

cp : Heat capacity of fluid (J/kg.C°)

$\frac{dT}{dt}$  or  $\frac{\Delta T}{\Delta t}$  : Slope of temperature with time (C°/s)

The mean heat capacity of water at the temperature range is 4184 J/kg.C°, and the amount of water charge is 0.6 kg. The slopes of measuring temperature with time for all heating rate are given in Table (C.1), as well as the actual heating rates.

**Table C-1** Actual Heating Rates for Heater Reading

Heater index	$\Delta T/\Delta t$ (C°/min)	$\Delta T/\Delta t$ (C°/s)	Q (Watt)
1	3.50	0.0583	146
2	2.13	0.0355	90
3	1.55	0.0258	65



## C.4 Calibration of Thermometers

### 1. Bottom temperature

	<u>Observed C°</u>	<u>Real C°</u>
Boiling	100.5	100
Freezing	0	0

$$T_{real} = 0.995 * T_{obs} \tag{C.5}$$

### 2. Top temperature

	<u>Observed C°</u>	<u>Real C°</u>
Boiling	99.6	100
Freezing	1	0

$$T_{real} = 1.014199 * T_{obs} - 1.014199 \tag{A.6}$$

## Appendix (D)

### Results Data

#### D.1 Experimental Results of Changing the FMR

Table D-1 Data of Figure (5.1)

Component	FMR=1:1	FMR=2:1	FMR=4:1
H <sub>2</sub> O	0.16333	0.17559	0.14842
ETBE	0.05619	0.03909	0.03417
ETOH	0.23031	0.42642	0.57024
TBA	0.55017	0.3589	0.24717

#### D.2 Experimental Results of Changing the Rr

Table D-2 Liquid Mole Fractions at Reflux Ratio=3

Distillate				
Component	H <sub>2</sub> O	ETBE	ETOH	TBA
2hr	0.24861	0.05492	0.19224	0.50423
3hr	0.17835	0.08551	0.23882	0.49732
4hr	0.1729	0.09918	0.25505	0.47287
5hr	0.16931	0.10062	0.29489	0.43518
6hr	0.15837	0.11135	0.31621	0.41407
Residue				
Component	H <sub>2</sub> O	ETBE	ETOH	TBA
6hr	0.9534	0.00806	0.0175	0.02104

**Table D-3** Liquid Mole Fractions at Reflux Ratio=4

Distillate				
Component	H <sub>2</sub> O	ETBE	ETOH	TBA
2hr	0.16511	0.05626	0.29724	0.48139
3hr	0.17714	0.08783	0.35717	0.37786
4hr	0.16296	0.12021	0.38823	0.3286
5hr	0.24319	0.12631	0.29531	0.33519
6hr	0.27078	0.1304	0.30266	0.29616
Residue				
Component	H <sub>2</sub> O	ETBE	ETOH	TBA
6hr	0.95405	0.0045	0.03028	0.0117

**Table D-4** Liquid Mole Fractions at Reflux Ratio=5

Distillate				
Component	H <sub>2</sub> O	ETBE	ETOH	TBA
2hr	0.12956	0.06301	0.30203	0.5054
3hr	0.12917	0.1105	0.28477	0.47556
4hr	0.11177	0.10989	0.29993	0.45809
5hr	0.12325	0.13315	0.31321	0.42803
6hr	0.11667	0.1487	0.32012	0.41451
Residue				
Component	H <sub>2</sub> O	ETBE	ETOH	TBA
6hr	0.95775	0.01131	0.01245	0.01849

### D.3 Experimental Results of Changing the Boiler Heat Duty

**Table D-5** Liquid Mole Fractions at Reflux Ratio=5, Heat Duty=65W

Distillate				
Component	H <sub>2</sub> O	ETBE	ETOH	TBA
2hr	0.12747	0.09416	0.34277	0.4356
3hr	0.10774	0.12993	0.35123	0.4111
4hr	0.13873	0.13109	0.34129	0.38889
5hr	0.12105	0.12516	0.36053	0.39326
6hr	0.12414	0.12551	0.36449	0.38586
Residue				
Component	H <sub>2</sub> O	ETBE	ETOH	TBA
6hr	0.95498	0.00215	0.02162	0.02125

**Table D-6** Liquid Mole Fractions at Reflux Ratio=5, Heat Duty=90W

Distillate				
Component	H <sub>2</sub> O	ETBE	ETOH	TBA
2hr	0.20572	0.09339	0.28586	0.41503
3hr	0.15189	0.11196	0.3176	0.41855
4hr	0.15779	0.13776	0.31172	0.39271
5hr	0.15482	0.13655	0.30128	0.40735
6hr	0.13405	0.13027	0.33924	0.39644
Residue				
Component	H <sub>2</sub> O	ETBE	ETOH	TBA
6hr	0.97184	0.00073	0.01257	0.01486

## D.4 Experimental Results of Changing the Catalyst Type

**Table D-7** Liquid Mole Fractions with 90% water, catalyst H<sub>2</sub>SO<sub>4</sub>

Distillate				
Component	H <sub>2</sub> O	ETBE	ETOH	TBA
2hr	0.10881	0.08425	0.57032	0.23662
3hr	0.10166	0.13317	0.68115	0.08402
4hr	0.1007	0.18739	0.69242	0.01949
5hr	0.13617	0.16799	0.69197	0.00387
6hr	0.1492	0.16615	0.6846	0.00005
Residue				
Component	H <sub>2</sub> O	ETBE	ETOH	TBA
6hr	0.98934	0.00003	0.01044	0.00019

**Table D-8** Liquid Mole Fractions with 0% water, catalyst KHSO<sub>4</sub>

Distillate				
Component	H <sub>2</sub> O	ETBE	ETOH	TBA
2hr	0.04016	0.20149	0.43937	0.31898
3hr	0.0444	0.26045	0.39158	0.30357
4hr	0.04466	0.27929	0.38129	0.29476
5hr	0.04938	0.2925	0.3695	0.28862
6hr	0.05503	0.29996	0.36051	0.2845
Residue				
Component	H <sub>2</sub> O	ETBE	ETOH	TBA
6hr	0.14405	0.06175	0.4141	0.3801

**Table D-9** Liquid Mole Fractions with 0% water, catalyst H<sub>2</sub>SO<sub>4</sub>

Distillate				
Component	H <sub>2</sub> O	ETBE	ETOH	TBA
2hr	0.06311	0.23208	0.35364	0.35117
3hr	0.07337	0.37727	0.28745	0.26191
4hr	0.07943	0.50228	0.22684	0.19145
5hr	0.082	0.59274	0.18172	0.14354
6hr	0.13149	0.61317	0.15112	0.10422
Residue				
Component	H <sub>2</sub> O	ETBE	ETOH	TBA
6hr	0.20774	0.09645	0.39148	0.30433

## D.5 Experimental Results of Increasing the Catalyst Amount

**Table D-10** Liquid Mole Fractions with 0% water, catalyst 3\* KHSO<sub>4</sub>

Distillate				
Component	H <sub>2</sub> O	ETBE	ETOH	TBA
2hr	0.04766	0.20159	0.44891	0.30184
3hr	0.03831	0.26811	0.406	0.28758
4hr	0.13015	0.31441	0.30648	0.24896
5hr	0.1677	0.36668	0.26104	0.20458
6hr	0.18831	0.41622	0.21768	0.17779
Residue				
Component	H <sub>2</sub> O	ETBE	ETOH	TBA
6hr	0.29764	0.14474	0.29008	0.26764

## D.6 Experimental Results of Intermediate Reactive Section

**Table D-11** Liquid Mole Fractions

Distillate				
Component	H <sub>2</sub> O	ETBE	ETOH	TBA
2hr	0.05389	0.22155	0.34634	0.37822
3hr	0.10612	0.58584	0.1352	0.17282
4hr	0.16078	0.74679	0.0411	0.05133
5hr	0.16674	0.76528	0.03638	0.0316
6hr	0.17643	0.79407	0.0188	0.0107
Residue				
Component	H <sub>2</sub> O	ETBE	ETOH	TBA
6hr	0.40481	0.18135	0.22214	0.1917

## D.7 Experimental Results of Purification Experiments

**Table D-12** Liquid Mole Fractions, 0% Water in Feed, H<sub>2</sub>SO<sub>4</sub>

Component	1:1	2:1	4:1
H <sub>2</sub> O	15.97	14.565	14.143
ETBE	62.661	68.004	69.128
ETOH	11.641	10.286	10.284
TBA	9.728	7.145	6.445

**Table D-13** Liquid Mole Fractions, Three Times Catalyst KHSO<sub>4</sub>

Component	1:1	2:1	4:1
H <sub>2</sub> O	19.82	15.548	15.188
ETBE	59.143	67.122	68.241
ETOH	11.995	10.013	9.342
TBA	9.042	7.317	7.229

**Table D-14** Liquid Mole Fractions, Intermediate Reactive Section

Component	1:1	2:1	4:1
H <sub>2</sub> O	15.502	12.539	11.389
ETBE	82.713	86.333	87.142
ETOH	0.990	0.910	0.930
TBA	0.795	0.218	0.539

## D.8 Operating Conditions for Checking the Validity of EQ Model

**Table D-15** Operating Conditions for Comparison of Proposed EQ Program and Aspen Plus (Assabumrungrat et al., 2004)

Pressure (Pa)	101325
Feed molar ratio (TBA:ETOH:H <sub>2</sub> O)	1:1:38
Composition [% mol]	
ETOH	2.5
TBA	2.5
H <sub>2</sub> O	95
Feed flow rate (mol/s)	$2.7 \cdot 10^{-3}$
Reflux ratio	1.5
Catalyst weight per stage (kg)	0.04
Total stages	16
Rectification stages	5
Reaction stages	6
Stripping stages	5
Feed stage	12
Boiler Heat duty (W)	26.3



**Table D-16** Liquid Mole Fractions, Distillate of ASPEN PLUS

Component	H <sub>2</sub> O	ETBE	ETOH	TBA
Initial	0.950	0.000	0.025	0.025
1hr	0.780	0.063	0.067	0.090
2hr	0.405	0.171	0.189	0.235
3hr	0.272	0.201	0.215	0.312
4hr	0.270	0.191	0.206	0.333
5hr	0.270	0.186	0.188	0.356
6hr	0.270	0.185	0.186	0.359

**Table D-17** Liquid Mole Fractions, Distillate of Proposed Program

Component	H <sub>2</sub> O	ETBE	ETOH	TBA
Initial	0.950	0.000	0.025	0.025
1hr	0.622	0.092	0.097	0.189
2hr	0.388	0.170	0.165	0.277
3hr	0.292	0.193	0.189	0.326
4hr	0.268	0.192	0.193	0.347
5hr	0.301	0.184	0.189	0.326
6hr	0.311	0.185	0.187	0.317

## D.9 Theoretical Results of Equilibrium Model

**Table D-18** Liquid Mole Fractions, Rr=3

Distillate				
Component	H <sub>2</sub> O	ETBE	ETOH	TBA
2hr	0.175	0.062	0.286	0.457
3hr	0.1754	0.095	0.311	0.4186
4hr	0.176	0.126	0.314	0.384
5hr	0.151	0.127	0.357	0.365
6hr	0.145	0.128	0.356	0.371

**Table D-19** Liquid Mole Fractions, Rr=4

Distillate				
Component	H <sub>2</sub> O	ETBE	ETOH	TBA
2hr	0.1954	0.0663	0.3458	0.3925
3hr	0.1954	0.1263	0.3458	0.3325
4hr	0.2239	0.1256	0.32	0.3305
5hr	0.2595	0.124	0.26	0.32
6hr	0.3524	0.1155	0.2281	0.3039

**Table D-20** Liquid Mole Fractions, Rr=5

Distillate				
Component	H <sub>2</sub> O	ETBE	ETOH	TBA
2hr	0.18	0.071	0.2554	0.4936
3hr	0.1818	0.125	0.250	0.4432
4hr	0.160	0.1274	0.240	0.4726
5hr	0.130	0.139	0.230	0.501
6hr	0.090	0.160	0.217	0.533

**Table D-21** Liquid Mole Fractions, Heat Duty=65W

Distillate				
Component	H <sub>2</sub> O	ETBE	ETOH	TBA
2hr	0.09	0.08	0.42	0.41
3hr	0.162	0.098	0.301	0.44
4hr	0.1481	0.09898	0.303	0.449
5hr	0.139	0.108	0.304	0.449
6hr	0.159	0.11	0.301	0.43

**Table D-22** Liquid Mole Fractions, Heat Duty=90W

Distillate				
Component	H <sub>2</sub> O	ETBE	ETOH	TBA
2hr	0.083	0.09	0.21	0.617
3hr	0.09	0.098	0.32	0.492
4hr	0.103	0.16	0.37	0.367
5hr	0.106	0.13	0.41	0.354
6hr	0.11	0.117	0.43	0.343

**Table D-23** Liquid Mole Fractions, 0% Water in Feed, KHSO<sub>4</sub>

Distillate				
Component	H <sub>2</sub> O	ETBE	ETOH	TBA
2hr	0.031	0.19	0.429	0.35
3hr	0.041	0.201	0.428	0.33
4hr	0.048	0.2238	0.3332	0.395
5hr	0.051	0.2412	0.2778	0.43
6hr	0.0605	0.2532	0.2535	0.4328

**Table D-24** Liquid Mole Fractions, Three Times KHSO<sub>4</sub>

Distillate				
Component	H <sub>2</sub> O	ETBE	ETOH	TBA
2hr	0.031	0.19	0.429	0.35
3hr	0.0401	0.2319	0.428	0.33
4hr	0.048	0.254	0.333	0.365
5hr	0.091	0.311	0.237	0.371
6hr	0.122	0.373	0.153	0.352

**Table D-25** Liquid Mole Fractions, Intermediate Reactive Section

Distillate				
Component	H <sub>2</sub> O	ETBE	ETOH	TBA
2hr	0.123	0.191	0.355	0.331
3hr	0.139	0.415	0.192	0.254
4hr	0.203	0.571	0.091	0.135
5hr	0.195	0.691	0.053	0.061
6hr	0.193	0.721	0.031	0.055

## D.10 Theoretical Results if the Non-Equilibrium Model

**Table D-26** Liquid Mole Fractions, Rr=3

Distillate				
Component	H <sub>2</sub> O	ETBE	ETOH	TBA
2hr	0.1606	0.0602	0.225	0.5542
3hr	0.1619	0.0911	0.2855	0.4615
4hr	0.1644	0.1188	0.316	0.4008
5hr	0.1657	0.1212	0.3164	0.3967
6hr	0.167	0.1224	0.3169	0.3937

**Table D-27** Liquid Mole Fractions, Rr=4

Distillate				
Component	H <sub>2</sub> O	ETBE	ETOH	TBA
2hr	0.1763	0.0663	0.3048	0.4526
3hr	0.1971	0.1273	0.3437	0.3319
4hr	0.198	0.1283	0.3426	0.3311
5hr	0.2089	0.1311	0.3415	0.3185
6hr	0.2197	0.1314	0.3394	0.3095

**Table D-28** Liquid Mole Fractions, Rr=5

Distillate				
Component	H <sub>2</sub> O	ETBE	ETOH	TBA
2hr	0.1229	0.0592	0.2874	0.5305
3hr	0.1222	0.1194	0.2779	0.4805
4hr	0.1236	0.1208	0.2889	0.4467
5hr	0.115	0.1336	0.2793	0.4721
6hr	0.1164	0.1394	0.2698	0.4744

**Table D-29** Liquid Mole Fractions, Heat Duty=65W

Distillate				
Component	H <sub>2</sub> O	ETBE	ETOH	TBA
2hr	0.1285	0.0866	0.3288	0.4561
3hr	0.1309	0.1378	0.3378	0.3935
4hr	0.142	0.139	0.3368	0.3822
5hr	0.1432	0.1314	0.3248	0.4006
6hr	0.1534	0.1326	0.3238	0.3902

**Table D-30** Liquid Mole Fractions, Heat Duty=90W

Distillate				
Component	H <sub>2</sub> O	ETBE	ETOH	TBA
2hr	0.0981	0.0991	0.2317	0.5711
3hr	0.1093	0.1004	0.3225	0.4678
4hr	0.1118	0.1318	0.3218	0.4346
5hr	0.1131	0.1331	0.3525	0.4013
6hr	0.1144	0.1359	0.3649	0.3848

**Table D-31** Liquid Mole Fractions, 0% Water in Feed, KHSO<sub>4</sub>

Distillate				
Component	H <sub>2</sub> O	ETBE	ETOH	TBA
2hr	0.0574	0.1617	0.4410	0.3399
3hr	0.0511	0.1852	0.4200	0.3437
4hr	0.0569	0.2111	0.3982	0.3338
5hr	0.0631	0.2394	0.3344	0.3631
6hr	0.0689	0.2699	0.2981	0.3631

**Table D-32** Liquid Mole Fractions, Three Times KHSO<sub>4</sub>

Distillate				
Component	H <sub>2</sub> O	ETBE	ETOH	TBA
2hr	0.0376	0.1876	0.4289	0.3459
3hr	0.0382	0.2377	0.4161	0.308
4hr	0.0389	0.2678	0.3239	0.3694
5hr	0.04029	0.3377	0.2555	0.36651
6hr	0.04097	0.3879	0.1972	0.37393

**Table D-33** Liquid Mole Fractions, Intermediate Reactive Section

Distillate				
Component	H <sub>2</sub> O	ETBE	ETOH	TBA
2hr	0.1753	0.2571	0.3600	0.2076
3hr	0.1780	0.5330	0.1667	0.1223
4hr	0.2475	0.6252	0.1125	0.0148
5hr	0.2811	0.6931	0.0261	0.0197
6hr	0.2276	0.7467	0.0252	0.0005

## شكر و تقدير

فيما أنا اتم هذا الجهد المتواضع لا يسعني الا ان اتقدم بالشكر الجزيل والامتنان الكبير الى الاستاذ الدكتور ندى بجحت نقاش لاضافتها العلميه القيمه لكل فقره من فقرات البحث بما يتناسب ومكانتها العلميه المرموقه وما ابدته من نصح و توجيه كان له الاثر الكبير في انجاز هذا البحث.

كما اتوجه بالشكر الجزيل الى رئيس قسم الهندسه الكيمياويه لما ابداه من دعم خلال مرحله البحث, وشكري الجزيل لجميع كادر قسم الهندسه الكيمياويه.

و اود ان اعبر عن خالص امتناني وشكري لجميع افراد عائلتي لما قدموه من تشجيع و دعم على كافة الاصعده خلال سنوات دراسي.



## أخلاقه

يُستخدم الاثيل ثلاثي بيوتيل أليثير (ETBE) بصورة رئيسية في إنتاج كازولين عالي عدد الأوكتان. يتم إنتاج مادة ETBE من تفاعل الأيثانول و ثلاثي البيوتانول بوجود عامل مساعد حامضي حيث يُنتج الماء أيضاً كنتاج ثانوي باستخدام وحدة التقطير التفاعلي والتي يمكن اعتبارها كوحدة تفاعل و وحدة تقطير مدمجتين في وحدة تشغيل واحدة.

يُصنف العمل الحالي إلى جزأين: الجزء العملي و الجزء النظري. الغرض الرئيسي من الجزء العملي هو تصميم و بناء منظومة تقطير ذات الحشوات والتي تعمل بنظام الدفعاة بعمود تقطير طوله ٧١ سم و قطر داخلي ٣،٥ سم مُعبأ بحشوات من نوع Rasching Ring طولها ١٠ ملم و قطريها الداخلي و الخارجي ٦ ملم و ٣ ملم على التوالي. و من ثم تستخدم المنظومة المُصممة لإنتاج مادة ETBE. قبل إنتاج ETBE باستخدام منظومة التقطير التفاعلي أُجريت ثلاث تجارب بنسب قليلة و باستخدام التفاعل فقط لغرض التحقق من أداء العامل المساعد المستخدم و قابليته لإنتاج ETBE، من التجارب الثلاثة السابقه تبين فشل الزيولايت (13X) كعامل مساعد لإنتاج مادة ETBE، أما مادتي  $H_2SO_4$  و  $KHSO_4$  فقد أنتجتا مادة ETBE بنسب متفاوتة.

عند استخدام وحدة التقطير التفاعلي لإنتاج مادة ETBE تمت دراسة تأثير بعض العوامل التشغيلية على نقاوة مادة ETBE كنسبة الداخيل من الأيثانول إلى ثلاثي البيوتانول (١:١، ١:٢، و ١:٤)، نسبة الراجع (٣، ٤، و ٥)، الحمل الحراري لانهاء الغلايه (٦٥، ٩٠، و ١٤٦ واط)، نوع العامل المساعد ( $H_2SO_4$  و  $KHSO_4$ )، و كمية العامل المساعد عند إضافته مع المواد المُتفاعله في إناء الغلايه. كما تم إجراء تجرُبه أخرى لإنتاج مادة ETBE باستخدام جزء تفاعل وسطي حيث أُضيف العامل المساعد  $KHSO_4$  إلى جيوب قماشيه و تمت تعبأها في الجزء الوسطي من عمود التقطير. جميع التجارب تم إجراؤها تحت ضغط ١ جو.

أما في الجزء النظري فقد تم تطوير نموذجين رياضيين في حالي التوازن و الألاتوازن باستخدام لغة الماتلاب ( $R2009b$ ) بواسطة حل معادلات MESHR وهي مختصر لانتقال الماده و علاقة التوازن و جمع التراكيب و انتقال أطافه بالاضافه

إلى مُعادلة التفاعل. أُجْزَ الموديل الرياضي في حالة التوازن وقد قورنت نتائجه مع نتائج برنامج جَاهِر (ASPEN 10.2 PLUS) لظروف تشغيله مُعيّنه أظهرَ خلالها الموديل الرياضي توافقاً جيداً بنسبة خطأ  $\pm 10\%$ . إنَّ النمذج الرياضي في حالة التوازن لا يأخذ بنظر الاعتبار تأثير انتقال الكُتله و الطاقه ولهذا فقد تم عمل نموذج رياضي لحالة الألاتوازن مع إضافة فقرات مُكافئه لمعدل انتقال الكُتله و الطاقه.

تم تشغيل برنامجي التوازن والألاتوازن حسب الضروف العمليّه و مقارنتهما مع نتائج الجزء العملي وقد كانت نسبة الخطأ  $\pm 10\%$  لكلاهما. بالإضافة إلى مُقارنة نتائج حالة التوازن مع حالة الألاتوازن التي أظهرت انحرافاً ترجع أسبابه إلى أخذ تأثير انتقال الكُتله و الطاقه في برنامج الألاتوازن و اعتبار كفاءة البخار (Murphee) تساوي ١.

من خلال النتائج العمليه والنظريه تبين أن أفضل الظروف التشغيليه هي: نسبة الداخل ١:١، نسبة الرجاع ٥، الحِمل الحراري لانياء الغلايه ١٤٦ واط. كما إنَّ العاملُ المُساعد  $H_2SO_4$  أعطى نسبة نقاوه لمادة ETBE أعلى من التي أعطاهها العاملُ المُساعد  $KHSO_4$  حتى عند استخدام كميّه أكبر بثلاث مرّات. أمّا تفاعل الجزء الوسطي فأعطى نسبة نقاوه أعلى من التي أُستحصِلت عندما تمّ التفاعل في إناء الغلايه إلا أنه يحتاج إلى كميّه أكبر من العاملُ المُساعد.

# ألمحاكاة نظريا و عمليا لانتاج الاثيل ثلاثي بيوتيل أالاثر بأستخدام ألتقطير ألتفاعلي

رساله

مقدمة إلى كلية الهندسه في جامعة النهري  
وهي جزء من متطلبات نيل درجة ماجستير علوم  
في الهندسه الكيمياويه

من قبل

نادين خالد محمد الجنابي  
(بكالوريوس, ٢٠٠٨)

١٤٣١

٢٠١٠

ذو الحجه

تشرين الثاني